iScience

CellPress
OPEN ACCESS

Article

Coevolution of enamel, ganoin, enameloid, and their matrix SCPP genes in osteichthyans

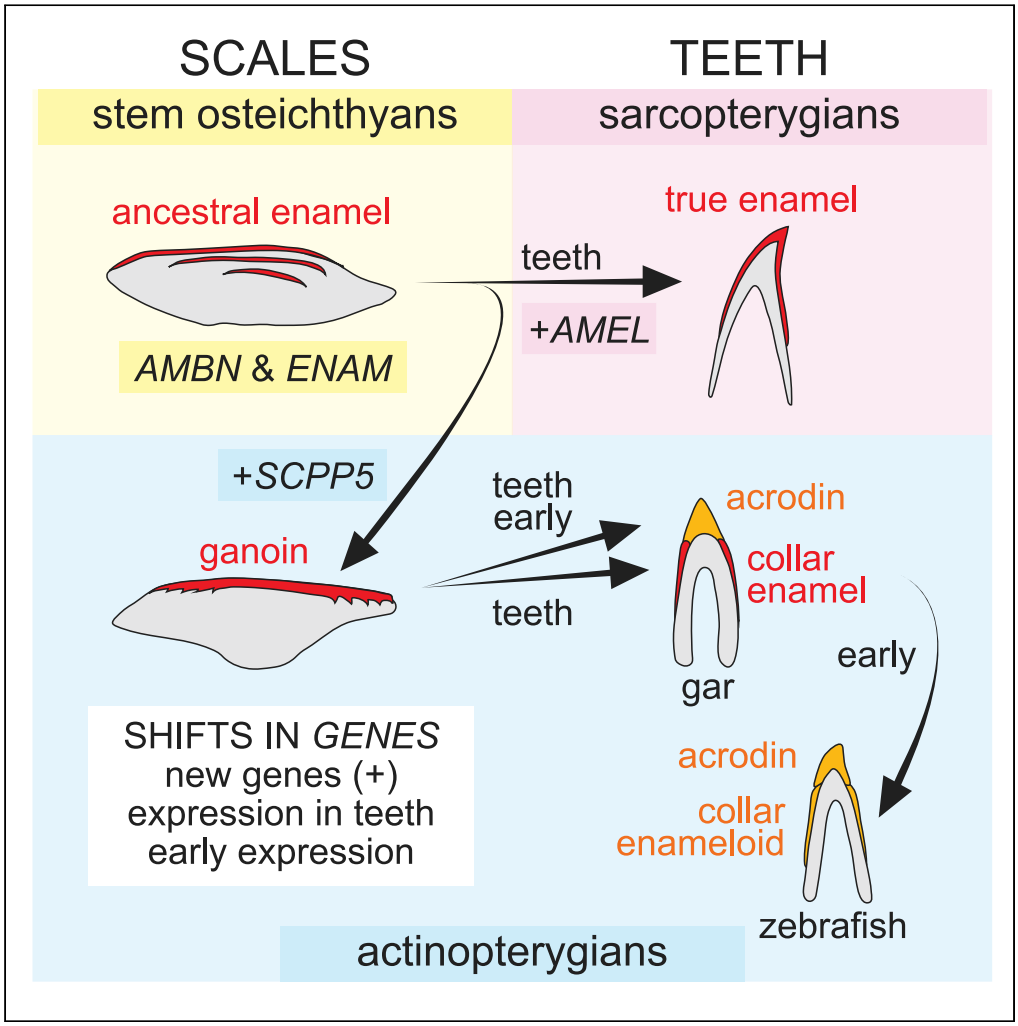

Kazuhiko Kawasaki, Joseph N. Keating, Mitsushiro Nakatomi, ..., Mark N. Puttick, Philip C.J. Donoghue, Mikio Ishiyama

kuk2@psu.edu

HIGHLIGHTS

Ganoin emerged in actinopterygians; true enamel arose in sarcopterygians

Dental enamel, acrodin, and enameloid in actinopterygians are related to ganoin

SCPP5 evolved in association with ganoin, whereas *AMEL* evolved with true enamel

Shifts in SCPP gene expression explain the evolution of hypermineralized tissues

Kawasaki et al., iScience *24*, 102023
January 22, 2021
https://doi.org/10.1016/j.isci.2020.102023

iScience

CellPress
OPEN ACCESS

Article

Coevolution of enamel, ganoin, enameloid, and their matrix SCPP genes in osteichthyans

Kazuhiko Kawasaki,[1,9,*] Joseph N. Keating,[2,8] Mitsushiro Nakatomi,[3,8] Monique Welten,[2,8] Masato Mikami,[4,8] Ichiro Sasagawa,[5,8] Mark N. Puttick,[2,6] Philip C.J. Donoghue,[2] and Mikio Ishiyama[7]

SUMMARY

We resolve debate over the evolution of vertebrate hypermineralized tissues through analyses of matrix protein-encoding secretory calcium-binding phosphoprotein (SCPP) genes and phylogenetic inference of hypermineralized tissues. Among these genes, *AMBN* and *ENAM* are found in both sarcopterygians and actinopterygians, whereas *AMEL* and *SCPP5* are found only in sarcopterygians and actinopterygians, respectively. Actinopterygian *AMBN*, *ENAM*, and *SCPP5* are expressed during the formation of hypermineralized tissues on scales and teeth: ganoin, acrodin, and collar enamel in gar, and acrodin and collar enameloid in zebrafish. Our phylogenetic analyses indicate the emergence of an ancestral enamel in stem-osteichthyans, whereas ganoin emerged in stem-actinopterygians and true enamel in stem-sarcopterygians. Thus, *AMBN* and *ENAM* originated in concert with ancestral enamel, *SCPP5* evolved in association with ganoin, and *AMEL* evolved with true enamel. Shifts in gene expression domain and timing explain the evolution of different hypermineralized tissues. We propose that hypermineralized tissues in osteichthyans coevolved with matrix SCPP genes.

INTRODUCTION

The vertebrate skeleton is composed principally of cartilage, bone, dentine, enamel, and enameloid (Donoghue et al., 2006; Hall, 2015), all of which are critical to vertebrate adaptations, including protective body armor, an endoskeleton for locomotion, and teeth for feeding (Donoghue and Keating, 2014). As such, mineralized tissues comprise a key innovation underlying much of vertebrate evolutionary success. Among these skeletal tissues, the origin of hypermineralized tissues, enamel, enameloid, and their histological derivatives, remains controversial, partly because their classification in fossils varies among researchers (Friedman and Brazeau, 2010; Schultze, 2016) and partly because genes encoding their matrix proteins are well understood only for true enamel in sarcopterygians. Here we investigate the evolution of various hypermineralized tissues through genomic and developmental analyses, combined with estimation of ancestral states based on data available from living and fossil vertebrates. We draw these disparate approaches together to obtain a holistic understanding of the origin and diversification of vertebrate hypermineralized tissues. Our results reveal evidence for the coevolution of hypermineralized tissues in osteichthyans and their matrix secretory calcium-binding phosphoprotein (SCPP) genes.

RESULTS

Enamel and enameloid have been classified into different types depending on their location and histological characteristics (Figure 1A). Mineralization of enamel and enameloid progresses in organic matrices (Berkovitz and Shellis, 2016) that are subsequently removed as they mature into hypermineralized inorganic tissues (Sasagawa, 1997; Fincham et al., 1999). Enamel grows in a non-collagenous matrix secreted by ameloblasts of epithelial origin (Fincham et al., 1999) and occurs in three main types: (1) true enamel, considered equivalent to mammalian tooth enamel (Smith, 1989); (2) multilayered ganoin (Schultze, 2016) on scales and their derivatives, found only in bichirs and gars among extant clades, as well as in diverse fossil actinopterygians (Sire et al., 2009); and (3) tooth collar enamel, which occurs in actinopterygians, including bichirs, gars, and extinct clades (Smith, 1995; Ishiyama et al., 1999; Sasagawa et al., 2013). Enameloid forms in a collagenous matrix secreted by both inner dental epithelial (IDE) cells and mesenchyme-derived odontoblasts (Poole, 1967), often characterized histologically by protruding dentine tubules (Smith, 1995). Enameloid constitutes an acrodin tooth cap in various extant and extinct actinopterygians

[1]Department of Anthropology, Pennsylvania State University, University Park, PA 16802, USA

[2]School of Earth Sciences, University of Bristol, Bristol BS8 1TQ, UK

[3]Division of Anatomy, Kyushu Dental University, Kitakyushu, Fukuoka 803-8580, Japan

[4]Department of Microbiology, School of Life Dentistry at Niigata, the Nippon Dental University, Niigata, Niigata 951-8580, Japan

[5]Advanced Research Center, School of Life Dentistry at Niigata, the Nippon Dental University, Niigata, Niigata 951-8580, Japan

[6]Milner Centre for Evolution, Department of Biology and Biochemistry, University of Bath, Bath BA2 7AY, UK

[7]Department of Histology, School of Life Dentistry at Niigata, the Nippon Dental University, Niigata, Niigata 951-8580, Japan

[8]These authors contributed equally

[9]Lead Contact

*Correspondence: kuk2@psu.edu

https://doi.org/10.1016/j.isci.2020.102023

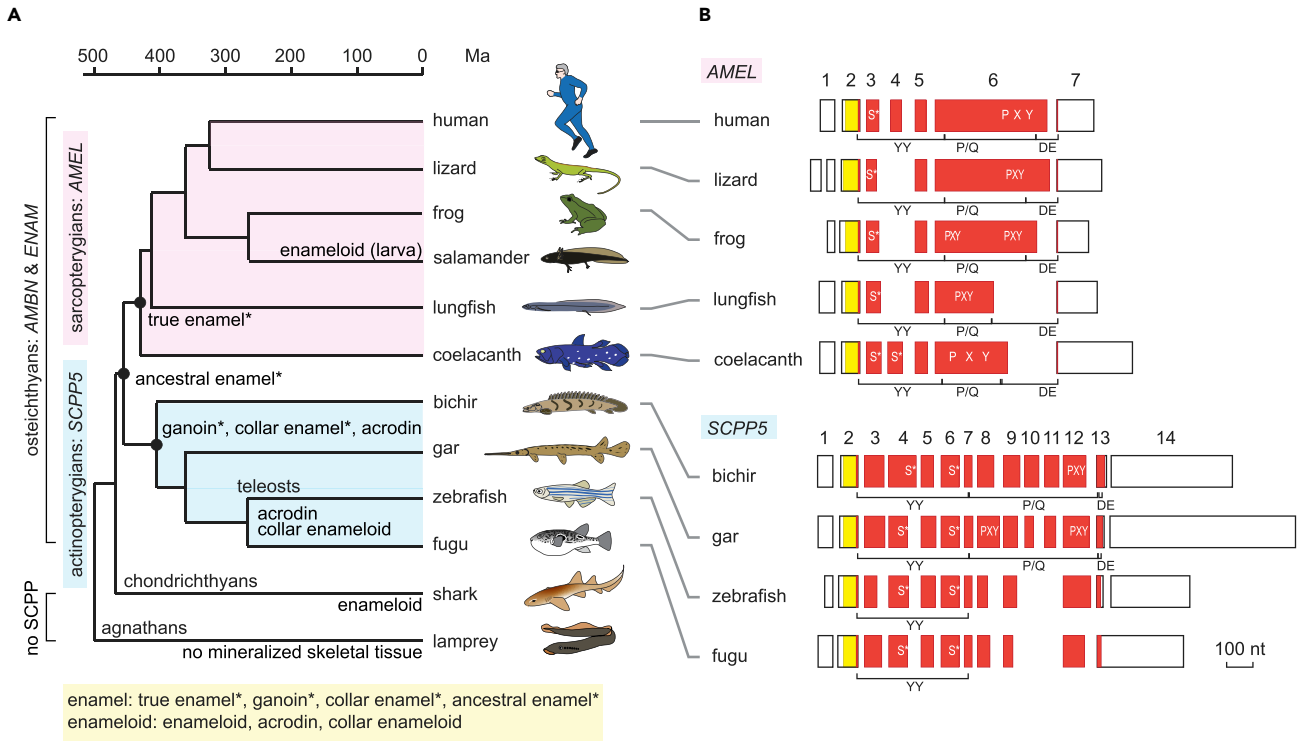

Figure 1. Phylogenetic distribution of enamel and enameloid matrix genes, and exon-intron structure of *AMEL* and *SCPP5*

(A) Phylogenetic distribution of enamel, enameloid, and their matrix genes. Hypermineralized tissues classified as enamel are denoted by an asterisk. Divergence times are based on previous studies: most sarcopterygian taxa (Hedges and Kumar, 2009), actinopterygian taxa (Near et al., 2012), lungfish-tetrapods and chondrichthyans-osteichthyans (Giles et al., 2017), and agnathans-gnathostomes (Kuraku and Kuratani, 2006).

(B) Exon-intron structure of *AMEL* and *SCPP5*. Separate boxes represent exons. Open areas in exons show 5′ and 3′ untranslated regions. The areas encoding the signal peptide and mature protein are shown in yellow and vermilion, respectively. Exon numbers are indicated for human *AMEL* (*AMELX*) and bichir *scpp5*. Locations encoding phospho-Ser residues (S*) (Kawasaki and Amemiya, 2014) and Pro-Xaa-Yaa (Xaa and Yaa represent any amino acids; PXY) repeats are illustrated within exon boxes. Regions encoding the three modules, the N-terminal aromatic residue-rich region (YY), the Pro/Gln-rich core region containing uninterrupted PXY repeats (P/Q), and the C-terminal hydrophilic region (DE), are indicated below exon boxes. Scale bar, 100 nucleotides (nt). See Figure S1A for details.

(Shellis and Miles, 1974; Sasagawa et al., 2013; Schultze, 2016). Tooth collar enameloid occurs in teleosts (Shellis and Miles, 1974; Sasagawa, 1988; Smith, 1995). Enameloid is also found on the dental and dermal skeleton in chondrichthyans (including acanthodians), as well as in extinct jawed and jawless stem-gnathostomes (Donoghue et al., 2006; Rücklin et al., 2011; Keating et al., 2015).

Enamel and enameloid matrix genes in sarcopterygians and actinopterygians

The amelogenin (*AMEL*), ameloblastin (*AMBN*), and enamelin (*ENAM*) genes encode the principal enamel matrix proteins (Fincham et al., 1999) in tetrapods (presumably also coelacanth [Kawasaki and Amemiya, 2014]), whereas *SCPP5* is thought to encode an enameloid matrix protein in *Fugu rubripes* (fugu) and *Danio rerio* (zebrafish) (Kawasaki et al., 2005, 2009). *AMEL* has been found only in sarcopterygians and *SCPP5* only in actinopterygians (Figure S1A) (Qu et al., 2015; Braasch et al., 2016; Kawasaki et al., 2017). *AMBN* and *ENAM* are also found in actinopterygians, including *Lepisosteus oculatus* (referred to below as "gar") and zebrafish (Figures S1B and S1C) (Braasch et al., 2016; Kawasaki et al., 2017). All four genes belong to the SCPP gene family that arose by gene duplication (Kawasaki and Weiss, 2003; Kawasaki et al., 2017). It is notable that no SCPP genes have been identified in chondrichthyans (Figure 1A) (Venkatesh et al., 2014; Enault et al., 2018).

We identified *amel* and *ambn* in *Lepidosiren paradoxa* (lungfish); *ambn*, *enam*, and *scpp5* in *Polypterus senegalus* (referred to below as "bichir") and various teleosts; and *ambn* in *Acipenser sinensis* (sturgeon; Figure S1); *AMEL* was not identified in actinopterygians. All three modules characteristic of tetrapod

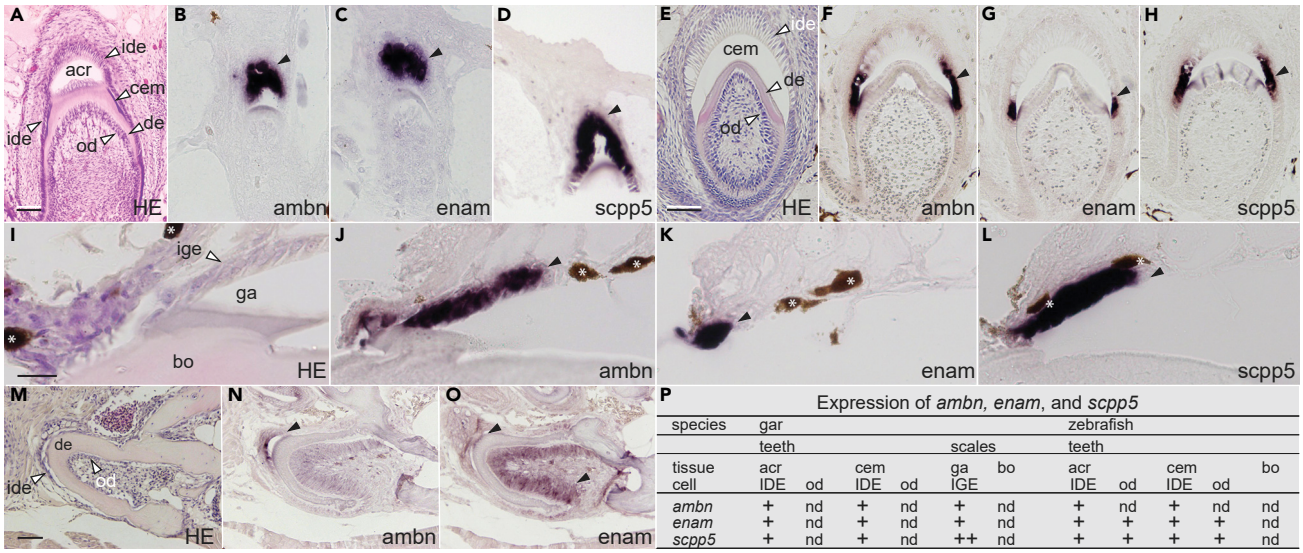

P

Expression of *ambn*, *enam*, and *scpp5*

species	gar						zebrafish				
	teeth				scales		teeth				
tissue	acr		cem		ga	bo	acr		cem		bo
cell	IDE	od	IDE	od	IGE		IDE	od	IDE	od	
ambn	+	nd	+	nd	+	nd	+	nd	+	nd	nd
enam	+	nd	+	nd	+	nd	+	+	+	+	nd
scpp5	+	nd	+	nd	++	nd	+	+	+	+	nd

Figure 2. Expression of *ambn*, *enam*, and *scpp5* in teeth and scales of gar and teeth of zebrafish

(A) Hematoxylin-eosin (H&E) staining of a developing gar tooth immediately after acrodin formation. Scale bar, 50 μm.

(B–D) Our *in situ* hybridization (ISH) analysis reveals expression of gar *ambn* (B), *enam* (C), and *scpp5* (D) in IDE cells during the matrix formation stage of acrodin formation (closed arrowheads).

(E) H&E staining of a developing gar tooth forming collar enamel. Scale bar, 50 μm.

(F–H) ISH analysis reveals expression of gar *ambn* (F), *enam* (G), and *scpp5* (H) in IDE cells during the secretory stage of collar enamel formation (closed arrowheads).

(I) H&E staining of a gar scale forming ganoin. Ganoin was lost during decalcification. Scale bar, 50 μm.

(J–L) ISH analysis reveals expression of gar *ambn* (J), *enam* (K), and *scpp5* (L) in IGE cells during the secretory stage of ganoin formation (closed arrowheads). Brown pigments are shown by asterisks.

(M) H&E staining of a developing zebrafish tooth. Scale bar, 50 μm.

(N and O) ISH analysis reveals expression of zebrafish *ambn* (N) in IDE cells (a closed arrowhead) and *enam* (O) in matrix-formation stage IDE cells and odontoblasts (closed arrowheads).

(P) Summary of matrix SCPP gene expression in mineralized tissues. In gar scales, relative expression levels were determined by RNA-seq analysis (Table S1) and the highest expression level of *scpp5* among all SCPP genes is shown as "++." Expression of zebrafish *scpp5* (Kawasaki et al., 2017) and stages of hypermineralized tissue formation in gar and teleosts were described previously (Sasagawa, 1995, 1997; Sasagawa and Ishiyama, 2005; Sasagawa et al., 2008, 2013). See Figure S2A for negative controls and more results. Abbreviations: acr, acrodin; bo, bone; cem, collar enamel; de, dentine; ga, ganoin; ide, inner dental epithelial cells; ige, inner ganoin epithelial cells; od, odontoblasts.

and coelacanth amelogenins (YY-, P/Q-, and DE-rich regions; Figures 1B and S1A) (Toyosawa et al., 1998; Fincham et al., 1999) were detected in proteins encoded by *amel* in *L. paradoxa* and *scpp5* in bichir and gar. Nevertheless, in most sarcopterygians these modules are encoded by five exons in *AMEL*, but twelve exons in bichir and gar *scpp5* genes (Figure 1B). Furthermore, *AMEL* differs from *SCPP5* in genomic location, exon-intron organization, and exons encoding phospho-Ser residues (Figure S1A). These data support interpretation independent origin of *AMEL* and *SCPP5*. Teleosts do not possess enamel, and their *scpp5* genes lack two of these three modules (P/Q and DE; Figures 1B and S1A).

Expression of *ambn*, *enam*, and *scpp5* in teeth and scales of gar and teeth of zebrafish

In gar, expression of *ambn*, *enam*, and *scpp5* was detected during tooth formation in IDE cells, initially during acrodin matrix formation (matrix formation stage of enameloid; Figures 2A–2D) and then during collar enamel matrix formation (secretory stage of enamel; Figures 2E–2H) (Sasagawa and Ishiyama, 2005; Sasagawa et al., 2008). During scale formation, expression of *ambn*, *enam*, and *scpp5* was detected in inner ganoin epithelial (IGE) cells that secrete the ganoin matrix on scales (secretory stage; Figures 2I–2L). We detected no other expression domains of these genes (Figure S2A). Given the limited expression domain of these genes in gar skin, their relative expression levels in IGE cells can be determined by RNA sequencing (RNA-seq) analysis of the skin (Qu et al., 2015; Braasch et al., 2016). Expression of *scpp5* was the highest among these genes and among all SCPP genes (Table S1).

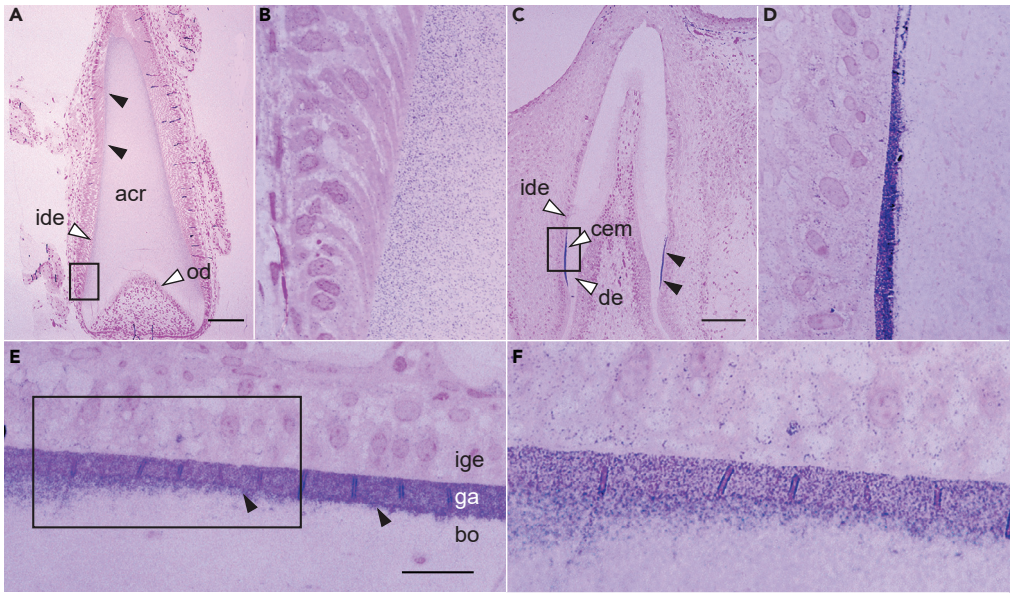

Figure 3. Distribution of gar Scpp5 in the matrix of teeth and scales detected using optical IHC analysis

(A–F) Optical IHC analysis of gar Scpp5 in acrodin (A and B) and collar enamel (C and D) in teeth, and ganoin in a scale (E and F). The rectangular region in (A), (C), and (E) is enlarged in (B), (D), and (F), respectively. IHC signals in (A), (C), and (E) are shown by closed arrowheads. Vertical lines in the ganoin layer (E and F) are artifacts of sectioning. See the legend of Figure 2 for abbreviations. Scale bar, 100 μm (A and C) or 20 μm (E). The contrast of these images was enhanced uniformly over the entire field (see Figure S2B for original images).

In zebrafish, expression of *ambn* and *enam* was detected in IDE cells in the matrix formation stages of acrodin and collar enameloid (Figures 2M–2O and S2A); *enam* was also expressed in odontoblasts, but we detected no significant expression of *enam* or *ambn* in bone cells (Figures 2N and 2O). Expression of *enam* in odontoblasts appears to initiate during acrodin matrix formation and continue throughout collar enameloid and dentine matrix formation (Figures 2O and S2A) (Shellis and Miles, 1974). Results of our expression analysis are summarized in Figure 2P.

Distribution of gar Scpp5 in acrodin and collar enamel on teeth and in ganoin on scales

The results of our *in situ* hybridization analysis for gar *scpp5* are consistent with the results of our immunohistochemical (IHC) analysis using an antibody raised against gar Scpp5. In the mineralization stage of acrodin formation, which begins after the matrix formation stage (Sasagawa and Ishiyama, 2005), high levels of Scpp5 were detected near the outer surface, decreasing toward the core, close to odontoblasts (Figures 3A and 3B). In the collar enamel matrix, Scpp5 was detected uniformly and strongly in the secretory stage, except in proximity to acrodin (Figures 3C and 3D), where Scpp5 was presumably absorbed by IDE cells that advanced to the maturation stage (Sasagawa et al., 2008). Scpp5 was also detected weakly in dentine along the border with collar enamel. In scales, Scpp5 was detected uniformly and strongly in the ganoin matrix in the secretory stage (Figure 3E) and underlying bone, decreasing immediately in a deeper region of the bone (Figure 3F).

Since our optical IHC analysis detected specific distributions of Scpp5 in the matrix of developing teeth and scales, we furthered IHC analysis using transmission electron microscopy (TEM). The results revealed an association of Scpp5 with the edge of collagen fibrils in the mineralization stage of acrodin formation (Figure 4A). In the developing collar enamel, Scpp5 was associated with electron-dense fibrils (Figure 4B) postulated to form as organic sheaths surrounding slender crystals (Warshawsky, 1989). Scpp5 was also detected in the underlying dentine near the border with collar enamel (Figure 4C), corroborating optical microscopic observations (Figure 3D). As in collar enamel, most Scpp5 signals in developing ganoin were associated with electron-dense fibrils (Figures 4D and 4E), especially along fibril edges, suggesting interactions of Scpp5 with minerals or mineral-associated organic molecules. Weak but significant signals

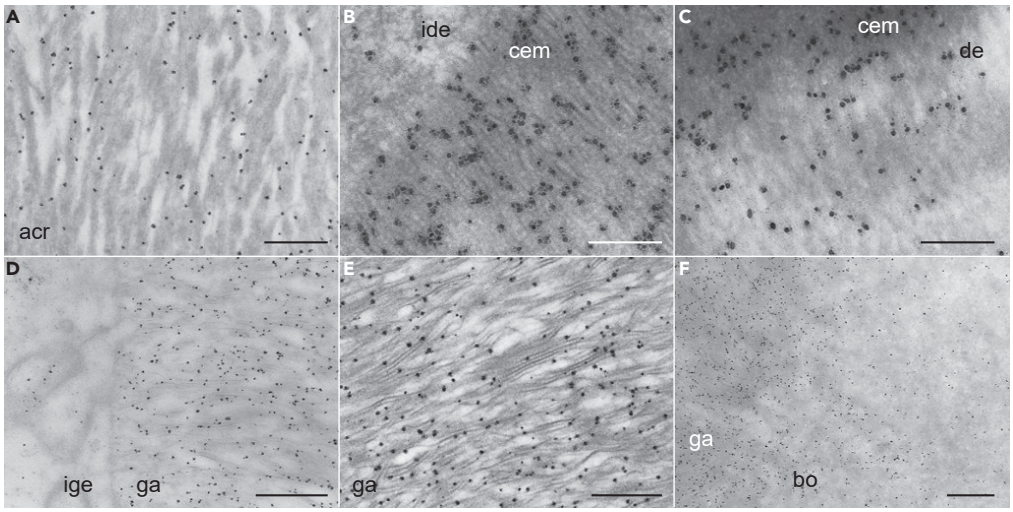

Figure 4. Distribution of gar Scpp5 in the matrix of teeth and scales detected using TEM IHC analysis

(A–F) TEM IHC analysis of gar Scpp5 in acrodin (A), collar enamel near IDE cells (B), collar enamel near dentine (C), ganoin near IGE cells (D), a middle portion of ganoin (E), and ganoin near bone (F). Dark dots show the distribution of Scpp5. Scale bar, 500 nm (A, D, E, and F) or 200 nm (B and C). See the legend of Figure 2 for abbreviations and Figure S2C for negative controls.

were also detected in bone underlying scale ganoin, but not in deeper regions (Figure 4F), as in dentine underlying collar enamel (Figure 4C).

Reconstructing ancestral states of hypermineralized tissues

We explored the evolution of acrodin, enameloid, enamel, and ganoin by reconstructing the ancestral states using data from living and fossil taxa (Table S2), stochastic character state mapping (Huelsenbeck et al., 2003), and phylogenetic hypotheses in which (1) *Guiyu*, *Achoania*, and *Psarolepis* (GAP clade) are constrained to stem-osteichthyans (King et al., 2017; Lu et al., 2017) and (2) these taxa are resolved as stem-sarcopterygians (Lu et al., 2016; Qiao et al., 2016; Choo et al., 2017) (Figures S3A and S3B).

Our results indicate that acrodin evolved in the actinopterygian stem-lineage (*Cheirolepis* and more crown-ward taxa); its presence in *Ligulalepis* is a consequence of convergence or the isolated tooth from which these data derive does not belong to *Ligulalepis* (Figures 5A, 5B, S3C, and S3D). Dental enameloid evolved late in the chondrichthyan stem-lineage (*Pucapampella* or more crown-ward taxa; Figures 5A, 5B, S3E, and S3F); the presence of dental enameloid in acanthodians is convergent. Dermal enameloid was resolved as primitive to the chondrichthyan total-group and, although it is also present in ostracoderms (Donoghue and Sansom, 2002; Keating et al., 2015), it is inferred absent from the dermal skeleton of stem-osteichthyans (Figures 5C, 5D, S3G, and S3H). Thus, dermal enameloid was lost in placoderms (Giles et al., 2013) and evolved convergently in stem-chondrichthyans after the divergence of *Ramirosuarezia* (Figures S3G and S3H). Taken together, these results suggest that, in both the dental and dermal skeletons, osteichthyan enameloid originated independently from chondrichthyan enameloid (but see below).

Our estimates of ancestral states were invariant to whether the GAP clade is resolved as stem-osteichthyan or stem-sarcopterygian (Figure 5). Dental enamel evolved early in the sarcopterygian stem-lineage (*Onychodus* and more crown-ward taxa), arising convergently as collar enamel in non-teleost actinopterygians (bichir and gar; Figures 5A, 5B, S3I, and S3J). Dermal enamel evolved deep in the osteichthyan stem-lineage (*Andreolepis* and more crown-ward taxa), was lost among early stem-actinopterygians (*Cheirolepis* and more crown-ward taxa), but retained in crown-sarcopterygians (Figures 5C, 5D, S3K, and S3L). Ganoin evolved among early stem-actinopterygians (*Cheirolepis* and more crown-ward taxa; Figures 5C, 5D, S3M, and S3N); the ganoin-like (Ørvig, 1978; Schultze, 2016) overlapping enamel in *Ligulalepis* (Schultze and Märss, 2004; Schultze, 2016) is resolved as convergent. If dermal enamel and ganoin are considered homologous, consistent with the expression patterns of *AMBN* and *ENAM* in both sarcopterygian enamel and gar ganoin, the ancestral tissue evolved deep in the osteichthyan-stem (*Andreolepis* and more crown-ward

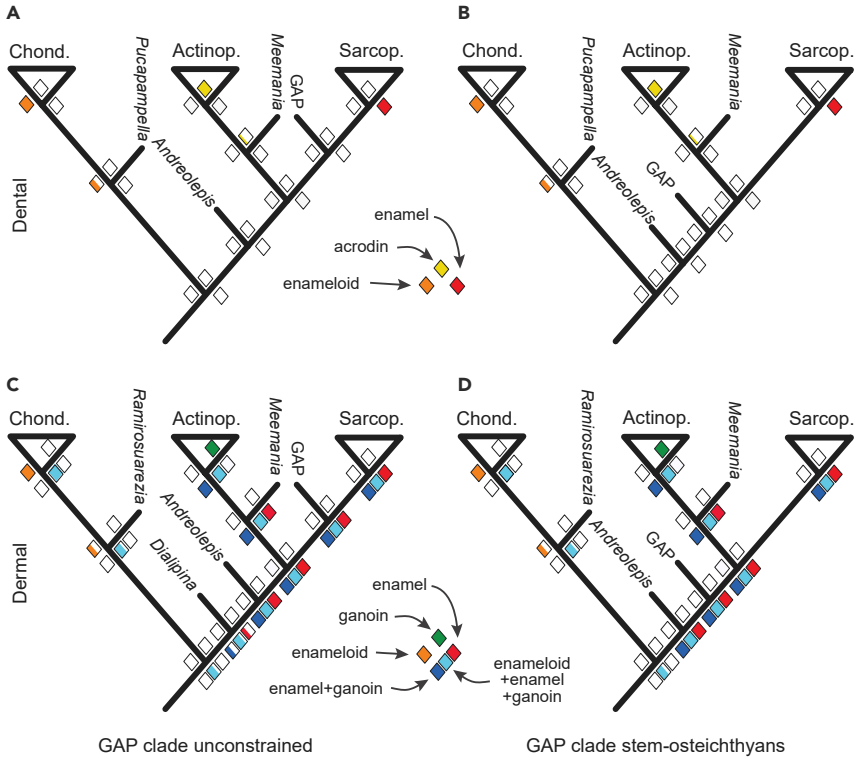

Figure 5. Reconstructing ancestral states of hypermineralized tissues

(A–D) Ancestral state reconstruction of the presence of hypermineralized tissues in the dental (A and B) and dermal (C and D) skeletons for trees, in which the GAP clade is resolved through unconstrained analysis to a stem-sarcopterygian affinity (A and C), or constrained to a stem-osteichthyan affinity (B and D). Diamonds at nodes express probability of the presence of a specific hypermineralized tissue, with the proportion of the color fill reflecting probability. The crown-chondrichthyans (Chond.), crown-actinopterygians (Actinop.), and crown-sarcopterygians (Sarcop.) are shown as triangles, and important stem taxa by bars (e.g., *Meemannia*). Tables S2 and S3 show data used to construct these trees.

taxa; Figures 5C, 5D, S3O, and S3P). Given the absence of SCPP genes in chondrichthyans, early enamel matrix SCPP genes likely evolved in concert with a prototypic enamel in stem-osteichthyans, from which true enamel and ganoin arose, respectively, in sarcopterygians and actinopterygians, as discussed below (Figure 1A).

Dermal enameloid is present in stem-gnathostomes, early members of placoderm plesia, and chondrichthyans (Giles et al., 2013). It has been hypothesized that enamel replaced enameloid through shifts in the timing of ameloblast and odontoblast activity (Smith, 1992, 1995). Ancestral state estimation provides support for this switch in a combined coding of dermal enamel, ganoin, and enameloid (Figures 5C, 5D, S3Q, and S3R). The initial enamel matrix SCPP gene may have originated in stem-gnathostomes and may have subsequently been lost in stem-chondrichthyans. As we discuss below, however, it is more likely that the enamel matrix SCPP genes are primitively absent from chondrichthyans and were never involved in dermal enameloid development. The origin of *AMBN* and *ENAM* in stem-osteichthyans may be invoked in the developmental evolution of enamel from an ancestral dermal enameloid (Donoghue and Sansom, 2002; Donoghue et al., 2006; Keating et al., 2015).

DISCUSSION

Similar formation of ganoin and collar enamel, and of acrodin and collar enameloid

We detected a similar expression pattern of gar *scpp5*, *ambn*, and *enam* in secretory-stage IGE cells and the uniform distribution of gar Scpp5 in the ganoin matrix (Figures 2J–2L, 3E, and 3F), which suggests that all these three genes encode ganoin matrix proteins. During collar enamel formation, expression of *scpp5*, *ambn*, and *enam* in IDE cells (Figures 2F–2H) and the uniform distribution of Scpp5 in the collar enamel

matrix (Figures 3C and 3D) were also detected. These results imply that ganoin and collar enamel form in a similar manner. Thus, collar enamel of gar is better described as collar ganoin, which corroborates the hypothesis obtained by histological studies of gars and many fossil actinopterygians (Ørvig, 1978; Schultze, 2016).

Acrodin forms below the basal lamina (BL) that originally separates odontoblasts from IDE cells (Smith, 1995). During acrodin formation in gar, odontoblasts retreat from the BL and secrete the bulk of the collagenous matrix (Sasagawa and Ishiyama, 2005), similar to dentine formation, while IDE cells secrete Scpp5, and presumably also Ambn and Enam, as suggested by the expression of *ambn* and *enam* in matrix formation-stage IDE cells. Thus, the region distal to the BL is formed principally by odontoblasts, whereas the contribution of IDE cells is large in the BL-proximal region (we observed the distribution of Scpp5 only near the outer surface; Figures 3A and 3B). This result suggests that gar acrodin forms as a dentine-ganoin composite, supporting the hypothesis for acrodin formation in teleosts (Shellis and Miles, 1974). Association of Scpp5 with collagen in the acrodin matrix during mineralization (Figure 4A) probably affects the mineralization and/or maturation processes, as previously inferred for teleosts (Shellis and Miles, 1974).

During acrodin formation in zebrafish, *ambn* and *enam* are expressed in IDE cells and *enam* are additionally expressed in odontoblasts. Similar to zebrafish *enam*, zebrafish and fugu *scpp5* genes are also expressed in both IDE cells and odontoblasts (Kawasaki et al., 2005; Kawasaki, 2009), unlike their gar orthologs (Figure 2P). Although the expression of these genes suggests conservation of acrodin in gar and zebrafish, expression of zebrafish *scpp5* and *enam* and fugu *scpp5* in odontoblasts implies a modification of acrodin. Because *ENAM* is expressed primarily in cells of epithelial origin during the formation of hypermineralized tissues in gar and sarcopterygians, the modification of acrodin is inferred to have occurred in teleosts. In zebrafish, a similar expression pattern of *ambn*, *enam*, and *scpp5* in IDE cells and odontoblasts was also detected during collar enameloid formation (Figure 2P) (Kawasaki, 2009). These results suggest that acrodin and collar enameloid form in a similar matrix in zebrafish and support the inference, obtained by studying various teleosts, that acrodin and collar enameloid are homologous, formed by both IDE cells and odontoblasts in a similar manner (Shellis and Miles, 1974; Sasagawa and Ishiyama, 1988).

Coevolution of hypermineralized tissues and SCPP genes

Our results suggest that enameloid evolved independently in chondrichthyans and actinopterygians. Although it is difficult to distinguish enameloid of chondrichthyans from enameloid of actinopterygians by histological characteristics (Reif, 1979), independent evolution of these tissues is supported by their different mineralization processes. In various actinopterygians, mineralization of enameloid initiates in matrix vesicles, and fine crystals accumulate along collagen fibrils, similar to mineralization of bone and dentine (Shellis and Miles, 1976; Sasagawa, 1988, 1997; Sasagawa et al., 2019). By contrast, mineralization of enameloid in various chondrichthyans begins in tubular vesicles, which are not found in osteichthyans, and no crystals concentrate along fibrillar structures (Sasagawa, 1998, 2002). The unique mineralization process of chondrichthyan enameloid reinforces the idea that this tissue evolved independently of SCPP genes (Kawasaki et al., 2017).

In gar, *scpp5* and presumably also *ambn* and *enam* encode ganoin matrix proteins, whereas *AMEL*, *AMBN*, and *ENAM* encode true enamel matrix proteins in sarcopterygians. The difference in matrix proteins of ganoin in gar and true enamel in sarcopterygians supports histological classification of true dental enamel in most stem- and crown-sarcopterygians and ganoin on scales in total-group actinopterygians (Qu et al., 2015). *AMEL* is found only in sarcopterygians; *SCPP5* only in actinopterygians (Figure S1). Gar *scpp5* shows the highest expression level among all SCPP genes in the skin during ganoin formation (Table S1), reminiscent of *AMEL* that encodes the most abundant enamel matrix protein (Fincham et al., 1999). Sarcopterygian *AMEL* genes and gar and bichir *scpp5* genes encode a similar modular structure, which is not encoded by *scpp5* in teleosts that do not possess enamel (Figure 1). Furthermore, expression of bichir *scpp5* was confirmed in the skin during ganoin formation (Figure S1A). These results suggest that sarcopterygian *AMEL* genes and gar and bichir *scpp5* genes have overlapping functions and that either *AMEL* or *scpp5* is sufficient for these overlapping functions during the formation of true enamel and ganoin. We thus assume that *AMEL* evolved in concert with true enamel and *SCPP5* evolved with ganoin.

Given the narrow expression domains and timings of *AMBN* and *ENAM*, similar spatiotemporal expression patterns of these genes during the formation of true enamel in sarcopterygians and ganoin in gar imply an

evolutionary relationship of these two tissues, rather than independent and coincidental employment of *AMBN* and *ENAM* in sarcopterygian true enamel and gar ganoin. Since sarcopterygians and gar phylogenetically bracket sarcopterygians and actinopterygians (Figure 1A) (Witmer, 1995), we hypothesize that both *AMBN* and *ENAM* were expressed during the formation of ancestral enamel (see below) in the most recent common ancestor of sarcopterygians and actinopterygians. The evolutionary relationship of true enamel and ganoin in gar and many fossil actinopterygians is supported by the common rod-like arrangement of crystallites, known as the protoprismatic microstructure (Ørvig, 1978; Smith, 1989; Sasagawa et al., 2016). A unique mineralization process of true enamel and ganoin in gar and bichir also supports their evolutionary relationship. During the formation of true enamel and ganoin, enamel ribbons form the mineralization front along the distal membrane of ameloblasts or IGE cells (Sire, 1995; Simmer et al., 2010). The close relationship of true enamel and ganoin suggests their homology: either one tissue derived from the other or both derived from an ancestral enamel.

Enamel and ganoin are considered homologous (Sire et al., 1987; Sasagawa et al., 2013; Qu et al., 2015), and the ancestral character estimation analysis assuming this (Figures 5C and 5D) is phylogenetically congruent, requiring an ancestral dermal hypermineralized tissue in stem-osteichthyans. Within the context of SCPP gene evolution, either *AMEL* or *SCPP5* was initially employed during the formation of an ancestral enamel in stem-osteichthyans; *SCPP5* was subsequently replaced by *AMEL* in sarcopterygians, or *AMEL* was replaced by *SCPP5* in actinopterygians. It is also conceivable, however, that *AMEL* arose in sarcopterygians and *SCPP5* in actinopterygians. Studies of gene-disrupted mice showed that both *AMBN* and *ENAM* are necessary for enamel ribbon formation, the unique mineralization process of enamel, whereas *AMEL* is not (Smith et al., 2016; Liang et al., 2019). Furthermore, a thin enamel can form in *AMEL*-deficient mice and in toothed whales that have deleterious mutations in *AMEL*, if both *AMBN* and *ENAM* are functional (Gibson et al., 2001; Kawasaki et al., 2020). These studies support the presence of ancestral enamel that formed enamel ribbons in a matrix containing AMBN and ENAM, but no AMEL or SCPP5. We hypothesize that both true enamel and ganoin originated from this ancestral enamel (Figures 1A and 5).

Dental acrodin arose with dermal ganoin among stem-actinopterygians. It was previously hypothesized that acrodin of teleosts is a composite of dentine and enamel (Shellis and Miles, 1974). Our observation of acrodin formation in gar confirms this hypothesis. Thus, acrodin evolution can be explained partly by early expression of ganoin matrix genes on the tooth cap during dentine formation, as previously suggested (Smith, 1992, 1995). Acrodin is similar in gar and zebrafish, but odontoblasts contribute more to acrodin formation in zebrafish by expressing *scpp5* and *enam*.

Ancestral state estimates suggest that dental enamel arose independently in stem-sarcopterygians and non-teleost actinopterygians. As we discussed above, collar enamel is better described as collar ganoin in gar and many fossil actinopterygians, which suggests that ganoin matrix gene expression on the tooth collar was critical to the evolution of collar enamel. Expression of *scpp5*, *ambn*, and *enam* during the formation of collar enamel in gar and collar enameloid in zebrafish suggests an evolutionary relationship of these two tissues and reinforces the previous hypothesis that the evolution of collar enameloid involved early expression of ganoin matrix genes during dentine formation (Smith, 1992, 1995). Consequently, collar enamel found in various non-teleost actinopterygians (Ørvig, 1978; Schultze, 2016) was replaced by collar enameloid in teleosts (Figure 1A). Enameloid is also found on teeth in larval urodeles (Assaraf-Weill et al., 2014; Berkovitz and Shellis, 2016), but in no other sarcopterygians (Figures S3C–S3F), indicating its independent origin in urodeles.

The results of our present study and previous studies using other methods and other species suggest that various hypermineralized tissues in modern osteichthyans can be classified genetically into true enamel, ganoin, and a diversity of enameloids; collar enamel, acrodin, and collar enameloid in actinopterygians are evolutionarily related to scale ganoin. A previous study supported the homology between ganoin and enamel largely based on the expression of gar *ambn* and *enam* in the skin (Qu et al., 2015); however, if acrodin and collar enameloid arose as a composite of dentine and ganoin, neither acrodin nor collar enameloid could be a ganoin homolog, even though *AMBN* and *ENAM* are expressed during formation. Our results show that orthologous SCPP gene expression may be insufficient to explain the differences between these tissues. The evolution of true enamel, ganoin, and enameloids can be better explained by various

changes of matrix SCPP genes, including spatiotemporal shifts in their expression. Hypermineralized tissues in osteichthyans appear to have coevolved with their matrix SCPP genes.

Limitations of the study

In extant actinopterygians, ganoin is found only in bichirs and gars. Although scales of bichirs consist of ganoin, dentine, and bone, scales of gars lack dentine. However, ganoin formation is similar in both clades (Sire, 1995), and bichir *ambn*, *enam*, and *scpp5* are presumably also expressed during scale and tooth formation in a manner similar to their gar orthologs. In teleosts, comprising ~30,000 species (Nelson et al., 2016), both acrodin and collar enameloid are found in various species. It was reported, however, that acrodin and collar enameloid of the common eel are covered with a hypermineralized layer formed by IDE cells, hence a type of enamel (Shellis and Miles, 1976). Although this layer remains to be confirmed, hypermineralized tissues may vary in some teleosts. Moreover, *ambn*, *enam*, and *scpp5* are all found in zebrafish and fugu (Figure S1), whereas *ambn* and/or *enam* were secondarily lost in some teleosts (Lv et al., 2017). The lack of these genes suggests modifications of acrodin and collar enameloid, or a loss of hypermineralized tissues. Examination of hypermineralized tissues in various teleosts would elucidate the evolution and adaptation of hypermineralized tissues in diverse teleosts.

Resource availability

Lead contact

Further information and requests for resources and reagents should be directed to and will be fulfilled by the Lead Contact, Kazuhiko Kawasaki (kuk2@psu.edu).

Materials availability

The anti-gar Scpp5 antibody generated in this study is available from the Lead Contact with a completed Materials Transfer Agreement.

Data and code availability

The nucleotide sequences generated during this study are available at GenBank (accession numbers: MG010658-MG010662).

METHODS

All methods can be found in the accompanying Transparent Methods supplemental file.

SUPPLEMENTAL INFORMATION

Supplemental Information can be found online at https://doi.org/10.1016/j.isci.2020.102023.

ACKNOWLEDGMENTS

K.K. is grateful to Prof. Joan T. Richtsmeier at Penn State University for critical reading of the manuscript. We acknowledge funding from the National Science Foundation (BCS0725227) and the Penn State Evan Pugh Professors Research Fund to Prof. Kenneth M. Weiss, from the European Commission Marie Curie scheme to M.W. (626424), from the Royal Commission for the Exhibition of 1851 (1851 Research Fellowship) to M.N.P., from a Royal Society Wolfson Merit Award to P.C.J.D., from the Natural Environment Research Council (NE/N002067/1; NE/P013678/1) to P.C.J.D., from the Biotechnology and Biological Sciences Research Council (BB/N000919/1) to P.C.J.D., from the Ministry of Education, Science, and Culture of Japan (Grant-in-Aid 18592013) to M.I., and from the Nippon Dental University to I.S. (NDUF-13-10, NDUF-14-12, and NDU Grants N-15015) and to M.I. (NDUF-10-04, NDUF-11-03, NDUF-14-07, NDUF-15-04, and NDU Grants N-17006).

AUTHOR CONTRIBUTIONS

Conceptualization, K.K., P.C.J.D., and M.I.; Investigation, all authors; Writing and Supervision, K.K. and P.C.J.D.

DECLARATION OF INTERESTS

The authors declare no competing interests.

Received: September 7, 2020
Revised: November 14, 2020
Accepted: December 29, 2020
Published: January 22, 2021

REFERENCES

Assaraf-Weill, N., Gasse, B., Silvent, J., Bardet, C., Sire, J.Y., and Davit-Beal, T. (2014). Ameloblasts express type I collagen during amelogenesis. J. Dent. Res. *93*, 502–507.

Berkovitz, B., and Shellis, R.P. (2016). The Teeth of Non-mammalian Vertebrates (Academic Press).

Braasch, I., Gehrke, A.R., Smith, J.J., Kawasaki, K., Manousaki, T., Pasquier, J., Amores, A., Desvignes, T., Batzel, P., Catchen, J., et al. (2016). The spotted gar genome illuminates vertebrate evolution and facilitates human-teleost comparisons. Nat. Genet. *48*, 427–437.

Choo, B., Zhu, M., Qu, Q., Yu, X., Jia, L., and Zhao, W. (2017). A new osteichthyan from the late Silurian of Yunnan, China. PLoS One *12*, e0170929.

Donoghue, P.C.J., and Keating, J.N. (2014). Early vertebrate evolution. Palaeontology *57*, 879–893.

Donoghue, P.C.J., and Sansom, I.J. (2002). Origin and early evolution of vertebrate skeletonization. Microsc. Res. Tech. *59*, 352–372.

Donoghue, P.C.J., Sansom, I.J., and Downs, J.P. (2006). Early evolution of vertebrate skeletal tissues and cellular interactions, and the canalization of skeletal development. J. Exp. Zool. B Mol. Dev. Evol. *306*, 278–294.

Enault, S., Munoz, D., Simion, P., Venteo, S., Sire, J.-Y., Marcellini, S., and Debiais-Thibaud, M. (2018). Evolution of dental tissue mineralization: an analysis of the jawed vertebrate *SPARC* and *SPARC-L* families. BMC Evol. Biol. *18*, 127.

Fincham, A.G., Moradian-Oldak, J., and Simmer, J.P. (1999). The structural biology of the developing dental enamel matrix. J. Struct. Biol. *126*, 270–299.

Friedman, M., and Brazeau, M.D. (2010). A reappraisal of the origin and basal radiation of the Osteichthyes. J. Vertebr. Paleontol. *30*, 36–56.

Gibson, C.W., Yuan, Z.A., Hall, B., Longenecker, G., Chen, E., Thyagarajan, T., Sreenath, T., Wright, J.T., Decker, S., Piddington, R., et al. (2001). Amelogenin-deficient mice display an amelogenesis imperfecta phenotype. J. Biol. Chem. *276*, 31871–31875.

Giles, S., Rücklin, M., and Donoghue, P.C.J. (2013). Histology of "placoderm" dermal skeletons: implications for the nature of the ancestral gnathostome. J. Morphol. *274*, 627–644.

Giles, S., Xu, G.H., Near, T.J., and Friedman, M. (2017). Early members of 'living fossil' lineage imply later origin of modern ray-finned fishes. Nature *549*, 265–268.

Hall, B.K. (2015). Bones and Cartilage (Elsevier).

Hedges, S.B., and Kumar, S. (2009). The Time Tree of Life (Oxford University Press).

Huelsenbeck, J.P., Nielsen, R., and Bollback, J.P. (2003). Stochastic mapping of morphological characters. Syst. Biol. *52*, 131–158.

Ishiyama, M., Inage, T., and Shimokawa, H. (1999). An immunocytochemical study of amelogenin proteins in the developing tooth enamel of the gar-pike, *Lepisosteus oculatus* (Holostei, Actinopterygii). Arch. Histol. Cytol. *62*, 191–197.

Kawasaki, K. (2009). The SCPP gene repertoire in bony vertebrates and graded differences in mineralized tissues. Dev. Genes Evol. *219*, 147–157.

Kawasaki, K., and Amemiya, C.T. (2014). SCPP genes in the coelacanth: tissue mineralization genes shared by sarcopterygians. J. Exp. Zool. B Mol. Dev. Evol. *322*, 390–402.

Kawasaki, K., Buchanan, A.V., and Weiss, K.M. (2009). Biomineralization in humans: making the hard choices in life. Annu. Rev. Genet. *43*, 119–142.

Kawasaki, K., Mikami, M., Goto, M., Shindo, J., Amano, M., and Ishiyama, M. (2020). The evolution of unusually small amelogenin genes in cetaceans; pseudogenization, X-Y gene conversion, and feeding strategy. J. Mol. Evol. *88*, 122–135.

Kawasaki, K., Mikami, M., Nakatomi, M., Braasch, I., Batzel, P., J, H.P., Sato, A., Sasagawa, I., and Ishiyama, M. (2017). SCPP genes and their relatives in gar: rapid expansion of mineralization genes in osteichthyans. J. Exp. Zool. B Mol. Dev. Evol. *328*, 645–665.

Kawasaki, K., Suzuki, T., and Weiss, K.M. (2005). Phenogenetic drift in evolution: the changing genetic basis of vertebrate teeth. Proc. Natl. Acad. Sci. U S A *102*, 18063–18068.

Kawasaki, K., and Weiss, K.M. (2003). Mineralized tissue and vertebrate evolution: the secretory calcium-binding phosphoprotein gene cluster. Proc. Natl. Acad. Sci. U S A *100*, 4060–4065.

Keating, J.N., Marquart, C.L., and Donoghue, P.C. (2015). Histology of the heterostracan dermal skeleton: insight into the origin of the vertebrate mineralised skeleton. J. Morphol. *276*, 657–680.

King, B., Qiao, T., Lee, M.S.Y., Zhu, M., and Long, J.A. (2017). Bayesian morphological clock methods resurrect placoderm monophyly and reveal rapid early evolution in jawed vertebrates. Syst. Biol. *66*, 499–516.

Kuraku, S., and Kuratani, S. (2006). Time scale for cyclostome evolution inferred with a phylogenetic diagnosis of hagfish and lamprey cDNA sequences. Zool. Sci. *23*, 1053–1064.

Liang, T., Hu, Y., Smith, C.E., Richardson, A.S., Zhang, H., Yang, J., Lin, B., Wang, S.K., Kim, J.W., Chun, Y.H., et al. (2019). *AMBN* mutations causing hypoplastic amelogenesis imperfecta and *Ambn* knockout-NLS-lacZ knockin mice exhibiting failed amelogenesis and *Ambn* tissue-specificity. Mol. Genet. Genom. Med. *7*, e929.

Lu, J., Giles, S., Friedman, M., den Blaauwen, J.L., and Zhu, M. (2016). The oldest actinopterygian highlights the cryptic early history of the hyperdiverse ray-finned fishes. Curr. Biol. *26*, 1602–1608.

Lu, J., Giles, S., Friedman, M., and Zhu, M. (2017). A new stem sarcopterygian illuminates patterns of character evolution in early bony fishes. Nat. Commun. *8*, 1932.

Lv, Y., Kawasaki, K., Li, J., Li, Y., Bian, C., Huang, Y., You, X., and Shi, Q. (2017). A genomic survey of SCPP family genes in fishes provides novel insights into the evolution of fish scales. Int. J. Mol. Sci. *18*, 2432.

Near, T.J., Eytan, R.I., Dornburg, A., Kuhn, K.L., Moore, J.A., Davis, M.P., Wainwright, P.C., Friedman, M., and Smith, W.L. (2012). Resolution of ray-finned fish phylogeny and timing of diversification. Proc. Natl. Acad. Sci. U S A *109*, 13698–13703.

Nelson, J.S., Grande, T.C., and Wilson, M.V.H. (2016). Fishes of the World (Wiley).

Ørvig, T. (1978). Microstructure and growth of dermal skeleton in fossil actinopterygian fishes - *Birgeria* and *Scanilepis*. Zool. Scr. *7*, 33–56.

Poole, D.F.G. (1967). Phylogeny of tooth tissues: enameloid and enamel in recent vertebrates, with a note on the history of cementum. In Structural and Chemical Organization of Teeth, A.E.W. Miles, ed. (Academic Press), pp. 111–149.

Qiao, T., King, B., Long, J.A., Ahlberg, P.E., and Zhu, M. (2016). Early gnathostome phylogeny revisited: multiple method consensus. PLoS One *11*, e0163157.

Qu, Q., Haitina, T., Zhu, M., and Ahlberg, P.E. (2015). New genomic and fossil data illuminate the origin of enamel. Nature *526*, 108–111.

Reif, W.-E. (1979). Structural convergences between enameloid of actinopterygian teeth and of shark teeth. Scan. Electron. Micros. *II*, 547–554.

Rücklin, M., Giles, S., Janvier, P., and Donoghue, P.C. (2011). Teeth before jaws? Comparative analysis of the structure and development of the external and internal scales in the extinct jawless vertebrate *Loganellia scotica*. Evol. Dev. *13*, 523–532.

Sasagawa, I. (1988). The appearance of matrix vesicles and mineralization during tooth development in three teleost fishes with well-

developed enameloid and orthodentine. Arch. Oral Biol. *33*, 75–86.

Sasagawa, I. (1997). Fine structure of the cap enameloid and of the dental epithelial cells during enameloid mineralisation and early maturation stages in the tilapia, a teleost. J. Anat. *190* (Pt 4), 589–600.

Sasagawa, I. (1995). Fine structure of tooth germs during the formation of enameloid matrix in *Tilapia nilotica*, a teleost fish. Arch. Oral Biol. *40*, 801–814.

Sasagawa, I. (1998). Mechanisms of mineralization in the enameloid of elasmobranchs and teleosts. Connect. Tissue Res. *39*, 207–214, discussion 221-225.

Sasagawa, I. (2002). Mineralization patterns in elasmobranch fish. Microsc. Res. Tech. *59*, 396–407.

Sasagawa, I., and Ishiyama, M. (2005). Fine structural and cytochemical mapping of enamel organ during the enameloid formation stages in gars, *Lepisosteus oculatus*, Actinopterygii. Arch. Oral Biol. *50*, 373–391.

Sasagawa, I., and Ishiyama, M. (1988). The structure and development of the collar enameloid in two teleost fishes, *Halichoeres poecilopterus* and *Pagrus major*. Anat. Embryol. (Berl.) *178*, 499–511.

Sasagawa, I., Ishiyama, M., Yokosuka, H., and Mikami, M. (2008). Fine structure and development of the collar enamel in gars, *Lepisosteus oculatus*, Actinopterygii. Front. Mater. Sci. China *2*, 134–142.

Sasagawa, I., Ishiyama, M., Yokosuka, H., and Mikami, M. (2013). Teeth and ganoid scales in *Polypterus* and *Lepisosteus*, the basic actinopterygian fish: an approach to understand the origin of the tooth enamel. J. Oral Biosci. *55*, 76–84.

Sasagawa, I., Ishiyama, M., Yokosuka, H., Mikami, M., Oka, S., Shimokawa, H., and Uchida, T. (2019). Immunolocalization of enamel matrix protein-like proteins in the tooth enameloid of spotted gar, *Lepisosteus oculatus*, an actinopterygian bony fish. Connect. Tissue Res. *60*, 291–303.

Sasagawa, I., Oka, S., Mikami, M., Yokosuka, H., Ishiyama, M., Imai, A., Shimokawa, H., and Uchida, T. (2016). Immunohistochemical and Western blotting analyses of ganoine in the ganoid scales of *Lepisosteus oculatus*: an actinopterygian fish. J. Exp. Zool. B Mol. Dev. Evol. *326*, 193–209.

Schultze, H.-P. (2016). Scales, enamel, cosmine, ganoine, and early osteichthyans. C. R. Palevol. *15*, 83–102.

Schultze, H.-P., and Märss, T. (2004). Revisiting *Lophosteus*, a primitive osteichthyan. Acta Univ. Latv. *679*, 57–78.

Shellis, R.P., and Miles, A.E.W. (1974). Autoradiographic study of formation of enameloid and dentin matrices in teleost fishes using tritiated amino-acids. Proc. R. Soc. Lond. B. *185*, 51–72.

Shellis, R.P., and Miles, A.E.W. (1976). Observations with electron microscope on enameloid formation in common eel (*Anguilla anguilla*; Teleostei). Proc. R. Soc. Lond. B. *194*, 253–269.

Simmer, J.P., Papagerakis, P., Smith, C.E., Fisher, D.C., Rountrey, A.N., Zheng, L., and Hu, J.C. (2010). Regulation of dental enamel shape and hardness. J. Dent. Res. *89*, 1024–1038.

Sire, J.Y. (1995). Ganoine formation in the scales of primitive actinopterygian fishes, lepisosteids and polypterids. Connect. Tissue Res. *33*, 213–222.

Sire, J.Y., Donoghue, P.C., and Vickaryous, M.K. (2009). Origin and evolution of the integumentary skeleton in non-tetrapod vertebrates. J. Anat. *214*, 409–440.

Sire, J.Y., Geraudie, J., Meunier, F.J., and Zylberberg, L. (1987). On the origin of ganoine: histological and ultrastructural data on the experimental regeneration of the scales of *Calamoichthys calabaricus* (Osteichthyes, Brachyopterygii, Polypteridae). Am. J. Anat. *180*, 391–402.

Smith, C.E., Hu, Y., Hu, J.C., and Simmer, J.P. (2016). Ultrastructure of early amelogenesis in wild-type, *Amelx*$^{(-/-)}$, and *Enam*$^{(-/-)}$ mice: enamel ribbon initiation on dentin mineral and ribbon orientation by ameloblasts. Mol. Genet. Genom. Med. *4*, 662–683.

Smith, M.M. (1989). Distribution and variaion in enamel structure in the oral teeth of sarcopterygians: its significance for the evolution of a protoprismatic enamel. Hist. Biol. *3*, 97–126.

Smith, M.M. (1995). Heterochrony in the evolution of enamel in vertebrates. In Evolutionary Change and Heterochrony, K.J. McNamara, ed. (John Wiley & Sons), pp. 125–150.

Smith, M.M. (1992). Microstructure and evolution of enamel amongst osteichthyan fishes and early tetrapods. In Structure, Function, and Evolution of Teeth, P. Smith and E. Tchernov, eds. (Freund Publishing House), pp. 73–101.

Toyosawa, S., O'HUigin, C., Figueroa, F., Tichy, H., and Klein, J. (1998). Identification and characterization of amelogenin genes in monotremes, reptiles, and amphibians. Proc. Natl. Acad. Sci. U S A *95*, 13056–13061.

Venkatesh, B., Lee, A.P., Ravi, V., Maurya, A.K., Lian, M.M., Swann, J.B., Ohta, Y., Flajnik, M.F., Sutoh, Y., Kasahara, M., et al. (2014). Elephant shark genome provides unique insights into gnathostome evolution. Nature *505*, 174–179.

Warshawsky, H. (1989). Organization of crystals in enamel. Anat. Rec. *224*, 242–262.

Witmer, L.M. (1995). The extant phylogeny bracket and the importance of reconstructing soft tissues in fossils. In Functional Morphology in Vertebrate Paleontology, J.J. Thompson, ed. (Cambridge University Press), pp. 19–33.

iScience, Volume *24*

Supplemental Information

Coevolution of enamel, ganoin, enameloid, and their matrix SCPP genes in osteichthyans

Kazuhiko Kawasaki, Joseph N. Keating, Mitsushiro Nakatomi, Monique Welten, Masato Mikami, Ichiro Sasagawa, Mark N. Puttick, Philip C.J. Donoghue, and Mikio Ishiyama

A

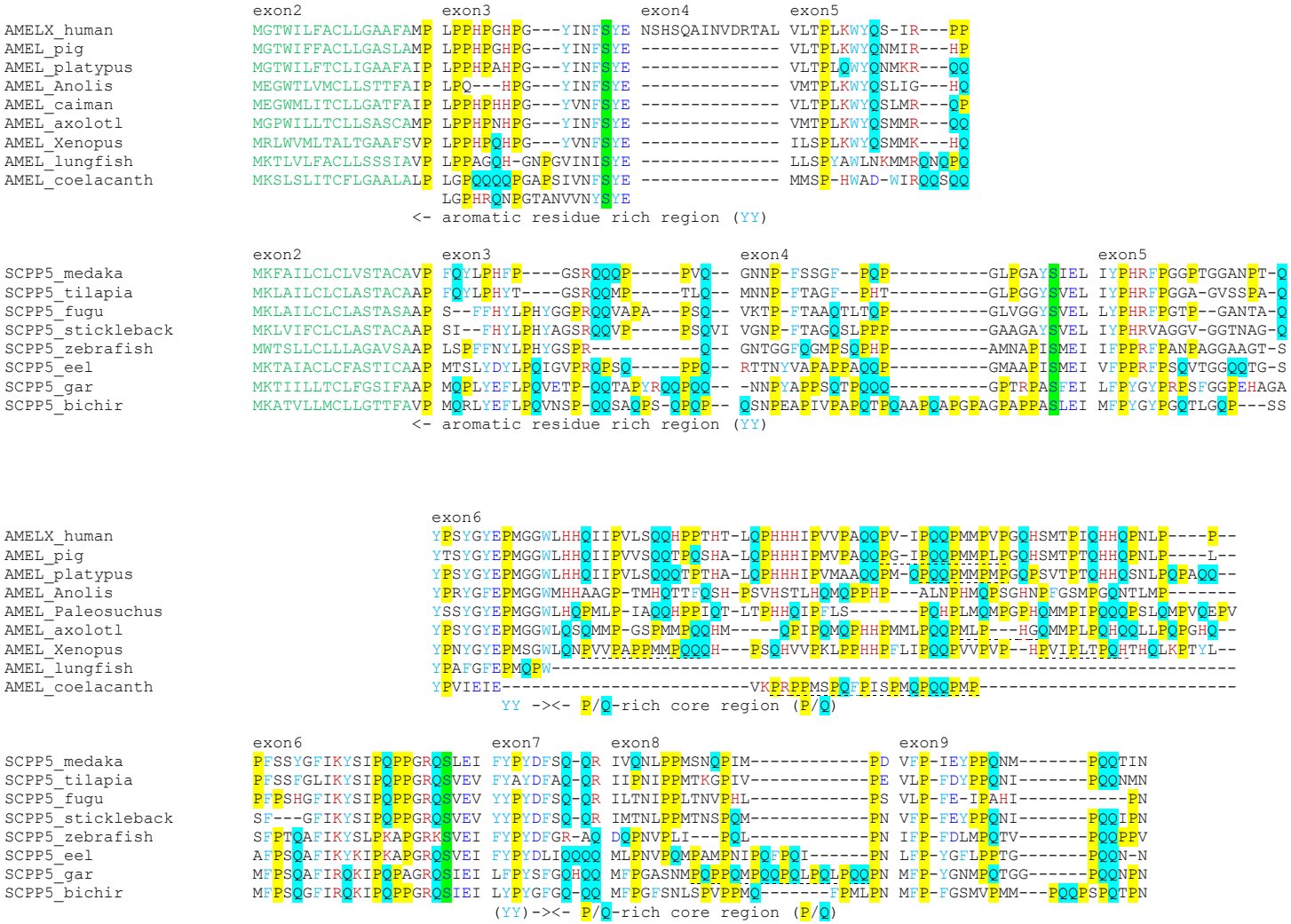
exon2
exon3
exon4
exon5
AMELX_human MGTWILFACLLGAAFAMP LPPHPGHPG---YINFSYE NSHSQAINVDRTAL VLTPLKWYQS-IR---PP
AMEL_pig MGTWIFFACLLGASLAMP LPPHPGHPG---YINFSYE -------------- VLTPLKWYQNMIR---HP
AMEL_platypus MGTWILFTCLIGAAFAIP LPPHPAHPG---YINFSYE -------------- VLTPLQWYQNMKR---QQ
AMEL_Anolis MEGWTLVMCLLSTTFAIP LPQ---HPG---YINFSYE -------------- VMTPLKWYQSLIG---HQ
AMEL_caiman MEGWMLITCLLGATFAIP LPPHPHHPG---YVNFSYE -------------- VLTPLKWYQSLMR---QP
AMEL_axolotl MGPWILLTCLLSASCAMP LPPHPNHPG---YINFSYE -------------- VMTPLKWYQSMMR---QQ
AMEL_Xenopus MRLWVMLTALTGAAFSVP LPPHPQHPG---YVNFSYE -------------- ILSPLKWYQSMMK---HQ
AMEL_lungfish MKTLVLFACLLSSSIAVP LPPAGQH-GNPGVINISYE -------------- LLSPYAWLNKMMRQNQPQ
AMEL_coelacanth MKSLSLITCFLGAALALP LGPQQQQQPGAPSIVNFSYE -------------- MMSP-HWAD-WIRQQSQQ
LGPHRQNPGTANVVNYSYE
<- aromatic residue rich region (YY)
exon2
exon3
exon4
exon5
SCPP5_medaka MKFAILCLCLVSTACAVP FQYLPHFP----GSRQQQP-----PVQ-- GNNP-FSSGF--PQP----------GLPGAYSIEL IYPHRFPGGPTGGANPT-Q
SCPP5_tilapia MKLAILCLCLASTACAAP FQYLPHYT----GSRQQMP-----TLQ-- MNNP-FTAGF--PHT----------GLPGGYSVEL IYPHRFPGGA-GVSSPA-Q
SCPP5_fugu MKLAILCLCLASTASAAP S--FFHYLPHYGGPRQQVAPA---PSQ-- VKTP-FTAAQTLTQP----------GLVGGYSVEL LYPHRFPGTP--GANTA-Q
SCPP5_stickleback MKLVIFCLCLASTACAAP SI--FHYLPHYAGSRQQVP-----PSQVI VGNP-FTAGQSLPPP----------GAAGAYSVEL IYPHRVAGGV-GGTNAG-Q
SCPP5_zebrafish MWTSLLCLLLAGAVSAAP LSPFFNYLPHYGSPR----------Q-- GNTGGFQGMPSQPHP----------AMNAPISMEI IFPPRFPANPAGGAAGT-S
SCPP5_eel MKTAIACLCFASTICAAP MTSLYDYLPQIGVPRQPSQ-----PPQ-- RTTNYVAPAPPAQQP----------GMAAPISMEI VFPPRFPSQVTGGQQTG-S
SCPP5_gar MKTIILLTCLFGSIFAAP MQPLYEFLPQVETP-QQTAPYRQQPQQ-- -NNPYAPPSQTPQQQ----------GPTRPASFEI LFPYGYPRPSFGGPEHAGA
SCPP5_bichir MKATVLLMCLLGTTFAVP MQRLYEFLPQVNSP-QQSAQPS-QPQP-- QSNPEAPIVPAPQTPQAAPQAPGPAGPAPPASLEI MFPYGYPGQTLGQP---SS
<- aromatic residue rich region (YY)
exon6
AMELX_human YPSYGYEPMGGWLHHQIIPVLSQQHPPTHT-LQPHHHIPVVPAQQPV-IPQQPMMPVPGQHSMTPIQHHQPNLP----P--
AMEL_pig YTSYGYEPMGGWLHHQIIPVVSQQTPQSHA-LQPHHHIPMVPAQQPG-IPQQPMMPLPGQHSMTPTQHHQPNLP----L--
AMEL_platypus YPSYGYEPMGGWLHHQIIPVLSQQQTPTHA-LQPHHHIPVMAAQQPM-QPQQPMMPMPGQPSVTPTQHHQSNLPQPAQQ--
AMEL_Anolis YPRYGFEPMGGWMHHAAGP-TMHQTTFQSH-PSVHSTLHQMQPPHP---ALNPHMQPSGHNPFGSMPGQNTLMP-------
AMEL_Paleosuchus YSSYGYEPMGGWLHQPMLP-IAQQHPPIQT-LTPHHQIPFLS-------PQHPLMQMPGPHQMMPIPQQQPSLQMPVQEPV
AMEL_axolotl YPSYGYEPMGGWLQSQMMP-GSPMMPQQQHM-----QPIPQMQPHHPMMLPQQPMLP---HGQMMPLPQHQQLLPQPGHQ--
AMEL_Xenopus YPNYGYEPMSGWLQNPVVPAPPMMPQQQH---PSQHVVPKLPPHHPFLIPQQPVVPVP--HPVIPLTPQHTHQLKPTYL--
AMEL_lungfish YPAFGFEPMQPW----------
AMEL_coelacanth YPVIEIE----------VKPRPPMSPQFPISPMQPQQPMP----------
YY -><- P/Q-rich core region (P/Q)
exon6
exon7
exon8
exon9
SCPP5_medaka PFSSYGFIKYSIPQPPGRQSLEI FYPYDFSQ-QR IVQNLPPMSNQPIM----------PD VFP-IEYPPQNM-------PQQTIN
SCPP5_tilapia PFSSFGLIKYSIPQPPGRQSVEV FYAYDFAQ-QR IIPNIPPMTKGPIV----------PE VLP-FDYPPQNI-------PQQNMN
SCPP5_fugu PFPSHGFIKYSIPQPPGRQSVEV YYPYDFSQ-QR ILTNIPPLTNVPHL----------PS VLP-FE-IPAHI----------PN
SCPP5_stickleback SF---GFIKYSIPQPPGRQSVEV YYPYDFSQ-QR IMTNLPPMTNSPQM----------PN VFP-FEYPPQNI-------PQQIPN
SCPP5_zebrafish SFPTQAFIKYSLPKAPGRKSVEI FYPYDFGR-AQ DQPNVPLI---PQL----------PN IFP-FDLMPQTV-------PQQPPV
SCPP5_eel AFPSQAFIKYKIPKAPGRQSVEI FYPYDLIQQQQ MLPNVPQMPAMPNIPQFPQI------PN LFP-YGFLPPTG-------PQQN-N
SCPP5_gar MFPSQAFIRQKIPQPAGRQSIEI LFPYSFGQHQQ MFPGASNMPQPPQMPQQPQLPQLPQQPN MFP-YGNMPQTGG------PQQNPN
SCPP5_bichir MFPSQGFIRQKIPQPPGRQSIEI LYPYGFGQ-QQ MFPGFSNLSPVPPMQ-------FPMLPN MFP-FGSMVPMM---PQQPSPQTPN
(YY)-><- P/Q-rich core region (P/Q)

```
A (continued)
                                                                                     (exon6 continued)                                                                                   exon7
AMELX_human                                                                          --------PAQQPYQPQPVQPQPHQPMQPQPPVHPMQPLPPQPPLPPMFPM-QPLPPMLPDLTLEAWPSTDKTKREEV D
AMEL_pig                                                                             --------PAQQPFQPQPVQPQPHQPLQPQSPMHPIQPLLPQPPLPPMFSM-Q---SLLPDLPLEAWPATDKTKREEV D
AMEL_platypus                                                                        ------------PFQPQVPQQPPHQPIQPQAPAHPMPPM-PQPPLPPMFPM-QPLPPLLPDLPLEQWPATDKTKREEV D
AMEL_Anolis                                                                          QFQ-PAHGGPIHHPFQPHAGEHPMHPQQTGNPVHPMHPQQPANPNSPIYPV-QQLPPLISDTPLESWPPADKTKQEEV D
AMEL_Paleosuchus                                                                     QPQAGEHPSPPVQPQQPGHPNPPMQPQLPGSPHPPMRPQQPGIPNPPMYPM-QPLPPLLPDMPLEPWRPMDKTKQEEI D
AMEL_axolotl                                                                         -------------PMQPMIPQQPSHVLQTAQANHPLQPHQPQHSGQPIYPVQQQQPPLLPDMPLEPWQPADKTNQEEQ D
AMEL_Xenopus                                                                         ---------------------SNPDSANTQPLEPFKPDHENKNGHPMFPL-QPLPPLFEERPQEPWQAAGNTNQEEL D
AMEL_lungfish                                                                        -------------PQQPFHPVQ-QGPQ-PAIPQIPGMPVMPQHPMFPTWVQEVEHVIPAQQQP-DQQQPN-QQAQQEL D
AMEL_coelacanth                                                                      -------PQYPMQPMQPQYSMQPQFPVQPQFAVQPPAPQQPVAPVEPIFP--WIQGMQQQQQPT-------KKTEKEQ D
                                                                                                                                                             P/Q -><- hydrophilic C-terminus (DE)

                                                                                        exon10                                           exon 11
SCPP5_medaka        ------------------------- ------------------------- KPT-SDAKAVPSQDP----------LQSLLQNKPTQASQ VHPKV-----
SCPP5_tilapia       ------------------------- ------------------------- IPQ-FDANALPSQDP----------PKLHLQDQPIQTSQ MPAKV-----
SCPP5_fugu          ------------------------- ------------------------- VAV-FDSP-PPSQDP----------LPPLQQDQPTQTSQ VPAKV-----
SCPP5_stickleback   ------------------------- ------------------------- IPS-FNPNALPSQDP----------MQPLQQDQPIQTSQ MPAKV-----
SCPP5_zebrafish     ------------------------- ------------------------- NPP-FQDGAPQTQEPQQQTQ---PEQQQQQQQQQAQTGQ VSTRP-----
SCPP5_eel           ------------------------- ------------------------- MFPSFGVQQQLPQEPVQAQQ---PAQSSQPAQPAQAGLN GPAAP-----
SCPP5_gar           VFHGFGNVP---------------PN LFPSFGNLPHL-----------PPN FIPNFGIPQPVPQEPTQPVQPVQPVQPVQPVQPVQPSQN TPV---EEQD
SCPP5_bichir        LPPSFGNM-------PQQPGQSDPN MFNPFANMPQL--------PAQNPN GVPNFGM----------PQDPSQPMQPAQPIPPVQPSPN IPVGGEQEVD
                                                                                                                 P/Q-><- hydrophilic C-terminus (DE)
```

Chromosomal locations of *AMEL* and *SCPP5*.

	ARHGAP6	*AMEL*	P/Q-rich SCPP genes	*SCPP5*
Homo sapiens	X	X, Y	4	ND
Anolis carolinensis	3	3	2, 5	ND
Xenopus tropicalis	2	2	1	ND
Latimeria chalumnae	JH126997	JH126997	JH128739, JH128762, JH129486	ND
Lepisosteus oculatus	17	ND	2, 4, 22	4
Danio rerio	7	ND	1, 5, 10, 23	1
Fugu rubripes	1	ND	17	17

Expression of bichir *scpp5* in the jaw and skin, detected by RT-PCR.

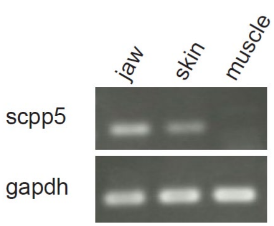

B


exon2
exon3
exon4
AMBN_human
AMBN_platypus
AMBN_caiman
AMBN_Anolis
AMBN_Xenopus
AMBN_lungfish
AMBN_coelacanth
AMBN_bichir
AMBN_sturgeon
AMBN_gar
AMBN_zebrafish
AMBN_medaka
AMBN_tilapia
AMBN_fugu
exon5
exon6

B (continued)

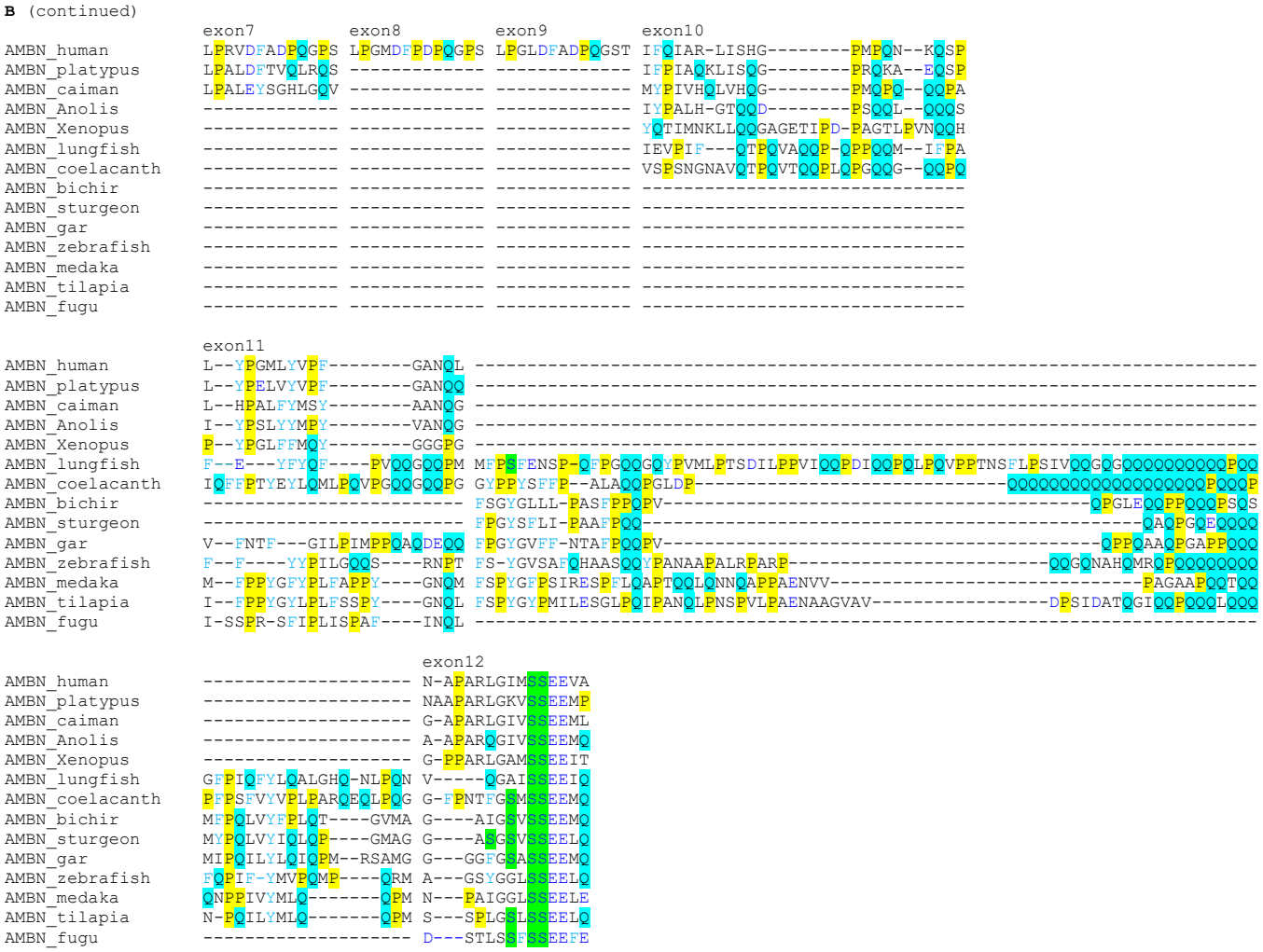
exon7 exon8 exon9 exon10
AMBN_human LPRVDFADPQGPS LPGMDFPDPQGPS LPGLDFADPQGST IFQIAR-LISHG--------PMPQN--KQSP
AMBN_platypus LPALDFTVQLRQS ------------ ------------ IFPIAQKLISQG--------PRQKA--EQSP
AMBN_caiman LPALEYSGHLGQV ------------ ------------ MYPIVHQLVHQG--------PMQPQ--QQPA
AMBN_Anolis ------------ ------------ ------------ IYPALH-GTQQD--------PSQQL--QQQS
AMBN_Xenopus ------------ ------------ ------------ YQTIMNKLLQQGAGETIPD-PAGTLPVNQQH
AMBN_lungfish ------------ ------------ ------------ IEVPIF---QTPQVAQQP-QPPQQM--IFPA
AMBN_coelacanth ------------ ------------ ------------ VSPSNGNAVQTPQVTQQPLQPGQQG--QQPQ
AMBN_bichir ------------ ------------ ------------ ----------
AMBN_sturgeon ------------ ------------ ------------ ----------
AMBN_gar ------------ ------------ ------------ ----------
AMBN_zebrafish ------------ ------------ ------------ ----------
AMBN_medaka ------------ ------------ ------------ ----------
AMBN_tilapia ------------ ------------ ------------ ----------
AMBN_fugu ------------ ------------ ------------ ----------
exon11
AMBN_human L--YPGMLYVPF--------GANQL ----------
AMBN_platypus L--YPELVYVPF--------GANQQ ----------
AMBN_caiman L--HPALFYMSY--------AANQG ----------
AMBN_Anolis I--YPSLYYMPY--------VANQG ----------
AMBN_Xenopus P--YPGLFFMQY--------GGGPG ----------
AMBN_lungfish F--E---YFYQF----PVQQGQQPM MFPSFFENSP-QFPGQQGQYPVMLPTSDILPPVIQQPDIQQPQLPQVPPTNSFLPSIVQQGQGQQQQQQQQQQPQQ
AMBN_coelacanth IQFFPTYEYLQMLPQVPGQQGQQPG GYPPYSFFP--ALAQQPGLDP----------QQQQQQQQQQQQQQQQQQQQPQQQP
AMBN_bichir ---------- FSGYGLLL-PASFPPQPV----------QPGLEQQPPQQQPSQS
AMBN_sturgeon ---------- FPGYSFLI-PAAFPQQ----------QAQPGQEQQQQ
AMBN_gar V--FNTF---GILPIMPPQAQDEQQ FPGYGVFF-NTAFPQQPV----------QPPQAAQPGAPPQQQ
AMBN_zebrafish F--F----YYPILGQQS----RNPT FS-YGVSAFQHAASQQYPANAAPALRPARP----------QQGQNAHQMRQPQQQQQQQQQ
AMBN_medaka M--FPPYGFYPLFAPPY----GNQM FSPYGFPSIRESPFLQAPTQQLQNNQAPPAENVV----------PAGAAPQQTQQ
AMBN_tilapia I--FPPYGYLPLFSSPY----GNQL FSPYGYPMILESGLPQIPANQLPNSPVLPAENAAGVAV----------DPSIDATQGIQQPQQQLQQQ
AMBN_fugu I-SSPR-SFIPLISPAF----INQL ----------
exon12
AMBN_human ---------- N-APARLGIMSSEEVA
AMBN_platypus ---------- NAAPARLGKVSSEEMP
AMBN_caiman ---------- G-APARLGIVSSEEML
AMBN_Anolis ---------- A-APARQGIVSSEEMQ
AMBN_Xenopus ---------- G-PPARLGAMSSEEIT
AMBN_lungfish GFPIQFYLQALGHQ-NLPQN V-----QGAISSEEIQ
AMBN_coelacanth PFPSFVYVPLPARQEQLPQG G-FPNTFGAMSSEEMQ
AMBN_bichir MFPQLVYFPLQT----GVMA G----AIGSVSSEEMQ
AMBN_sturgeon MYPQLVYIQLQP----GMAG G----ASGSVSSEELQ
AMBN_gar MIPQILYLQIQPM--RSAMG G---GGFGSASSEEMQ
AMBN_zebrafish FQPIF-YMVPQMP----QRM A---GSYGGLSSEELQ
AMBN_medaka QNPPIVYMLQ-------QPM N---PAIGGLSSEELE
AMBN_tilapia N-PQILYMLQ-------QPM S---SPLGSLSSEELQ
AMBN_fugu ---------- D---STLSSFSSEEFE

B (continued)

```
                exon13
AMBN_human      GGRE-DPMAYGAMFPGFGGMRP---------------------------------GFEGMPHNPAMGGDFTLEFDSPVAATKGPEN-------EEGGAQ----GSPMPEANPDNLENPAFLTELEPAPHAG-LLV
AMBN_platypus   GGGG-EPLAYGSIFPGFGSMRP---------------------------------GFGAMQINPALGKDFTLEDDSPTVAGK-PPG-------QGGEVL----GSPRDGAIPAGHPNPGLLPERISRLRSGAALT
AMBN_caiman     GGRG-GVPAYGAMIP---------------------------------------GFRGMPQDPALQGDFTTEDDNPATAHN-PAI-------QGGANQGFSRGSRFPAVNRAGHGSAILLPDGTPAGHEG----
AMBN_Anolis     GGGF-GAPAYRAPGPDLFAMDT--------------------------------RFGNSPLN--QPGDYTVEDDTLGITEQ-PDV-------KGGANA---------GANPSGKGNNAVLLDGTQGGALP----
AMBN_Xenopus    GGRTGAAHAFSSLYPGLLGMGP--------------------------------RLESHPQDPALQGDFTIEDDSPVAGQK-PTG-------QEVSQG--------PIESPQGVGSSIMIPGLEGSPTGQ-GET
AMBN_lungfish   GFPIQFYLQALGHQNLPQNVQGAISSEEIQANRAAGAAAAAVFNSMFPAFAANYPGFGSPVARPISPVDATIEDDHPVVGQGEQAGQGTGTPGVQGNLPNAVGT--------------PSSPAVNIPIPEGNPTG
AMBN_coelacanth AAGGGLS-PALGGIIPGYVGNIPG-FGAGVPSFGGSVPGAAANIPMF--------GFPNTAVNPAGQGGVTVEDDPPPAAEK-PASPGN-SPGT-GANPSGQGGSAPNPEGNPTGQVGSIPNPQANPPPSEGTPS
AMBN_bichir     QSAGDMS-PPMAGFIPGFATPT---FGGGFPNFVGSGPAVGGTVPV---AGGI--PTAQGTQPGVLPEV-------------------------------------------------------------KLPIPV
AMBN_sturgeon   AAGG-IS-PGFAGFIPGFAGQA---FGGSIPSFGGSVPGAEGSIPF---AGGV--PTGQGTNP-VVPEA-------------------------------------------------------------GLPTVEILPA
AMBN_gar        AAGG-VA--GFGGFVPGFAGSG---YGGFGGTVPGTE--GVFPTGQGILPVAPDAGLF-PVGQGG-------------------------------------------------------------SPTAPAVFPA
AMBN_zebrafish  NMGR-VNMHLPAIRGNVFPVSGPQTVVPIGPVRPPNPFPATGMTYPGITELQQPSIIAVPPSRDAIPATGGSH----------PNSAVLPSRISGTQDRDRAPCVGAEIPLTNSFAPLD--SGHGAFISADVP--
AMBN_medaka     MQAK-LNQMSV--YSVLTNLPAGAGPVQPENQAAGLTNPGEQGATPHVGGSA-----------------------------------------AGVRSLQGPACSGSLLNSNSVPAGVKTAVPEANAVQTQNHAK
AMBN_tilapia    MAAT-MGQLGV--YMPNVLTNQPAGAVQPESQAAGLTHPFQQGVQPAVGTSA-----------------------------------------AGAQPIKALPC-SGSQPNASGFSAG-LAGPDAATAQTPAEPQ
AMBN_fugu       --------VNI--YLSTALTDPSAATVQPVKQAAGL-----QNLVSTVGTPS-----------------------------------------TGAPQNQ-VPTSSGPPMDTNGVPVG-SEKPAEEMATVQHPVE
```

```
                exon13 (continued)
AMBN_human      ---------------------FLKDDIPGLPRDPSGKMKGLPSVTPAAVDPLMTPELADVYRTYDADMTTSVDFQEEATMDTTMAPNSLQTSMPGNKAQ----------------------EPEMMHDAWHFQEP
AMBN_platypus   ---------------------FPSDFIPHRGQGPAGQSKLPPGVTPPPADPLMTPGPSDPLEFFEGDGTTPLGLQREALLDTTMTPDTQSTYMPGNEAQ----------------------QMQVTQDQWQFQEP
AMBN_caiman     -------------------FLPNINDMPGQGVNPVGQ-RGTPEVTPTATAPELTQGIPDSFMTFGAEGTVPLGIQKEVTADPTMFPEAQHTLMAGNGAE----------------------QPQVMQDVWHFQEP
AMBN_Anolis     ----------------------NANSHLFSPAGQSQGLSGLAQATAAPHATQG---PFLPLDAADPS-------MPLDATMFPD-LYTSNVGNEAG----------------------LAQVGQDAWHFQEP
AMBN_Xenopus    ----------------------VPFPNINSPNMGFNPQSKIPPGVTP-ANAPRLTHDTGAGYVPFALDDTMPFGIQRENVISGDITRANNAKGIESPIMQH----------------------EVHLQNHNNYFQEP
AMBN_lungfish   QIGNPQIP-----------------------------QSNPSSPGQGGIMQNPDINPSNQGLPATPADIPAASAGNPSAATASPNEGGL----------------------------PVIYYEGLNHPAARGPWFP
AMBN_coelacanth VQGVPQPAPEGNLPNLEGN------PTGQVGNQPAPQSKGPMGGATTPASTKNLTPANVPGGPEGGIVPFGAGDTASAAARKVVPTIPAFFNPSLGGTAPTENNNAVRSNAAGVLPPIVVNEGLN-PLGGGWIYP
AMBN_bichir     GQG------GSPTIPEVIPIGQGNMPPKTEGAVPAQGGQQPSPQMKLPNMTPDGVLLDGPVPPEGTVQSFAPGSTQDTIGKKSPTAAPDPATVP---------------KAQAPTPPEVEMPDLDDYTANFYLHP
AMBN_sturgeon   GQG------GGPTIPEVIPTGQGSLP-----VMSKTGNQPAPQSKLPTVGLTTPAWVRMLTPGNSPAAA.
AMBN_gar        GHGNLPPTPGS-TVPV-----QGS------------NNQPAPQSRDPAFSMTTPAGVRAATVGNPPAAAAGTAQPNAAAAAATAAAE-----------------RVHVNHAERNIPADDEMPEADDYRAP-FIYP
AMBN_zebrafish  ------------------------------------------------------------------------------------TVHPDPQSSGPNLVPDPLPTAEYKEDLFPAAPP-LLSDTVDTNTAN-EMYP
AMBN_medaka     SLPTNRNLVRSKAN.
AMBN_tilapia    LQPMQETLV.
AMBN_fugu       AELLPLTQTRSV.
```

C

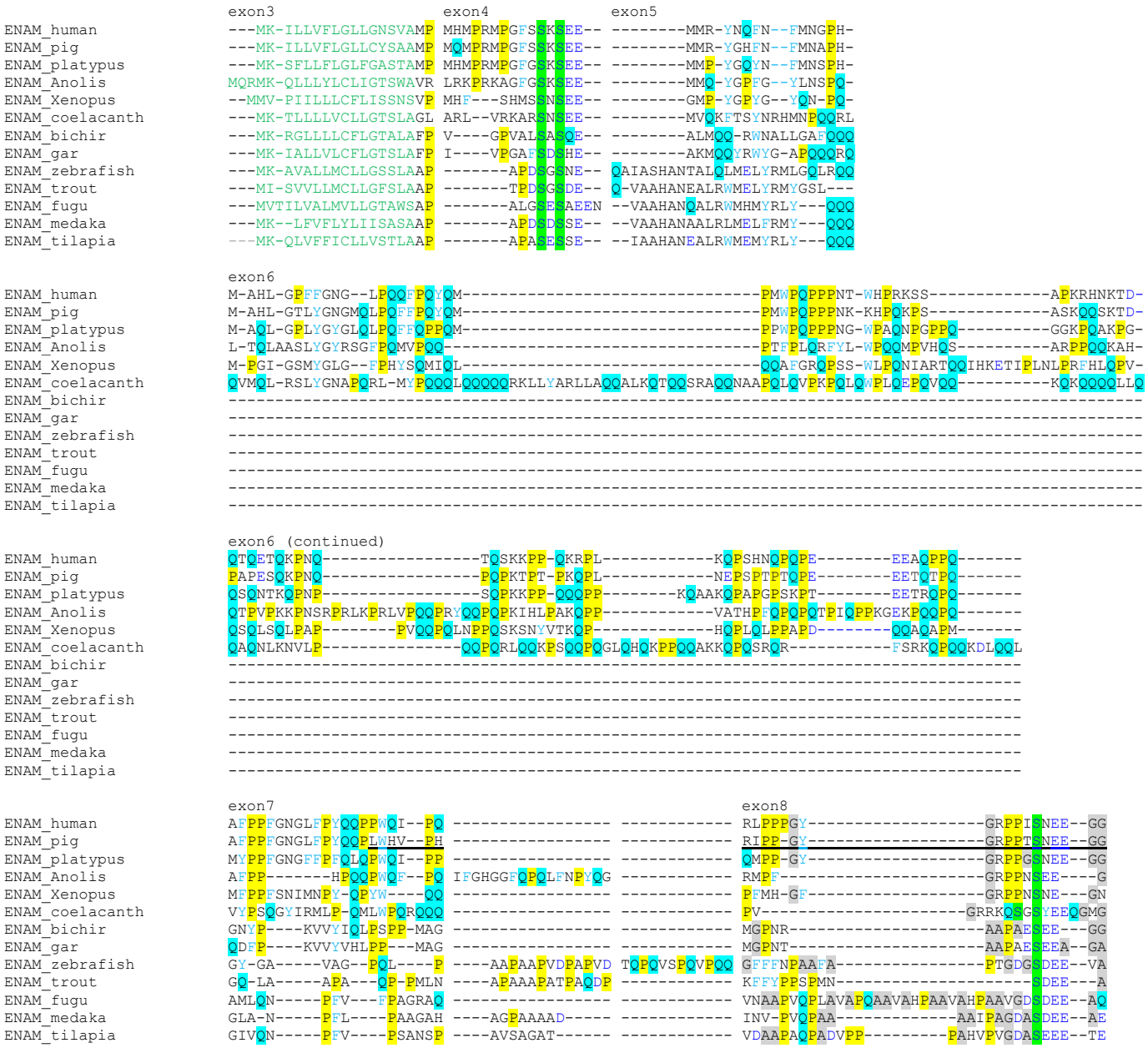
exon3
exon4
exon5
ENAM_human
ENAM_pig
ENAM_platypus
ENAM_Anolis
ENAM_Xenopus
ENAM_coelacanth
ENAM_bichir
ENAM_gar
ENAM_zebrafish
ENAM_trout
ENAM_fugu
ENAM_medaka
ENAM_tilapia
exon6
exon6 (continued)
exon7
exon8

C (continued)


exon9
ENAM_human -NPYFGY---------FGYHGFGG-RPPYYSEEMFEQDFEKPKEEDPPKAESPGTEPTANSTVTETNSTQ-PNPK----GSQGGNDTSPTGNSTPG---L
ENAM_pig -NPYFGF---------FGYHGFGG-RPPYYSEEMFEQDFEKPKEKDPPKTETPATEPSVNTTVPETNSTQ-PNAP----N-PRGNDTSPTGTSGQG---P
ENAM_platypus -NPYFGY---------FGHQGFGG-RPPYYSEEMKEEEKE------SPKEDSPSPEPTANSTVAETNSTQ-PSGP-SQAGSQGGNATDPGQSAGNGSPAQ
ENAM_Anolis -NPYFGP---------GYQGMGG-RPPYYSEEMFEQEDK-----EAPK-ESPATDPVTNST--DTNSTV-SNP-----ASQGGNGTMSGLSEKATGANS
ENAM_Xenopus -GNYFGF----------FGMGG-RAPYNSEEINEDEEPAKAEKESPKTESPVAE-TSNTTIADNNSTT-ISQ-------SQGNATTNNESMAGDITQS
ENAM_coelacanth -ISYFGA----------YYPEI-RRRPLESEEMYPESEG-----KSKKTED-------NSPVPEVSSPTSASPP----AGQDGNSTNAGGNHTVHGENL
ENAM_bichir QPQYAGYMPPAYGYGPYGGYGHFGKRMPL-SEEINEEGPAKAEGGKEPTKPPKAEEATPTPGGTATKPDGAAPNTEGGAPAAGGSPPAAEGSPNGQGGTP
ENAM_gar -PQYGGYVPSFYGYGPFG-FGNFGRRAPL-SEEINEVNEKESESPGKPEAPAATEAPKAEDLPPTPGGV--PTNTEGAGAAASANGTAANGAGNQPATEG
ENAM_zebrafish -PQYRGF------YPHYGYHQPAQPAAPLNSDEAEGAEAEGAEAEAGAEAGAEAGAEVGAEAE----PAGTAATVDAAAANEI---LPVDVAEPAA
ENAM_trout -PVPRYGGYGRY-YPYPGLAAPAAPAVPLNSDEVGEDEAAT-EAEAE----------PAVDHAAEEPAVVDTAAPVDPAD-AAPVDPAMDVPIDVVIPAA
ENAM_fugu -MQ--------------AAGPGAPAAPLNSDEAEEASEAEPAADPEAAGAAADATPAPAGA--EVAATAAADAPADAAAASGPEAAAADVPAAA-DVPA
ENAM_medaka -DGNP---------------GPGVGVAPLNSDEEEEVEEVEATEVE----------PAVVETAAEATAAPPAAAAEPAVVDVAVDAAPVDDVV-VDVPP
ENAM_tilapia -DGNP--------------ATKAAGPAPLNSDEVEEAEEVEAAEAD----------PAMVEAEPSANPAAVVEPAVVDVPIDV---APVDDAAAVDVPP

exon9 (continued)
ENAM_human NTGNNPSARNGI---GPLPAVNASGQGGPGSQIPW--RPSQPNIRENHPYPNI-RNFPSGRQWYF----------TGTVMGHRQNRPFYRNQQVQRG
ENAM_pig NPRSNPTGQNG-------PAVNVSGQGVPRSQSPW--GPRQTIIHENYPNPNI-RGFPARRQWRP----------PGPAMGHRRNGPFYRNQQIQRG
ENAM_platypus TPGHGTVPDNGE---PPGPLLNASDHGGARGPKPTGPGPGQPPFRGRPANPNAAPGFPAGRQRRPFVHPFGRPFDRPVGRPVGRRDHGPTYGNTPKARG
ENAM_Anolis PGLQ-NNMFSGNAVSTPLPTTQTSEGNGVA---QN--VLEQIRHRSKLPNGDVIQSFPSGRQHST----------MQVYNI---HKPHEHMEN----
ENAM_Xenopus STIA-LNAQNGH---IEGPPVIAVVHNKHKNTLHG--ASRQAHYVVRAPNPDTILSN----------HQPHQKYHI----
ENAM_coelacanth ---------PNTDINPSGQGDNTSNTGNVHFGRGDNP-QNPLSNPTGQEGSFPNPEFNPLGQGNMPPNTEVNPLGQGSTNPDPGYNSVGQGSIPPNTRY
ENAM_bichir ---------TNPEANPPASGGNSPANGQSQPDRGDSP-NQGVNQPN------PAQGINPMYPGNVNPFSG----------
ENAM_gar GPNTPGSSPPKPEGAPAGPGGNTPAVGPNLPGRGDSGPNAGPSSP-GVAGGFPVPGTNPLYP-NLDPFAG----------
ENAM_zebrafish DVIAAAV-----AAV---------DPALSPE----------APAVAMEIDTTV----------V---GPDVAAGEQVL----
ENAM_trout VDIPATV-----ATD---------IIVVDPA----------LIAPI---DTIV----------AADVPAEVDAGATDV----
ENAM_fugu D-AAAADVPVDAAAADVPVDAAGSGVPAAAAVDVPADAAAADVPVAAACS-DV--PAGAEAAAAEVPVDAAAADVPV---------RGDATAADVPTGV
ENAM_medaka VDVAAVD-----IAP---------EVAVDVA----------GPAAA-DI--PA----------AADVPAAGDTVATDA----
ENAM_tilapia VDVVPVDS--APAAP---------EVAVDPA----------APATA-DI--LA----------V----------

exon9 (continued)
ENAM_human P-RWNFFAWERKQVARPGNPVYHKAYPPTS-RGN--Y-PN-YAGNPANLRR-KPQGP-NKHPVGTTVAPLGPK-PGPVVRNEKIQNPKEKPLGPKEQI-
ENAM_pig P-RWNSFTLEGKQAVRPGYPTYRRVYGSTA-RSN--P-PN-YAGNSANLRR-KPEGP-NKNPMVTNVAPPGPK-HGTVDQNENIQNPREKQVSQKERT-
ENAM_platypus PLRWNAVTSEGKRVARPGYPMYRRPFPVAA-PGRG-F-PN-RAGNPLNLRK-NPQAP-AKHPGEANSGPVYSQRGGLMAPREPVASPQENPPSPREKP-
ENAM_Anolis --------I-KQNLISRGNPSIQSEDPTYP-MGNG-WNSN-HRGNIQNTNVNNPSTN-T----------R-HIPYGQQEQPHYPERNEFSQIDRV-
ENAM_Xenopus --------VDKILVGRGGFPSQNTIYHQEQITGKVPL-TNIHTEKSSYIRH-VPQTNSDKIPLRTVATKDGDS-F----------VREARGM
ENAM_coelacanth NPSGQGRIPPHTRANPPSQRSMSYPNTQRVGQKGIQPNPDYYPSGQESIPSNTRYHTFSQGSMTPNHIYKPSGEENIPPSPEYDPSDHGSIPPNHRYNP
ENAM_bichir ----------VFLPAGIRKVTPSPDTG----------
ENAM_gar ----------VMWPAGVRKVTPSPSAG----------
ENAM_zebrafish -------M----------AEAPDAALSV----------
ENAM_trout -------GA-APLDAEANMTGGPADPTATLLA----------
ENAM_fugu DAAAADTAAHADLAAEGPAAAGSSCPDATLLA----------
ENAM_medaka ----------AENEVTGGIADPALPV-M----------
ENAM_tilapia ----------AGPLDPTAL----------

exon9 (continued)
ENAM_human -IVPTKNPTSPWRNSQQYEVNKSNYKLPHSEGY---MPVPNFNSVDQHENSYYPRGDS--RKVPNS--DGQTQSQNLPKGIVLGSRRMPYESETNQSEL
ENAM_pig -VVPTRDPSGPWRNSQDYGINKSNYKLPQPEDN---MLVPNFNSIDQRENSYYPRGES--KRAPNS--DGQTQTQIIPKGIVLEPRRIPYESETNQPEL
ENAM_platypus -SFPTRGPAVPWRKPQNYGPGKPVYRPPLSEGR---PADPGPSPFDPRENPYYPRGDATDRRFLSS--GGSAPGRHFPEGIVLKP-------EDDQPPS
ENAM_Anolis -PFPSSDPVGQWNKDPIYRDNDPKNSPP--EGH---PLDPQFKTM-RIDNIYNARQDA--ERFQPS--GMHQSNALSHQGVNLATRRTPFEIETHQYDW
ENAM_Xenopus HFDPTMNTIGNDAIQQIYRNNVPDNASPKVDNEHLSFLVN-KNKTPNRKIILVQHQGR--EHFPGHIMESVIESEYAPRGIFSSHRNTPSYTQINKEDQ
ENAM_coelacanth SGQVNMPLNPNHKSFDKGGSSHIPQYSHLGHESVPPNPKYNPSGQESILPEQVYNPSGQE-RLTPYSKYNPPGQERIMPNSRYDLSGPENIQPNYRYSP
ENAM_bichir ----------STQILPGGFV-PSADGGATIP----------
ENAM_gar ----------ATQ----GFAEPGGED----A----------
ENAM_zebrafish ----------
ENAM_trout ----------
ENAM_fugu ----------
ENAM_medaka ----------
ENAM_tilapia ----------

C (continued)

```
                    exon9 (continued)
ENAM_human          KHSSYQPAVYPEEIPSP-A----KEHFPAGRNTW-------------------------DHQEISPP---FKEDPGRQEEHLPHPSHGSRGSV-FYPEY
ENAM_pig            KHSAYQPV-YTEGIPSP-A----KEHFPAGRNTW-------------------------NQQEISPP---FKEDPGRQEEHLPHLSHGSRVHV-YYPDY
ENAM_platypus       KQKPFHPV-TSERTPR---------EPSPTKPQR-------------------------TSPEPPPP---LEEGPGRQDKSLTYPPISPRSGI-PYPDH
ENAM_Anolis         REQPFNHI-DQKR----------GQFLSAQTPTW-------------------------NNREASQL---FQEAPPRQSSMYSSGSFNQREMP-TYSGK
ENAM_Xenopus        KLSVPNNG-DNSGN-INTAHIKSEDLFRGGEFFQHNGENAALYQKEGTASDIGTASDIGTAYDIGTAYDIGTATTGQQLESIYLVKHFPTNHFQVYGDN
ENAM_coelacanth     SGQESISPNSRYNPSGQEIHPPNSRYNPSGQENIPSNPNYNPSDQGRMLPHHEVNLPNKKSIQPNSGYHPSGQKNLSPRHMYNPSDHGSNPQNHEIDPL
ENAM_bichir         ----------------------VTSSPSGNNNAVLNIPYYPSNGG-------------------------------------------------NINPV
ENAM_gar            ----------------------TTPAPMGKGSPALNIPFSPSEGA-------------------------------------------------KRNPS
ENAM_zebrafish      ----------------------------------------------------------------------------------------------------
ENAM_trout          ----------------------------------------------------------------------------------------------------
ENAM_fugu           ----------------------------------------------------------------------------------------------------
ENAM_medaka         ----------------------------------------------------------------------------------------------------
ENAM_tilapia        ----------------------------------------------------------------------------------------------------

                    exon9 (continued)
ENAM_human          N-------PYDPRENSPYLRGNTWDERDDSPNTM--GQKESPL---YPI-NTP-DQKEIVPYNEEDPVDPTGDEVFPGQNRWG-EELSFKG--------
ENAM_pig            N-------PYDPRENSPYLRSNTWYERDDSPNTM--GQPENPH---YPM-NTP-DPKETIPYNEEDPIDPTGDEHFPGQSRWDMEELSFKE--------
ENAM_platypus       H-------PYDPK--------GTWDEGNEPTPSS--GPAEQPGRQPSPCSPRM-GQRGEVPYNEEDPVDPTGDEPNLGPGPWE-ETANGKE--------
ENAM_Anolis         KSYNQYTHPFPP---------RAWEDREHSPTISPSDQRESSP---YPP-VSPSDQIQRNTYY--RRIQPE-YEPYSRQDPWT-REQHLHD--------
ENAM_Xenopus        N-------PKNPS----HLLSNTWQKKPDQ--------LESPR---N---NLL-GQKEIYLYPDTELYHQTNNELPLGKQHWD-NEIDFSAVQFENPGS
ENAM_coelacanth     GQRHQPSSPVTNTLVQEDMSHYPRSNPLRQGGNSPNHETFSHGQKKYSHYDRSNHVRGKGNSPCHGSHPSGQVIHHKPQFKGNSQIHDENPWGQEGQMS
ENAM_bichir         GMRKTP----------------------VKNGC-------------------------------------------------------------
ENAM_gar            GIRKPP----------------------VQVPC-------------------------------------------------------------
ENAM_zebrafish      ----------------------------------------------------------------------------------------------------
ENAM_trout          ----------------------------------------------------------------------------------------------------
ENAM_fugu           ----------------------------------------------------------------------------------------------------
ENAM_medaka         ----------------------------------------------------------------------------------------------------
ENAM_tilapia        ----------------------------------------------------------------------------------------------------

                    exon9 (continued)
ENAM_human          -------------GPTVR--HYEGEQYT---SNQPKEYLPYSLDNPSKPREDFYYSEFYPWSPDENFPSYNTASTMPPPIESRGYYVNNAAGPEESTLF
ENAM_pig            -------------DPTVR--HYEGEQYT---SNQPKEYLPYSLDNPSKPREDFLYGEFYPWNPEENFPSYNTAPTVSSPVESRGYYANNAVGQEESTMF
ENAM_platypus       -------------DPS-R--YHKSPQYPQSRATEPQDYPPYPEGGLEK-HRDFPYGDFYPRGPEDNLQPYNGADQ--LPVEGRGYYTHDAVGQGGPLQF
ENAM_Anolis         --------------PD-N--QYSNSPYN---PTHHQTYQKYTTENPPSEISNLPYRKINQWTQEEHSPVH-TAGHL-RQMENVPYRTNSKFEQGE-RKF
ENAM_Xenopus        STYYMKDSQRQKQWPTASNNRVELDRQP---TDQPKYLLISKLD------------------PAKNTDVS--TFTTNEPMAQNGYITNQEAY----LQS
ENAM_coelacanth     NAGRIPSNRGDSSPYPGLFLSENRESSPYLASKPVNQGQISPNHEVYSSAQGGNRPYTGMIPTDKIISPNHGPSSSIQGDLSQNYRGYQSGKERNQPYT
ENAM_bichir         -------NMG-------------------------------------------------------NHGPTTV-------------------------
ENAM_gar            -------NKGP------------------------------------------------------HGPY-------------------------
ENAM_zebrafish      ----------------------------------------------------------------------------------------------------
ENAM_trout          ----------------------------------------------------------------------------------------------------
ENAM_fugu           ----------------------------------------------------------------------------------------------------
ENAM_medaka         ----------------------------------------------------------------------------------------------------
ENAM_tilapia        ----------------------------------------------------------------------------------------------------

                    exon9 (continued)
ENAM_human          PSRNSWDHRIQAQGQRERRPYFNRNIWDQATHLQKAPARPPDQKGNQPYYSNTPAGLQKNPIWHEG-E-NLNYGMQITRMNSPEREH------SSFPNF
ENAM_pig            PSWSSWDPRIQAQGQKEGRPYLNRNFWDQSTNLYKTPTSSPHQKENQPYSNNSPAGLQKNPTWHEG-E-NLNYGMQITRLNSPERDH------LAFPDL
ENAM_platypus       PSRDSWDWGLRSAAQERRAPYDERDSWDHAINS---PKSTAGATETLSPSHSVPAGIRGKPHEESV-D-WSYRGGQVSDLGVPEAEG------PALMEP
ENAM_Anolis         QNVGSGSPQQRNTFQEE-AQYAERNTWVPQRV------DPSAQKETAPYYNIYSTDFRGNPTHVEDRERIIHMNAPISTENAPRRRH------YLDRMG
ENAM_Xenopus        PNN--KSPFIFNKPSTDGILYIPIDELHDS--------------------QNNPVHLKLTP------------------YSKAHSENHSPGVFRSLQEV
ENAM_coelacanth     EVIPRGQKSIYSAPSGQRGNSENLRINPSGNSENLFYPERKPSGKESDLPSYRVYVKGQGENSPYSQPV-PSSQRIMTSDPLLNQSTQKGTMPYFTLNS
ENAM_bichir         ---------------------------------------EPVAPSAGNSEIPSFGE--------------------GILMA----------------------
ENAM_gar            ------------------------------------------GNGE-------------QPGFVDPMNPDAEGIILA----------------------
ENAM_zebrafish      ----------------------------------------------------------------------------------------------------
ENAM_trout          ----------------------------------------------------------------------------------------------------
ENAM_fugu           ----------------------------------------------------------------------------------------------------
ENAM_medaka         ----------------------------------------------------------------------------------------------------
ENAM_tilapia        ----------------------------------------------------------------------------------------------------
```

C (continued)

```
                    exon9 (continued)
ENAM_human          IPPSYPSGQKEAHL--------------------FHLS-QRG-SCCAGSSTGPKDNPLAL-------------------------------------
ENAM_pig            IPPDYPGGQKESHV--------------------FHLS-QRG-PCCAGGSMWPKNNPLAL-------------------------------------
ENAM_platypus       VARSDPADPREASS--------------------YPVAVARS-SCCAGGSPGPRDVPLAPPDYPPLALPGYLPLDPLDYPPLDRPDYLPPAPRDYPPP
ENAM_Anolis         YSDDYPKERRMIT---------------------SQST-ANQ-LCCADDSPMPRENRLAP-------------------------------------
ENAM_Xenopus        NPNIYPSSLRRQSLNPRKTGHYSCTIPLTGVDPTLEHSN-ALILVCCKLNDM-GQSHPSAN-------------------------------------
ENAM_coelacanth     PGQKTNSPYISENPSDQRGTSPKNRIYPAGQRARLPYPASSVFSQRDNHPIHGTNPSGQEDIPPNQDTNLLSKIGFTPYTLENPSEQRQSGPCPRNNQL
ENAM_bichir         ---------AAEAGSDGEGRT-------------------------------------------------------------------------------
ENAM_gar            ---------AADA---------------------------------------------------------------------------------------
ENAM_zebrafish      ---------------------------------------------------------------------------------------------------
ENAM_trout          ---------------------------------------------------------------------------------------------------
ENAM_fugu           ---------------------------------------------------------------------------------------------------
ENAM_medaka         ---------------------------------------------------------------------------------------------------
ENAM_tilapia        ---------------------------------------------------------------------------------------------------

                    exon9 (continued)
ENAM_human          ----------------------QDYTPSYGLAPGENQDTSPLYTDGSHTKQTRDII-SPTSILPGQRNSSE-----KRESQNPFRDGVSTLRRNTPCSI
ENAM_pig            ----------------------QDYTQSFGLAPGENPDTSIGYAEDSHIKYARQTV-SPTSIVPGQRNSSEKILPGESQNPSPFKDDVSTLRRSTPCSV
ENAM_platypus       DTPNYSPLDTPDYPPHYPPLAPQDYSSPLGLSLWELQVGGPRSPGGSRSRHVQQAA-SPVGYPAIRRNGTEEAPPTRREEPAPSRDGLA-PGRSPPCSL
ENAM_Anolis         ----------------------LRSAPQFRHALWEAKESST-YPDGSHANYVRHAH-SPAGIQA---NNPLKNGGREQEELGAFRVENAGSEKSLPCSN
ENAM_Xenopus        ----------------------EDNVHHLKVVLNEYKESVP-HQDQTHRQHTRDVIESPKFSI--Q-NNVMTVRPNSSNNHDNIQSSRGKSSDSVPCTS
ENAM_coelacanth     CQRSNSPDFKGNSPITERKSLGWRERTHSVGATPIHGNDHPDSFSPRKSQFPADNFPYQAGNPETPRRNQFVDRENMPITRDSPLGSEGNSMKPSLSEP
ENAM_bichir         ---------------------------------------------------------------------------------------------------
ENAM_gar            ----------------------------------IHGDS------------------------------------------------------------
ENAM_zebrafish      ---------------------------------------------------------------------------------------------------
ENAM_trout          ---------------------------------------------------------------------------------------------------
ENAM_fugu           ---------------------------------------------------------------------------------------------------
ENAM_medaka         ---------------------------------------------------------------------------------------------------
ENAM_tilapia        ---------------------------------------------------------------------------------------------------

                    exon9 (continued)
ENAM_human          KNQLGQKEI-MPFPEASSLQSKNTPCLKNDLGGDGNNILEQVFEDN-QLNERTVDLTPEQLVIGTPDEGSNPEGIQSQVQENESERQQQRPSN--ILHL
ENAM_pig            KSQLSQRGI-MPLPEANSLQSKNTPCLTSDLGGDGNNVLEQIFEGN-QLNERTVDLTPEQLVFGTPDKEPRPEGIPNEMQGNESERQQQRQSS--ILQL
ENAM_platypus       RPRASPRAG-LAFPEAGLPPAKPAPCFKSRLRGDVDSVPEQILDPD-PPVAGNDGPAPGDLAVVVPERDPGPVGIRGDP----EPGPEAGAPG--FQWV
ENAM_Anolis         SH-LSQDSKQEANLQRGLFKFRNMPCHGSNIRGDRHNPLAHLVGTGQSFGRGTLNFLPEQ--------FPQPHGIQSEALVSEDDGKEYAALG--AKRI
ENAM_Xenopus        KPSYEQNSE-YPY------AFPKKQCS---YRGDADSYLPPSQDESISLKK--RFLASENVYMPL-ANTPEPDL-PDRRI--KDDGKVKKGIGKLLEIL
ENAM_coelacanth     ---------------------------------RVNLFDRDNPALFSHTTNANNFEEGISTTSPKKEMPPPGVDLTRHATKSWIPAAAGDMLPAPIKKA
ENAM_bichir         ---------------------------------------------------------------------------------------------------
ENAM_gar            ---------------------------------------------------------------------------------------------------RV
ENAM_zebrafish      ---------------------------------------------------------------------------------------------------
ENAM_trout          ---------------------------------------------------------------------------------------------------
ENAM_fugu           ---------------------------------------------------------------------------------------------------
ENAM_medaka         ---------------------------------------------------------------------------------------------------
ENAM_tilapia        ---------------------------------------------------------------------------------------------------

                    exon9 (continued)
ENAM_human          PCFGSKLAKHHSSTT-----GTPS---------------SDGRQSP-----------FDGDSI--TPTE-------NPNTLVELA--TEEQFKS-----INVDP-
ENAM_pig            PCFGSKLANYHTSSI-----GTPS---------------SLGRQDS-----------FDGDPI--MPTE-------TPNSLAGLA--TGAQFQN-----INVDP-
ENAM_platypus       PCFGSETRDSK-SLL-----GMDGRSPWQREAGPIRAGVHRTRRDPGRGLWASDRGAFRGPQP--SPFIRTFTALQDPPVGSGRR--SGTTGSR-----LLVAP-
ENAM_Anolis         PCFGSWLKQYL-SNT-----EVPS---------------DDQQRDP-----------FYGENP--VPTE-------RPNSIPPKPEPISSSFLS-----NGVEE-
ENAM_Xenopus        TCPQDQEIHTNKKAINIAKTRPTA---------------SLLNHDK-----------LSADAIP-----------------------------------VLNTEQ
ENAM_coelacanth     PCFGDRTSPTSRDKIMSFGGSATLAGVRKAPPGNGDSMVLAVKPNLVPPASKTTVATDPKNDMALTSTLNKFPGTEKDALSAPPIAVNEDPRENRAPDCVLLRD-
ENAM_bichir         PCRVHDTATAGKESNFYY----------------------------------------------------------------------------------
ENAM_gar            PCVVHDSPAQAEENHYYY----------------------------------------------------------------------------------
ENAM_zebrafish      ---------------------------------------------------------------------------------------------------
ENAM_trout          ---------------------------------------------------------------------------------------------------
ENAM_fugu           ---------------------------------------------------------------------------------------------------
ENAM_medaka         ---------------------------------------------------------------------------------------------------
ENAM_tilapia        ---------------------------------------------------------------------------------------------------
```

Figure S1. Multiply aligned amino acid sequences encoded by matrix SCPP genes, Related to Figure 1.

(A) Multiply aligned amino acid sequences encoded by *AMEL* and *SCPP5*, their chromosomal locations, and expression of bichir *scpp5* in the jaw and skin. Aromatic residues, negatively charged residues, and positively charged residues are shown in sky blue, blue, and brown, respectively, while Pro, Gln, and potentially phosphorylated Ser residues (potential pSer residues: Ser residues in Ser-Xaa-Glu or Ser-Xaa-pSer sequences, where Xaa represents any amino acids, are known to be phosphorylated in SCPPs.) (Kawasaki and Amemiya, 2014) are highlighted in yellow, blue, and green, respectively. Uninterrupted Pro-Xaa-Yaa (Yaa also represents any amino acid; PXY) repeats are shown with dashed underlines. The three conserved modules, the aromatic residue-rich region (YY), the Pro/Gln-rich region containing uninterrupted PXY repeats (P/Q), and the hydrophilic C-terminus (DE) are shown at the bottom. Unaligned sequence gaps are shown by dashes. Amino acid sequences were retrieved from GenBank (accession numbers for *AMEL*: NP_873632.1 for humans, NP_998965.1 for pig, reconstructed from GCA_000002275 for platypus, XP_003228746.1 for *Anolis*, AAC78133.1 for caiman, AAZ23149.1 for axolotl, NP_001107153.1 for *Xenopus*, AYU58914.1 for lungfish, and reconstructed from GCA_000225785.1 for coelacanth; accession numbers for *SCPP5*: AYU58917.1 for bichir, XP_015200896.1 for gar, XP_035273951.1 for eel, NP_001138708.1 for zebrafish, reconstructed from GCA_000180675.1 for stickleback, NP_001032946.1 for fugu, reconstructed from GCA_000188235.2 for tilapia, and reconstructed from GCA_002234675.1 for medaka). Note that all teleost species used for multiple amino acid sequence alignments (A, B, and C) belong to different orders. In sarcopterygians, *AMEL* is located within intron 1 of *ARHGAP6*, while in actinopterygians *SCPP5* is located within a P/Q-rich SCPP gene cluster (Kawasaki et al., 2017). In *L. chalumnae*, locations of genes are shown as contig names (JHxxxxxx). Expression of bichir *scpp5* was detected in the jaw and skin that secretes the ganoin matrix on scales, but not in the skeletal muscle (negative control). Bichir *gapdh* (glyceraldehyde 3-phosphate dehydrogenase) was used as the positive control.

(B) Multiply aligned amino acid sequences encoded by *AMBN*. Cys residues is shown in red. See the legend above. *AMBN* in sturgeon, medaka, and tilapia has a small last exon, and the C-terminus is shown by a period. The amino acid sequences shown under exon 6 of human *AMBN* are encoded by two different exons in bichir, sturgeon, and gar (separated by an underscore). In a previous study, *ambn* was named *scpp6* in teleosts (Kawasaki, 2009). However, conservation of the amino acid sequences encoded by exons 11 and 12 (corresponds to exon 12 of human *AMBN*) between *AMBN* and *SCPP6*, the absence of the entirely untranslated last exon in both *ANBN* and *SCPP6*, the presence and locations of four potential pSer residues, and an equivalent chromosomal location of gar *ambn* and zebrafish *scpp6* (between *scpp3* genes and *scpp7*) implies the orthology of *AMBN* and *SCPP6* (Qu et al., 2015; Braasch et al., 2016; Kawasaki et al., 2017). In the present study, the orthology of *AMBN* and *SCPP6* was confirmed by a similar expression pattern during tooth development. Amino acid sequences were retrieved from GenBank (AAG35772.1 for humans, XP_007667389.2 for platypus,

AAK92227.1 for caiman, XP_016846623.1 for *Anolis*, XP_002938667.2 for *Xenopus*, AYU58913.1 for lungfish, XP_006011890.1 for coelacanth, AYU58915.1 for bichir, reconstructed from SRX424534 for sturgeon, AMD08894.1 for gar, NP_001138709.1 for zebrafish, reconstructed from GCA_002234675.1 for medaka, reconstructed from GCA_000188235.2 for tilapia, and NP_001032945.1 for fugu).

(C) Multiply aligned amino acid sequences encoded by exons 3, 4, 5, 6, 7, 8, and a 5' half of exon 9 of *ENAM*. The amino acid sequence of porcine 32-kDa enamelin (Tanabe et al., 1990; Yamakoshi et al., 1998) was underlined. Small amino acids (Ala and Gly) in the 32-kDa enamelin and corresponding regions are highlighted in grey. In the region corresponding to exon 6 of human *ENAM*, many small duplicate exons were identified in gar and bichir *enam* genes but are not shown in the figure. Amino acid sequence similarities in the portion located C-terminal to the 32-kDa enamelin (not highlighted or not shown in color) are low or undetectable between phylogenetically distant vertebrates (e.g., tetrapods and teleosts). In teleosts, *enam* was originally referred to as *fa93e10* (Goldsmith et al., 2003). However, sequence similarities in the 32-kDa enamelin and its N-terminal region encoded by *ENAM* and *FA93E10*, the absence of the entirely untranslated last exon in both *ENAM* and *FA93E10*, the presence and locations of four pSer residues, and an equivalent chromosomal location of far *enam* and zebrafish *enam* (immediately downstream of *scpp5*) imply the orthology of *ENAM* and *FA93E10* (Qu et al., 2015; Braasch et al., 2016; Kawasaki et al., 2017). In the present study, the orthology of *ENAM* and *FA93E10* was confirmed by a similar expression pattern during tooth development. Amino acid sequences were retrieved from GenBank (AAG43242.1 for humans, NP_999406.1 for pig, reconstructed from GCA_000002275.2 for platypus, ADJ67842.1 for *Anolis*, NP_001139215.1 for *Xenopus*, reconstructed from GCA_000225785.1 for coelacanth, AYU58916.1 for bichir, AMD08897.1 for gar, NP_001139028.1 for zebrafish, CDQ64219.1 for trout, reconstructed from GCA_000180735.1 for fugu, reconstructed from GCA_002234675.1 for medaka, and XP_003454248.1 for tilapia).

A

ISH: gar teeth

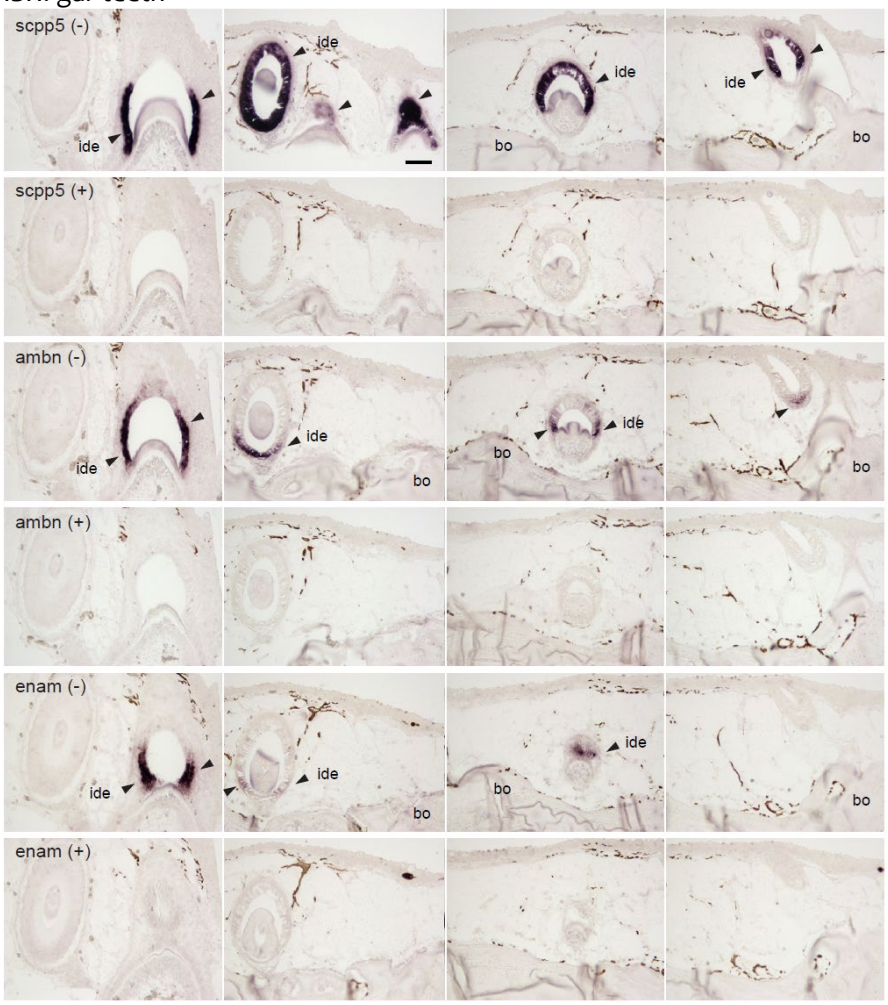

ISH: gar scales

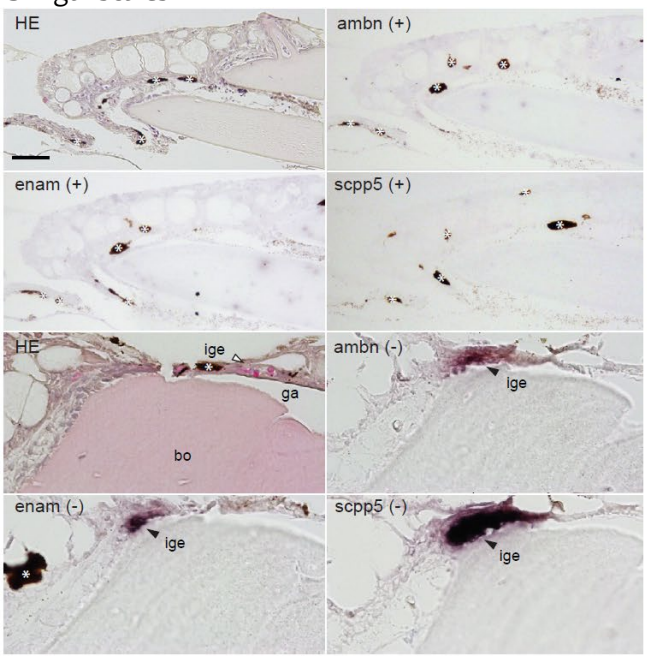

ISH: zebrafish teeth

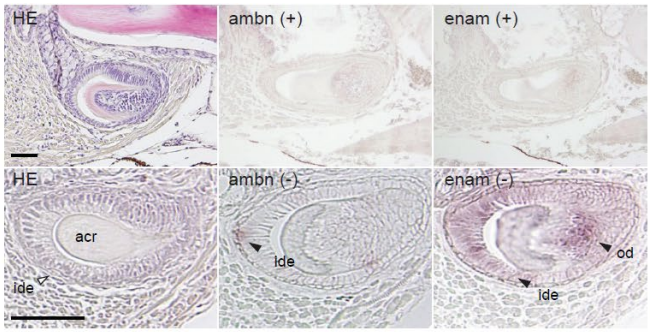

B

Optical IHC: gar acrodin, collar enamel, and ganoin

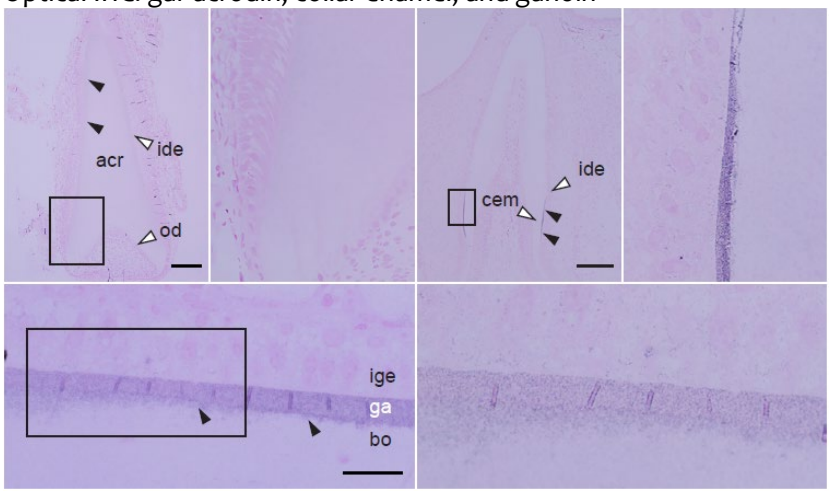

C

TEM IHC: gar acrodin, collar enamel, and ganoin

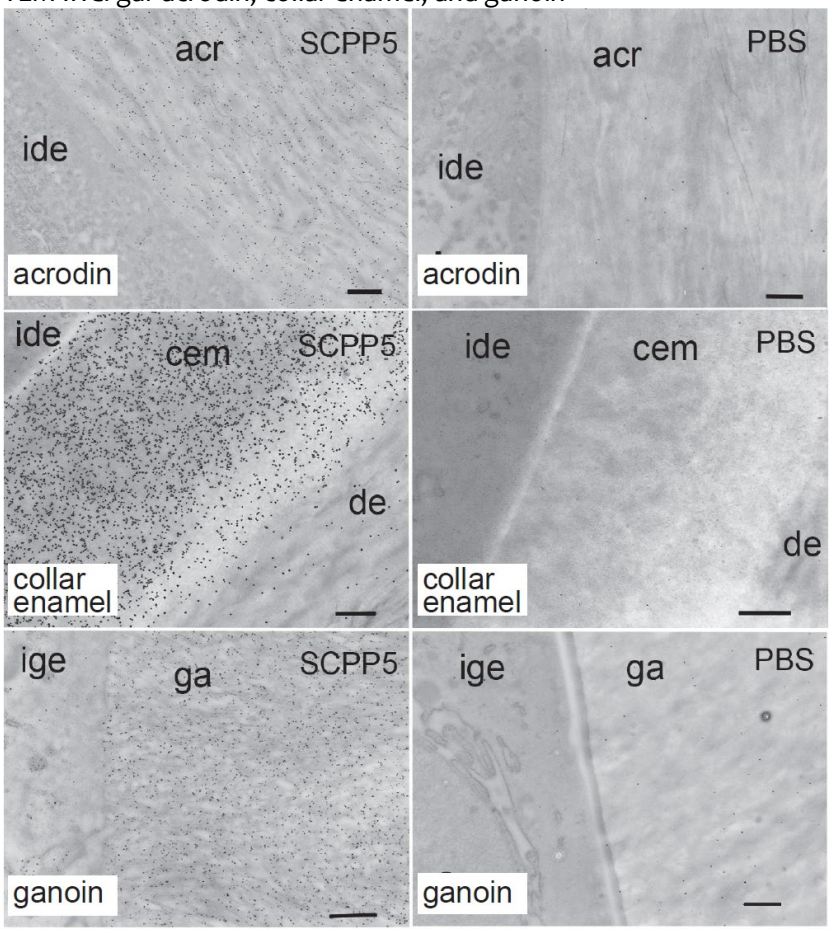

Figure S2. Expression of gar and zebrafish *scpp5*, *ambn*, and *enam* genes in teeth and/or scales, and distribution of gar Scpp5 in teeth and scales, Related to Figures 2-4.

(A) ISH analysis of gar teeth, gar scales, and zebrafish teeth. Expression of *scpp5*, *ambn*, and *enam* genes were detected using antisense (-) probes, but not using sense (+) probes, which serve as negative controls. Images of HE staining are shown for gar scales and zebrafish teeth. All our ISH results are summarized in Figure 2P. Abbreviations: acr, acrodin; bo, bone; ga, ganoin; ide, inner dental epithelial cells; ige, inner ganoin epithelial cells; od, odontoblasts. Scale bar, 50 μm.

(B) Original images for optical IHC analysis (Figures 3A-3F) without enhancing image contrast. See the legend of Figure 3. Scale bar, 100μm (upper row) or 20 μm (lower row).

(C) TEM IHC analysis of gar Scpp5 in acrodin, collar enamel, and ganoin. PBS was used as negative controls. Abbreviations: acr, acrodin, cem, collar enamel; de, dentine; ga, ganoin; ide, inner dental epithelial cells; ige, inner ganoin epithelial cells. Scale bar, 500 nm.

A

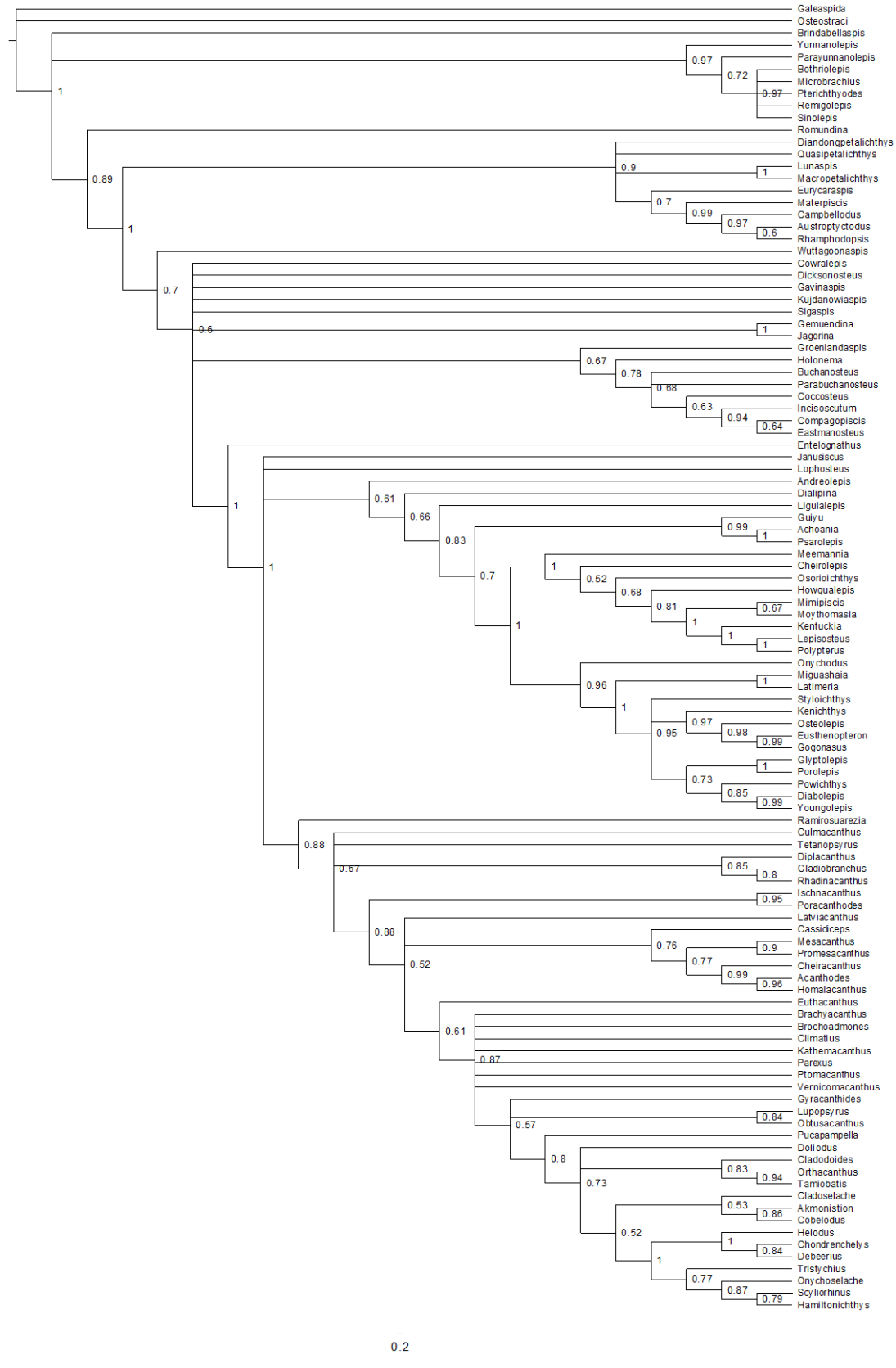
Galeaspida
Osteostraci
Brindabellaspis
Yunnanolepis
Parayunnanolepis
Bothriolepis
Microbrachius
Pterichthyodes
Remigolepis
Sinolepis
Romundina
Diandongpetalichthys
Quasipetalichthys
Lunaspis
Macropetalichthys
Eurycaraspis
Materpiscis
Campbellodus
Austroptyctodus
Rhamphodopsis
Wuttagoonaspis
Cowralepis
Dicksonosteus
Gavinaspis
Kujdanowiaspis
Sigaspis
Gemuendina
Jagorina
Groenlandaspis
Holonema
Buchanosteus
Parabuchanosteus
Coccosteus
Incisoscutum
Compagopiscis
Eastmanosteus
Entelognathus
Janusiscus
Lophosteus
Andreolepis
Dialipina
Ligulalepis
Guiyu
Achoania
Psarolepis
Meemannia
Cheirolepis
Osorioichthys
Howqualepis
Mimipiscis
Moythomasia
Kentuckia
Lepisosteus
Polypterus
Onychodus
Miguashaia
Latimeria
Styloichthys
Kenichthys
Osteolepis
Eusthenopteron
Gogonasus
Glyptolepis
Porolepis
Powichthys
Diabolepis
Youngolepis
Ramirosuarezia
Culmacanthus
Tetanopsyrus
Diplacanthus
Gladiobranchus
Rhadinacanthus
Ischnacanthus
Poracanthodes
Latviacanthus
Cassidiceps
Mesacanthus
Promesacanthus
Cheiracanthus
Acanthodes
Homalacanthus
Euthacanthus
Brachyacanthus
Brochoadmones
Climatius
Kathemacanthus
Parexus
Ptomacanthus
Vernicomacanthus
Gyracanthides
Lupopsyrus
Obtusacanthus
Pucapampella
Doliodus
Cladodoides
Orthacanthus
Tamiobatis
Cladoselache
Akmonistion
Cobelodus
Helodus
Chondrenchelys
Debeerius
Tristychius
Onychoselache
Scyliorhinus
Hamiltonichthys
0.2

B

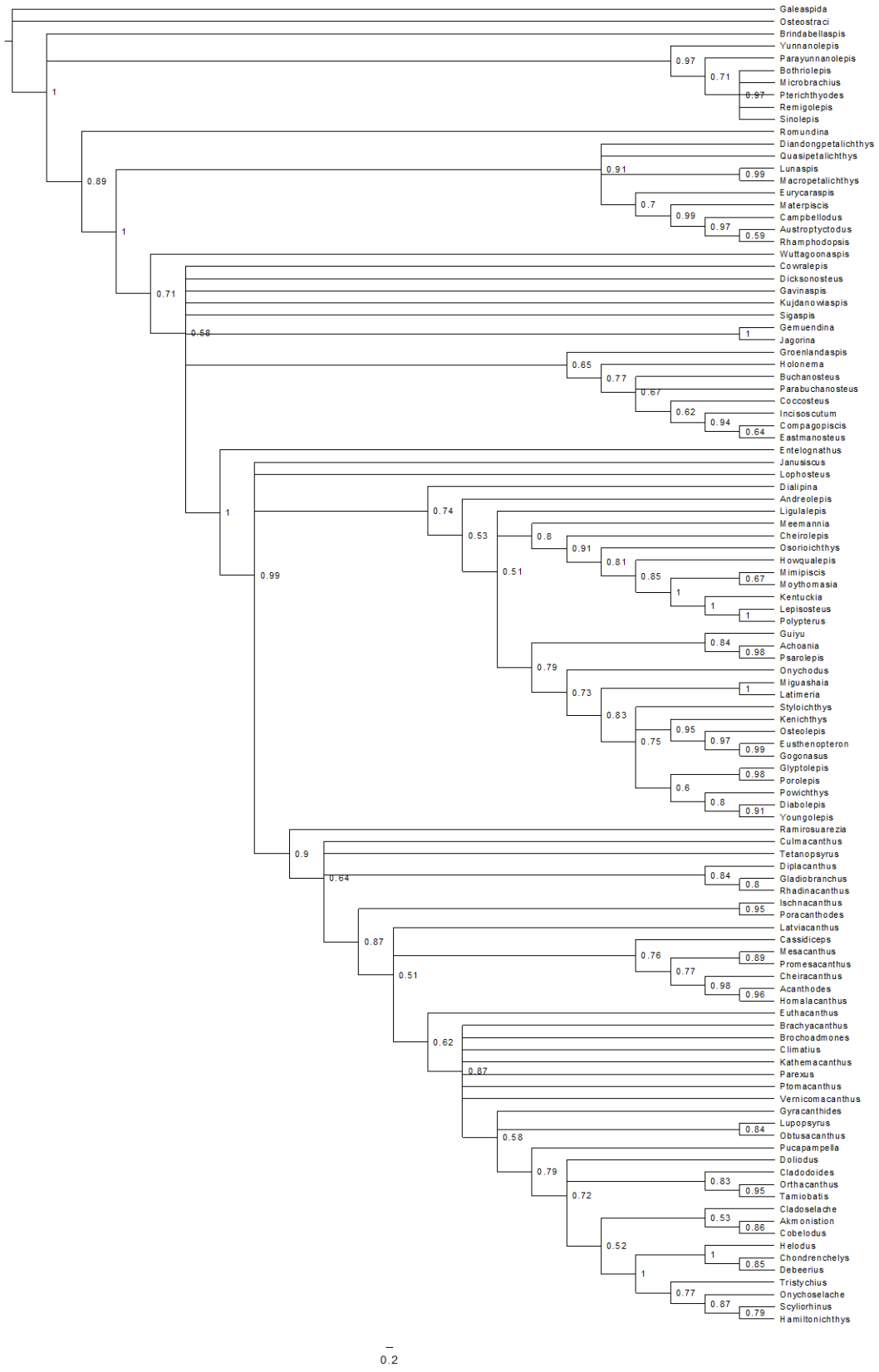
Galeaspida
Osteostraci
Brindabellaspis
Yunnanolepis
Parayunnanolepis
Bothriolepis
Microbrachius
Pterichthyodes
Remigolepis
Sinolepis
Romundina
Diandongpetalichthys
Quasipetalichthys
Lunaspis
Macropetalichthys
Eurycaraspis
Materpiscis
Campbellodus
Austroptyctodus
Rhamphodopsis
Wuttagoonaspis
Cowralepis
Dicksonosteus
Gavinaspis
Kujdanowiaspis
Sigaspis
Gemuendina
Jagorina
Groenlandaspis
Holonema
Buchanosteus
Parabuchanosteus
Coccosteus
Incisoscutum
Compagopiscis
Eastmanosteus
Entelognathus
Janusiscus
Lophosteus
Dialipina
Andreolepis
Ligulalepis
Meemannia
Cheirolepis
Osorioichthys
Howqualepis
Mimipiscis
Moythomasia
Kentuckia
Lepisosteus
Polypterus
Guiyu
Achoania
Psarolepis
Onychodus
Miguashaia
Latimeria
Styloichthys
Kenichthys
Osteolepis
Eusthenopteron
Gogonasus
Glyptolepis
Porolepis
Powichthys
Diabolepis
Youngolepis
Ramirosuarezia
Culmacanthus
Tetanopsyrus
Diplacanthus
Gladiobranchus
Rhadinacanthus
Ischnacanthus
Poracanthodes
Latviacanthus
Cassidiceps
Mesacanthus
Promesacanthus
Cheiracanthus
Acanthodes
Homalacanthus
Euthacanthus
Brachyacanthus
Brochoadmones
Climatius
Kathemacanthus
Parexus
Ptomacanthus
Vernicomacanthus
Gyracanthides
Lupopsyrus
Obtusacanthus
Pucapampella
Doliodus
Cladodoides
Orthacanthus
Tamiobatis
Cladoselache
Akmonistion
Cobelodus
Helodus
Chondrenchelys
Debeerius
Tristychius
Onychoselache
Scyliorhinus
Hamiltonichthys
0.2

C

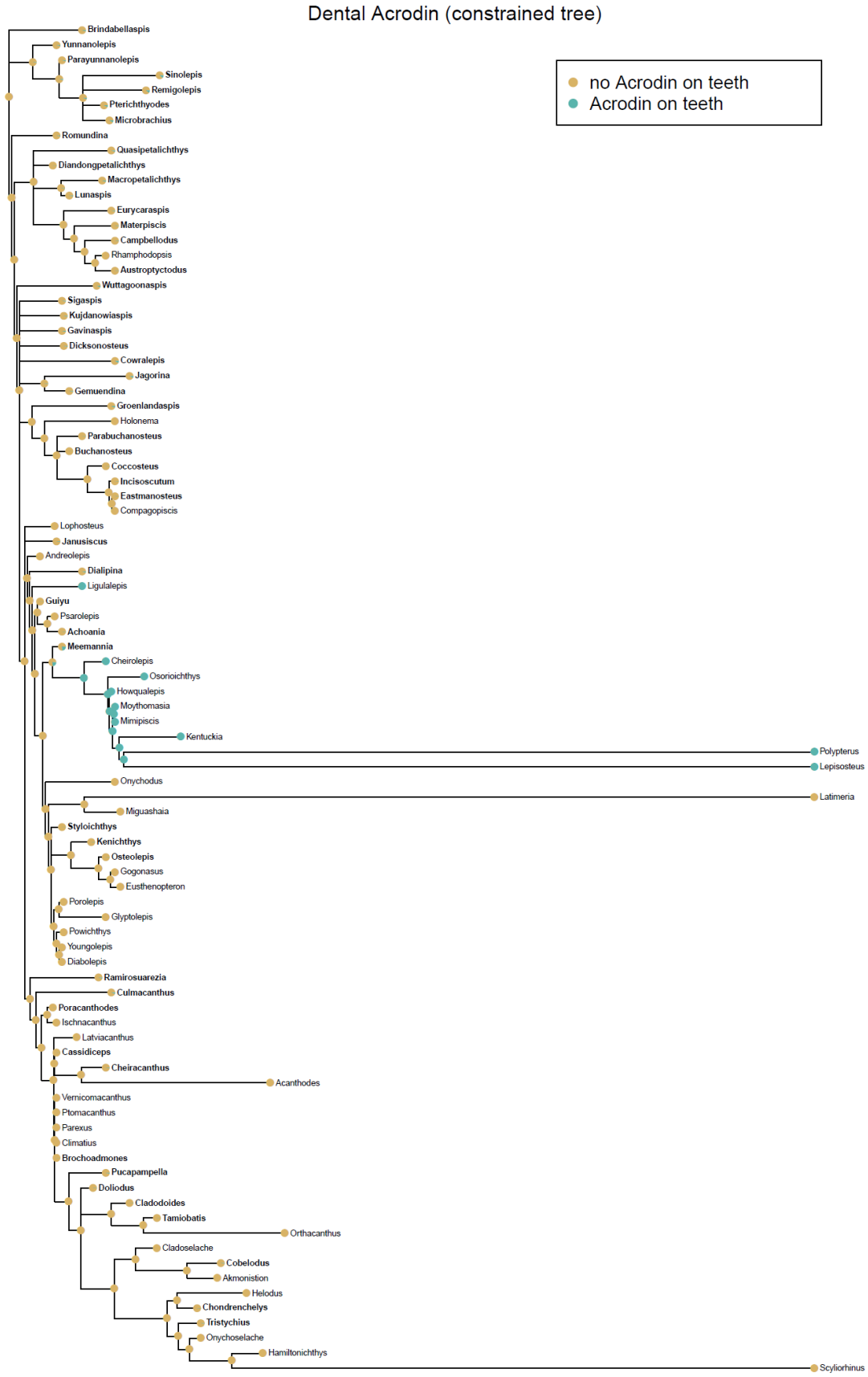
Dental Acrodin (constrained tree)
no Acrodin on teeth
Acrodin on teeth
Brindabellaspis
Yunnanolepis
Parayunnanolepis
Sinolepis
Remigolepis
Pterichthyodes
Microbrachius
Romundina
Quasipetalichthys
Diandongpetalichthys
Macropetalichthys
Lunaspis
Eurycaraspis
Materpiscis
Campbellodus
Rhamphodopsis
Austroptyctodus
Wuttagoonaspis
Sigaspis
Kujdanowiaspis
Gavinaspis
Dicksonosteus
Cowralepis
Jagorina
Gemuendina
Groenlandaspis
Holonema
Parabuchanosteus
Buchanosteus
Coccosteus
Incisoscutum
Eastmanosteus
Compagopiscis
Lophosteus
Janusiscus
Andreolepis
Dialipina
Ligulalepis
Guiyu
Psarolepis
Achoania
Meemannia
Cheirolepis
Osorioichthys
Howqualepis
Moythomasia
Mimipiscis
Kentuckia
Polypterus
Lepisosteus
Onychodus
Latimeria
Miguashaia
Styloichthys
Kenichthys
Osteolepis
Gogonasus
Eusthenopteron
Porolepis
Glyptolepis
Powichthys
Youngolepis
Diabolepis
Ramirosuarezia
Culmacanthus
Poracanthodes
Ischnacanthus
Latviacanthus
Cassidiceps
Cheiracanthus
Acanthodes
Vernicomacanthus
Ptomacanthus
Parexus
Climatius
Brochoadmones
Pucapampella
Doliodus
Cladodoides
Tamiobatis
Orthacanthus
Cladoselache
Cobelodus
Akmonistion
Helodus
Chondrenchelys
Tristychius
Onychoselache
Hamiltonichthys
Scyliorhinus

D

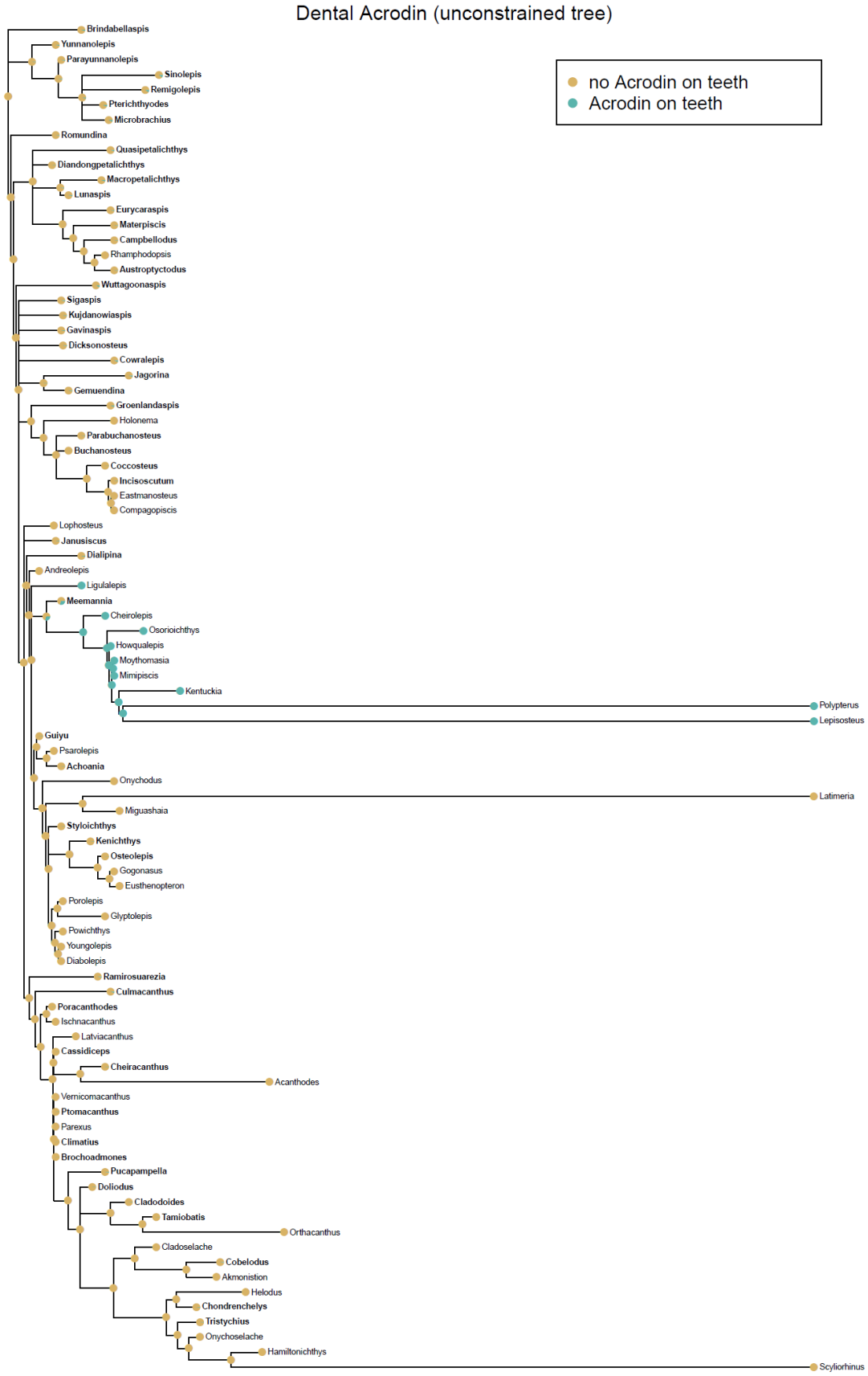
Dental Acrodin (unconstrained tree)
no Acrodin on teeth
Acrodin on teeth
Brindabellaspis
Yunnanolepis
Parayunnanolepis
Sinolepis
Remigolepis
Pterichthyodes
Microbrachius
Romundina
Quasipetalichthys
Diandongpetalichthys
Macropetalichthys
Lunaspis
Eurycaraspis
Materpiscis
Campbellodus
Rhamphodopsis
Austroptyctodus
Wuttagoonaspis
Sigaspis
Kujdanowiaspis
Gavinaspis
Dicksonosteus
Cowralepis
Jagorina
Gemuendina
Groenlandaspis
Holonema
Parabuchanosteus
Buchanosteus
Coccosteus
Incisoscutum
Eastmanosteus
Compagopiscis
Lophosteus
Janusiscus
Dialipina
Andreolepis
Ligulalepis
Meemannia
Cheirolepis
Osorioichthys
Howqualepis
Moythomasia
Mimipiscis
Kentuckia
Polypterus
Lepisosteus
Guiyu
Psarolepis
Achoania
Onychodus
Latimeria
Miguashaia
Styloichthys
Kenichthys
Osteolepis
Gogonasus
Eusthenopteron
Porolepis
Glyptolepis
Powichthys
Youngolepis
Diabolepis
Ramirosuarezia
Culmacanthus
Poracanthodes
Ischnacanthus
Latviacanthus
Cassidiceps
Cheiracanthus
Acanthodes
Vernicomacanthus
Ptomacanthus
Parexus
Climatius
Brochoadmones
Pucapampella
Doliodus
Cladodoides
Tamiobatis
Orthacanthus
Cladoselache
Cobelodus
Akmonistion
Helodus
Chondrenchelys
Tristychius
Onychoselache
Hamiltonichthys
Scyliorhinus

E

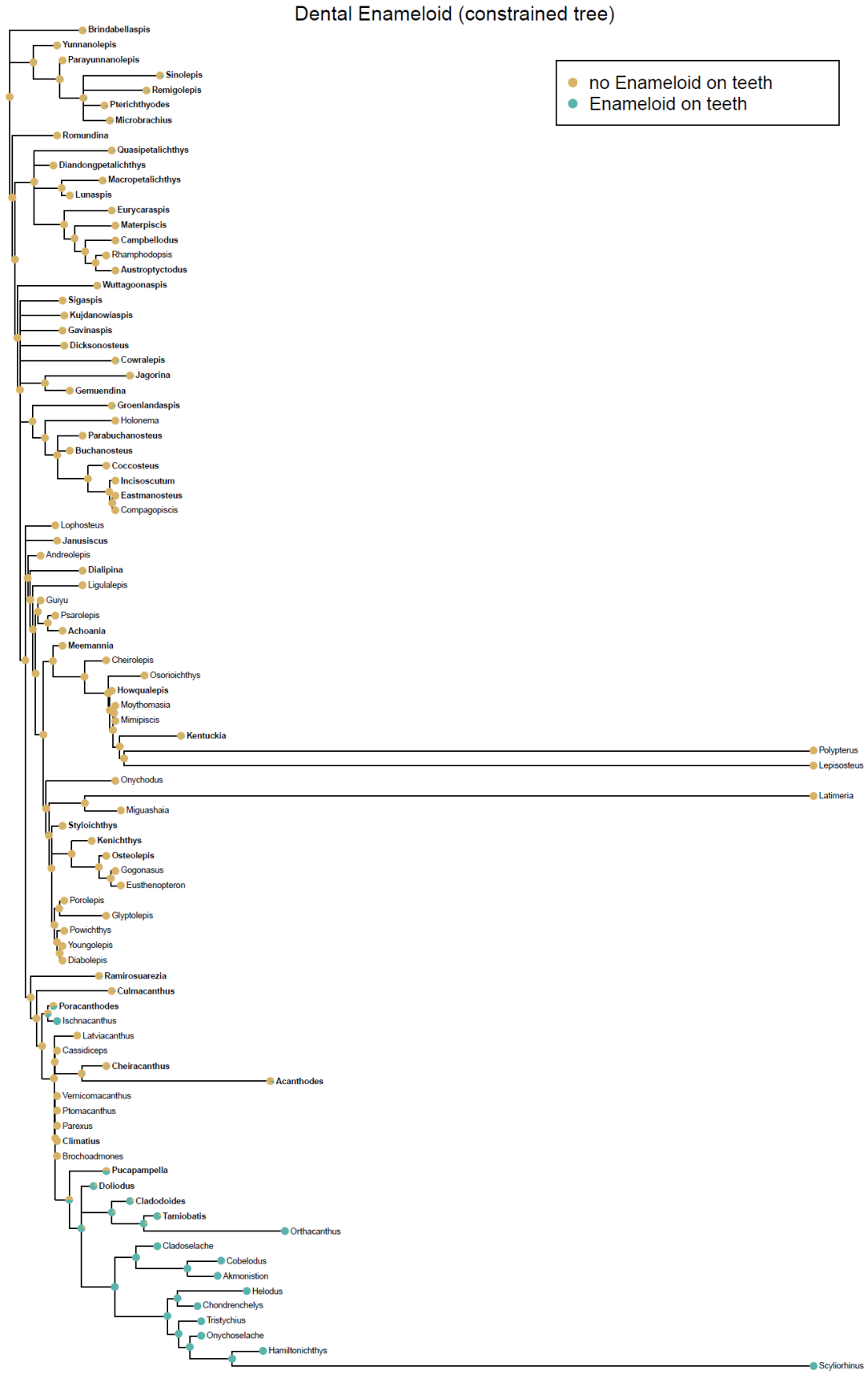
Dental Enameloid (constrained tree)
no Enameloid on teeth
Enameloid on teeth
Brindabellaspis
Yunnanolepis
Parayunnanolepis
Sinolepis
Remigolepis
Pterichthyodes
Microbrachius
Romundina
Quasipetalichthys
Diandongpetalichthys
Macropetalichthys
Lunaspis
Eurycaraspis
Materpiscis
Campbellodus
Rhamphodopsis
Austroptyctodus
Wuttagoonaspis
Sigaspis
Kujdanowiaspis
Gavinaspis
Dicksonosteus
Cowralepis
Jagorina
Gemuendina
Groenlandaspis
Holonema
Parabuchanosteus
Buchanosteus
Coccosteus
Incisoscutum
Eastmanosteus
Compagopiscis
Lophosteus
Janusiscus
Andreolepis
Dialipina
Ligulalepis
Guiyu
Psarolepis
Achoania
Meemannia
Cheirolepis
Osorioichthys
Howqualepis
Moythomasia
Mimipiscis
Kentuckia
Polypterus
Lepisosteus
Onychodus
Latimeria
Miguashaia
Styloichthys
Kenichthys
Osteolepis
Gogonasus
Eusthenopteron
Porolepis
Glyptolepis
Powichthys
Youngolepis
Diabolepis
Ramirosuarezia
Culmacanthus
Poracanthodes
Ischnacanthus
Latviacanthus
Cassidiceps
Cheiracanthus
Acanthodes
Vernicomacanthus
Ptomacanthus
Parexus
Climatius
Brochoadmones
Pucapampella
Doliodus
Cladodoides
Tamiobatis
Orthacanthus
Cladoselache
Cobelodus
Akmonistion
Helodus
Chondrenchelys
Tristychius
Onychoselache
Hamiltonichthys
Scyliorhinus

F

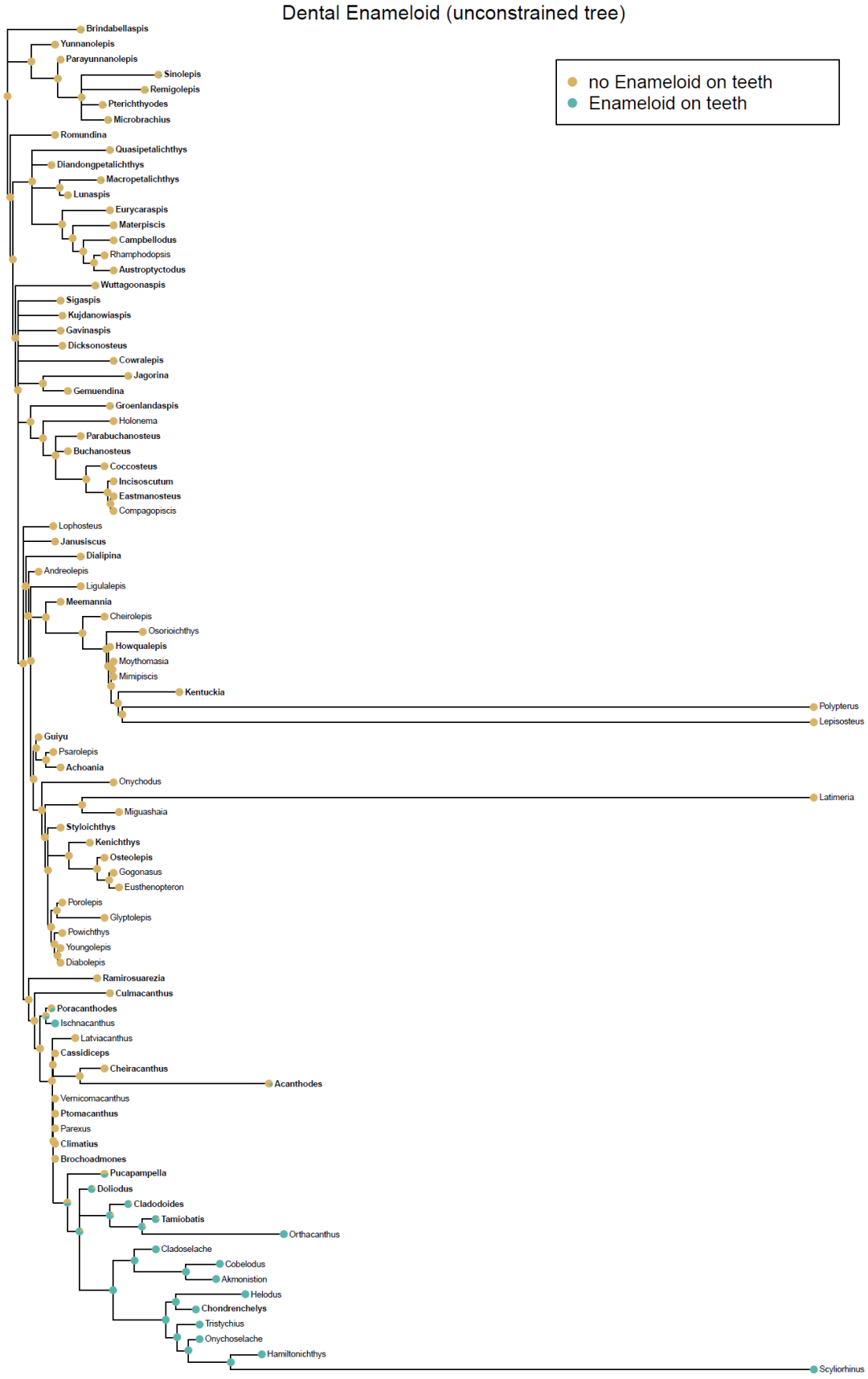
Dental Enameloid (unconstrained tree)
no Enameloid on teeth
Enameloid on teeth
Brindabellaspis
Yunnanolepis
Parayunnanolepis
Sinolepis
Remigolepis
Pterichthyodes
Microbrachius
Romundina
Quasipetalichthys
Diandongpetalichthys
Macropetalichthys
Lunaspis
Eurycaraspis
Materpiscis
Campbellodus
Rhamphodopsis
Austroptyctodus
Wuttagoonaspis
Sigaspis
Kujdanowiaspis
Gavinaspis
Dicksonosteus
Cowralepis
Jagorina
Gemuendina
Groenlandaspis
Holonema
Parabuchanosteus
Buchanosteus
Coccosteus
Incisoscutum
Eastmanosteus
Compagopiscis
Lophosteus
Janusiscus
Dialipina
Andreolepis
Ligulalepis
Meemannia
Cheirolepis
Osorioichthys
Howqualepis
Moythomasia
Mimipiscis
Kentuckia
Polypterus
Lepisosteus
Guiyu
Psarolepis
Achoania
Onychodus
Latimeria
Miguashaia
Styloichthys
Kenichthys
Osteolepis
Gogonasus
Eusthenopteron
Porolepis
Glyptolepis
Powichthys
Youngolepis
Diabolepis
Ramirosuarezia
Culmacanthus
Poracanthodes
Ischnacanthus
Latviacanthus
Cassidiceps
Cheiracanthus
Acanthodes
Vernicomacanthus
Ptomacanthus
Parexus
Climatius
Brochoadmones
Pucapampella
Doliodus
Cladodoides
Tamiobatis
Orthacanthus
Cladoselache
Cobelodus
Akmonistion
Helodus
Chondrenchelys
Tristychius
Onychoselache
Hamiltonichthys
Scyliorhinus

G

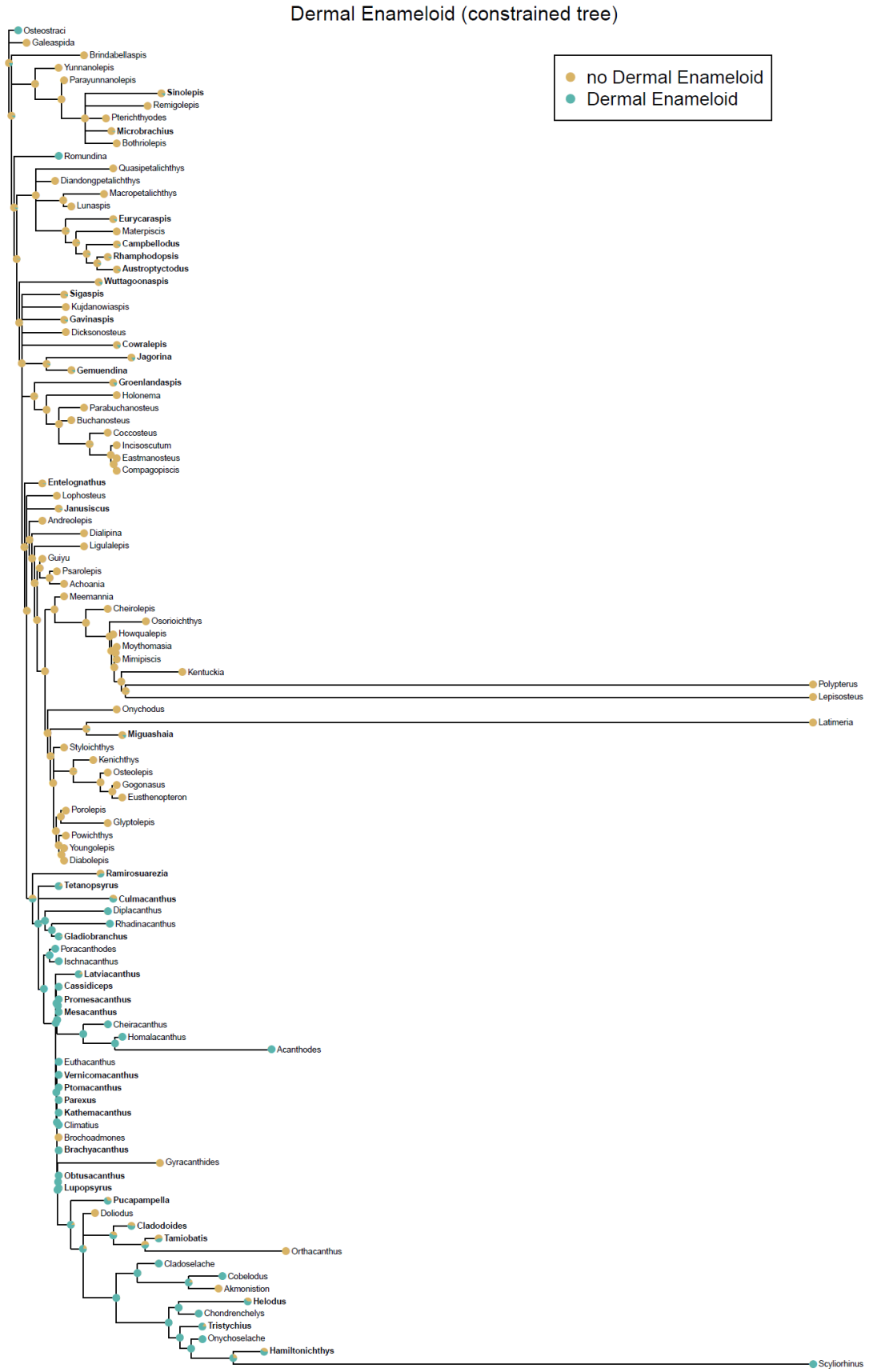
Dermal Enameloid (constrained tree)
no Dermal Enameloid
Dermal Enameloid
Osteostraci
Galeaspida
Brindabellaspis
Yunnanolepis
Parayunnanolepis
Sinolepis
Remigolepis
Pterichthyodes
Microbrachius
Bothriolepis
Romundina
Quasipetalichthys
Diandongpetalichthys
Macropetalichthys
Lunaspis
Eurycaraspis
Materpiscis
Campbellodus
Rhamphodopsis
Austroptyctodus
Wuttagoonaspis
Sigaspis
Kujdanowiaspis
Gavinaspis
Dicksonosteus
Cowralepis
Jagorina
Gemuendina
Groenlandaspis
Holonema
Parabuchanosteus
Buchanosteus
Coccosteus
Incisoscutum
Eastmanosteus
Compagopiscis
Entelognathus
Lophosteus
Janusiscus
Andreolepis
Dialipina
Ligulalepis
Guiyu
Psarolepis
Achoania
Meemannia
Cheirolepis
Osorioichthys
Howqualepis
Moythomasia
Mimipiscis
Kentuckia
Polypterus
Lepisosteus
Onychodus
Latimeria
Miguashaia
Styloichthys
Kenichthys
Osteolepis
Gogonasus
Eusthenopteron
Porolepis
Glyptolepis
Powichthys
Youngolepis
Diabolepis
Ramirosuarezia
Tetanopsyrus
Culmacanthus
Diplacanthus
Rhadinacanthus
Gladiobranchus
Poracanthodes
Ischnacanthus
Latviacanthus
Cassidiceps
Promesacanthus
Mesacanthus
Cheiracanthus
Homalacanthus
Acanthodes
Euthacanthus
Vernicomacanthus
Ptomacanthus
Parexus
Kathemacanthus
Climatius
Brochoadmones
Brachyacanthus
Gyracanthides
Obtusacanthus
Lupopsyrus
Pucapampella
Doliodus
Cladodoides
Tamiobatis
Orthacanthus
Cladoselache
Cobelodus
Akmonistion
Helodus
Chondrenchelys
Tristychius
Onychoselache
Hamiltonichthys
Scyliorhinus

H

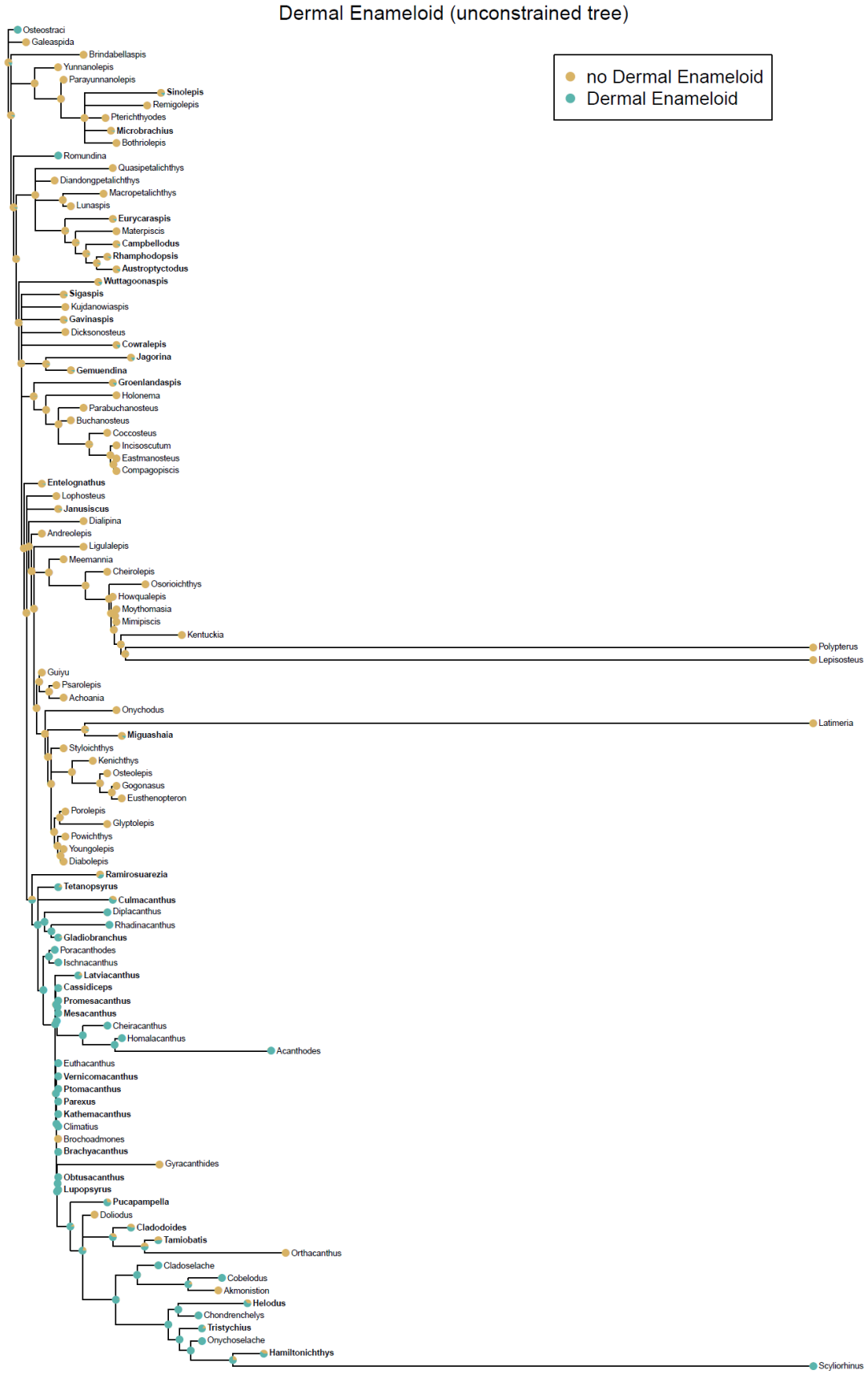
Dermal Enameloid (unconstrained tree)
no Dermal Enameloid
Dermal Enameloid
Osteostraci
Galeaspida
Brindabellaspis
Yunnanolepis
Parayunnanolepis
Sinolepis
Remigolepis
Pterichthyodes
Microbrachius
Bothriolepis
Romundina
Quasipetalichthys
Diandongpetalichthys
Macropetalichthys
Lunaspis
Eurycaraspis
Materpiscis
Campbellodus
Rhamphodopsis
Austroptyctodus
Wuttagoonaspis
Sigaspis
Kujdanowiaspis
Gavinaspis
Dicksonosteus
Cowralepis
Jagorina
Gemuendina
Groenlandaspis
Holonema
Parabuchanosteus
Buchanosteus
Coccosteus
Incisoscutum
Eastmanosteus
Compagopiscis
Entelognathus
Lophosteus
Janusiscus
Dialipina
Andreolepis
Ligulalepis
Meemannia
Cheirolepis
Osorioichthys
Howqualepis
Moythomasia
Mimipiscis
Kentuckia
Polypterus
Lepisosteus
Guiyu
Psarolepis
Achoania
Onychodus
Latimeria
Miguashaia
Styloichthys
Kenichthys
Osteolepis
Gogonasus
Eusthenopteron
Porolepis
Glyptolepis
Powichthys
Youngolepis
Diabolepis
Ramirosuarezia
Tetanopsyrus
Culmacanthus
Diplacanthus
Rhadinacanthus
Gladiobranchus
Poracanthodes
Ischnacanthus
Latviacanthus
Cassidiceps
Promesacanthus
Mesacanthus
Cheiracanthus
Homalacanthus
Acanthodes
Euthacanthus
Vernicomacanthus
Ptomacanthus
Parexus
Kathemacanthus
Climatius
Brochoadmones
Brachyacanthus
Gyracanthides
Obtusacanthus
Lupopsyrus
Pucapampella
Doliodus
Cladodoides
Tamiobatis
Orthacanthus
Cladoselache
Cobelodus
Akmonistion
Helodus
Chondrenchelys
Tristychius
Onychoselache
Hamiltonichthys
Scyliorhinus

I

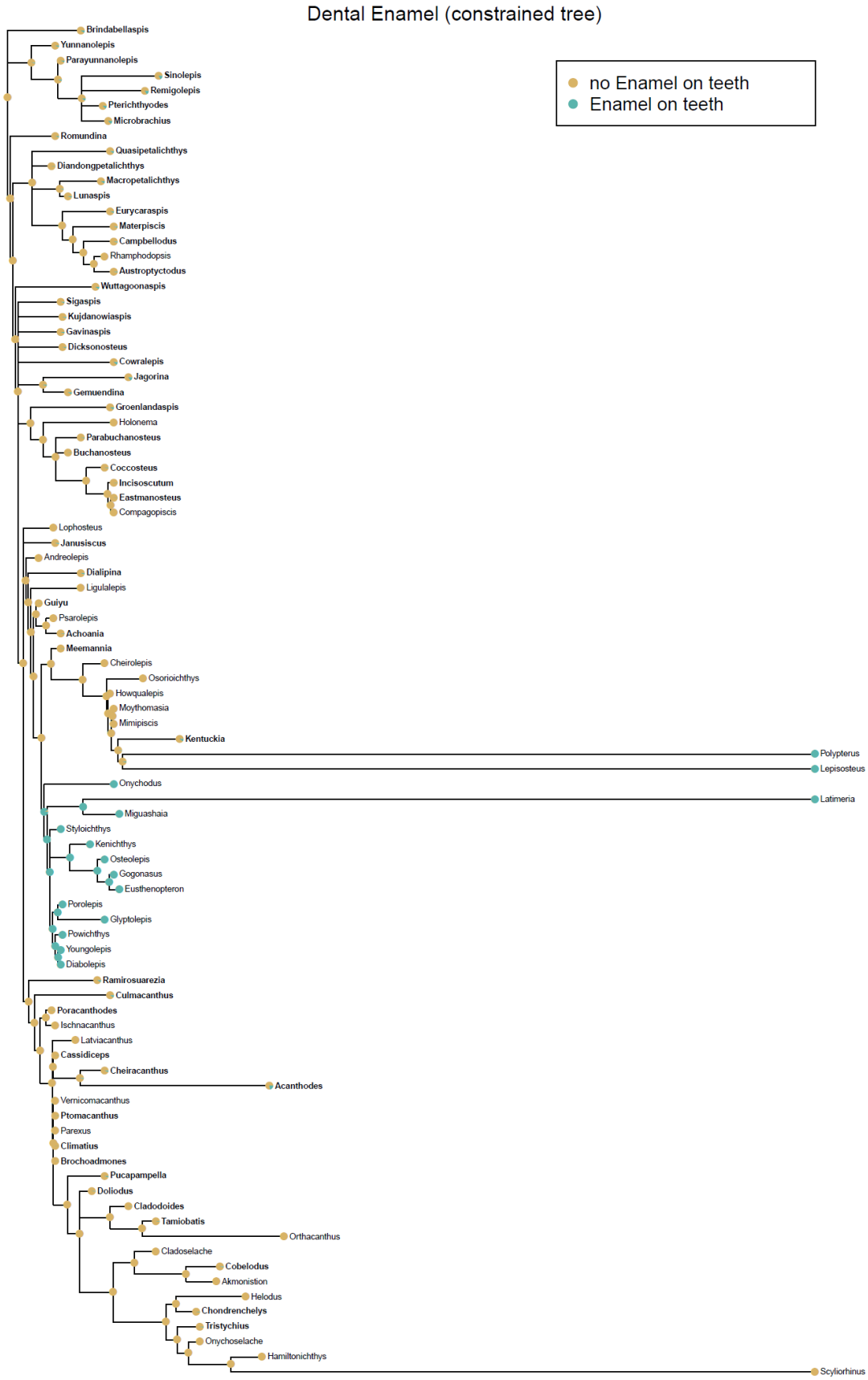
Dental Enamel (constrained tree)
no Enamel on teeth
Enamel on teeth
Brindabellaspis
Yunnanolepis
Parayunnanolepis
Sinolepis
Remigolepis
Pterichthyodes
Microbrachius
Romundina
Quasipetalichthys
Diandongpetalichthys
Macropetalichthys
Lunaspis
Eurycaraspis
Materpiscis
Campbellodus
Rhamphodopsis
Austroptyctodus
Wuttagoonaspis
Sigaspis
Kujdanowiaspis
Gavinaspis
Dicksonosteus
Cowralepis
Jagorina
Gemuendina
Groenlandaspis
Holonema
Parabuchanosteus
Buchanosteus
Coccosteus
Incisoscutum
Eastmanosteus
Compagopiscis
Lophosteus
Janusiscus
Andreolepis
Dialipina
Ligulalepis
Guiyu
Psarolepis
Achoania
Meemannia
Cheirolepis
Osorioichthys
Howqualepis
Moythomasia
Mimipiscis
Kentuckia
Polypterus
Lepisosteus
Onychodus
Latimeria
Miguashaia
Styloichthys
Kenichthys
Osteolepis
Gogonasus
Eusthenopteron
Porolepis
Glyptolepis
Powichthys
Youngolepis
Diabolepis
Ramirosuarezia
Culmacanthus
Poracanthodes
Ischnacanthus
Latviacanthus
Cassidiceps
Cheiracanthus
Acanthodes
Vernicomacanthus
Ptomacanthus
Parexus
Climatius
Brochoadmones
Pucapampella
Doliodus
Cladodoides
Tamiobatis
Orthacanthus
Cladoselache
Cobelodus
Akmonistion
Helodus
Chondrenchelys
Tristychius
Onychoselache
Hamiltonichthys
Scyliorhinus

J

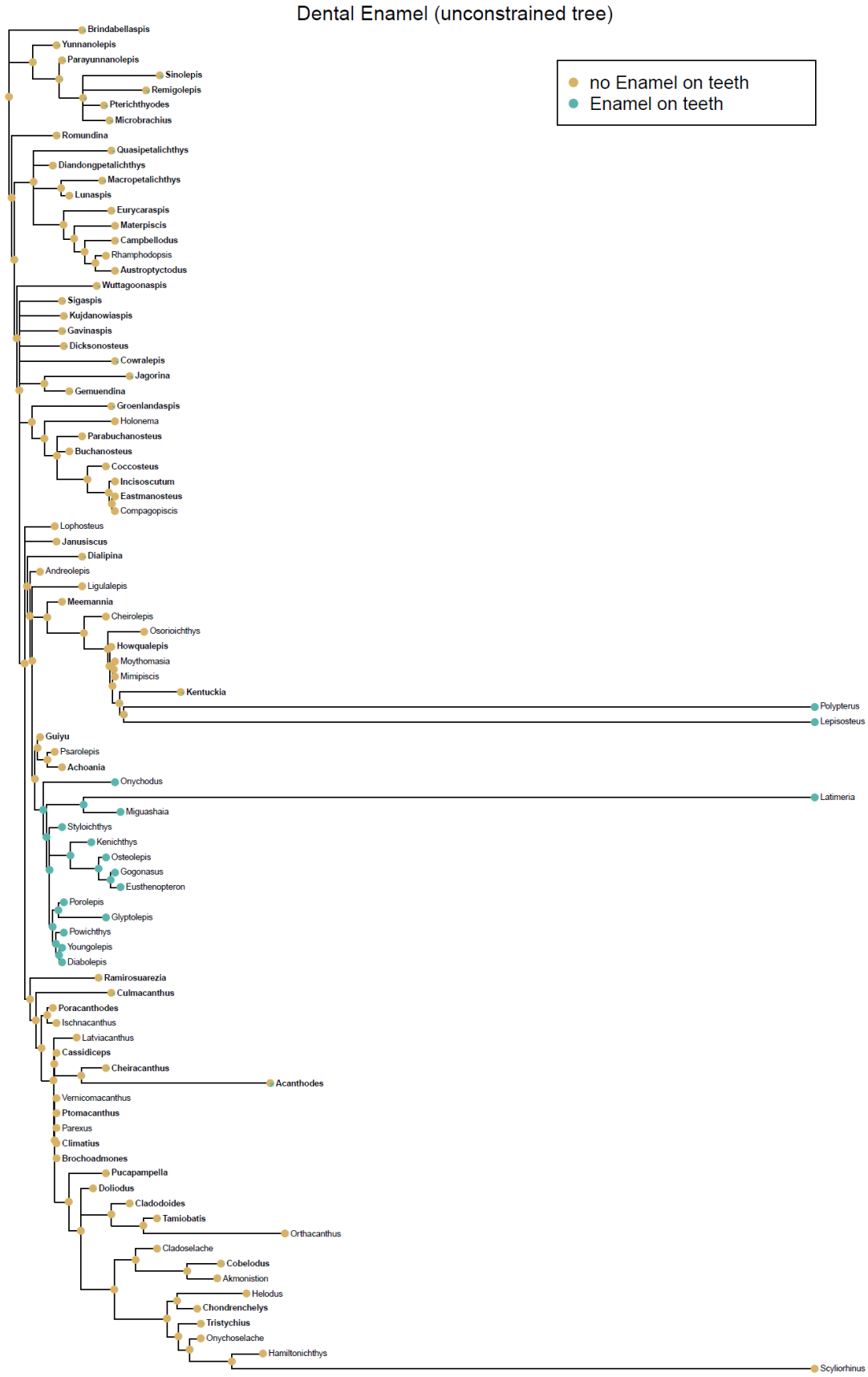
Dental Enamel (unconstrained tree)
no Enamel on teeth
Enamel on teeth
Brindabellaspis
Yunnanolepis
Parayunnanolepis
Sinolepis
Remigolepis
Pterichthyodes
Microbrachius
Romundina
Quasipetalichthys
Diandongpetalichthys
Macropetalichthys
Lunaspis
Eurycaraspis
Materpiscis
Campbellodus
Rhamphodopsis
Austroptyctodus
Wuttagoonaspis
Sigaspis
Kujdanowiaspis
Gavinaspis
Dicksonosteus
Cowralepis
Jagorina
Gemuendina
Groenlandaspis
Holonema
Parabuchanosteus
Buchanosteus
Coccosteus
Incisoscutum
Eastmanosteus
Compagopiscis
Lophosteus
Janusiscus
Dialipina
Andreolepis
Ligulalepis
Meemannia
Cheirolepis
Osorioichthys
Howqualepis
Moythomasia
Mimipiscis
Kentuckia
Polypterus
Lepisosteus
Guiyu
Psarolepis
Achoania
Onychodus
Latimeria
Miguashaia
Styloichthys
Kenichthys
Osteolepis
Gogonasus
Eusthenopteron
Porolepis
Glyptolepis
Powichthys
Youngolepis
Diabolepis
Ramirosuarezia
Culmacanthus
Poracanthodes
Ischnacanthus
Latviacanthus
Cassidiceps
Cheiracanthus
Acanthodes
Vernicomacanthus
Ptomacanthus
Parexus
Climatius
Brochoadmones
Pucapampella
Doliodus
Cladodoides
Tamiobatis
Orthacanthus
Cladoselache
Cobelodus
Akmonistion
Helodus
Chondrenchelys
Tristychius
Onychoselache
Hamiltonichthys
Scyliorhinus

K

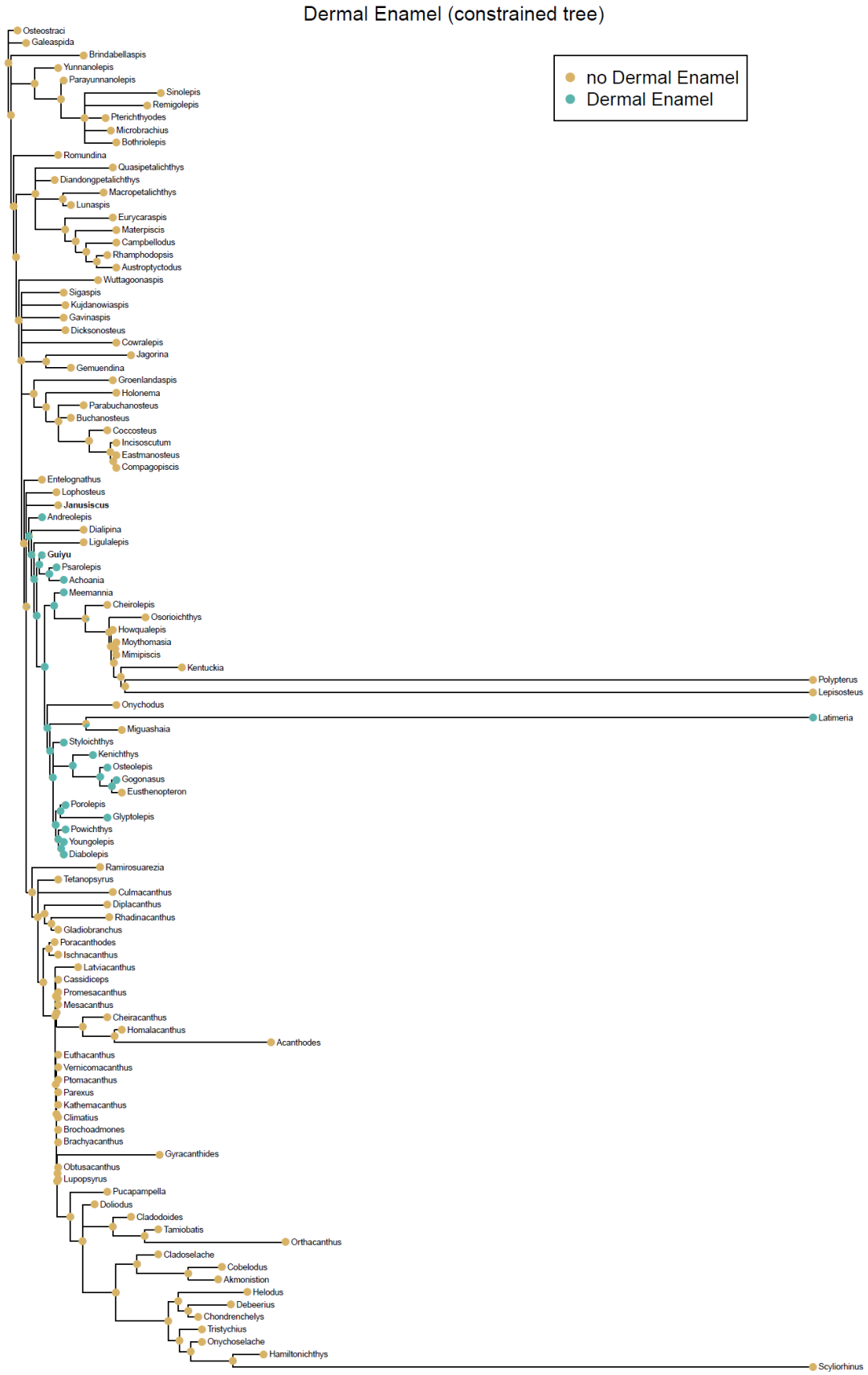
Dermal Enamel (constrained tree)
no Dermal Enamel
Dermal Enamel
Osteostraci
Galeaspida
Brindabellaspis
Yunnanolepis
Parayunnanolepis
Sinolepis
Remigolepis
Pterichthyodes
Microbrachius
Bothriolepis
Romundina
Quasipetalichthys
Diandongpetalichthys
Macropetalichthys
Lunaspis
Eurycaraspis
Materpiscis
Campbellodus
Rhamphodopsis
Austroptyctodus
Wuttagoonaspis
Sigaspis
Kujdanowiaspis
Gavinaspis
Dicksonosteus
Cowralepis
Jagorina
Gemuendina
Groenlandaspis
Holonema
Parabuchanosteus
Buchanosteus
Coccosteus
Incisoscutum
Eastmanosteus
Compagopiscis
Entelognathus
Lophosteus
Janusiscus
Andreolepis
Dialipina
Ligulalepis
Guiyu
Psarolepis
Achoania
Meemannia
Cheirolepis
Osorioichthys
Howqualepis
Moythomasia
Mimipiscis
Kentuckia
Polypterus
Lepisosteus
Onychodus
Latimeria
Miguashaia
Styloichthys
Kenichthys
Osteolepis
Gogonasus
Eusthenopteron
Porolepis
Glyptolepis
Powichthys
Youngolepis
Diabolepis
Ramirosuarezia
Tetanopsyrus
Culmacanthus
Diplacanthus
Rhadinacanthus
Gladiobranchus
Poracanthodes
Ischnacanthus
Latviacanthus
Cassidiceps
Promesacanthus
Mesacanthus
Cheiracanthus
Homalacanthus
Acanthodes
Euthacanthus
Vernicomacanthus
Ptomacanthus
Parexus
Kathemacanthus
Climatius
Brochoadmones
Brachyacanthus
Gyracanthides
Obtusacanthus
Lupopsyrus
Pucapampella
Doliodus
Cladodoides
Tamiobatis
Orthacanthus
Cladoselache
Cobelodus
Akmonistion
Helodus
Debeerius
Chondrenchelys
Tristychius
Onychoselache
Hamiltonichthys
Scyliorhinus

L

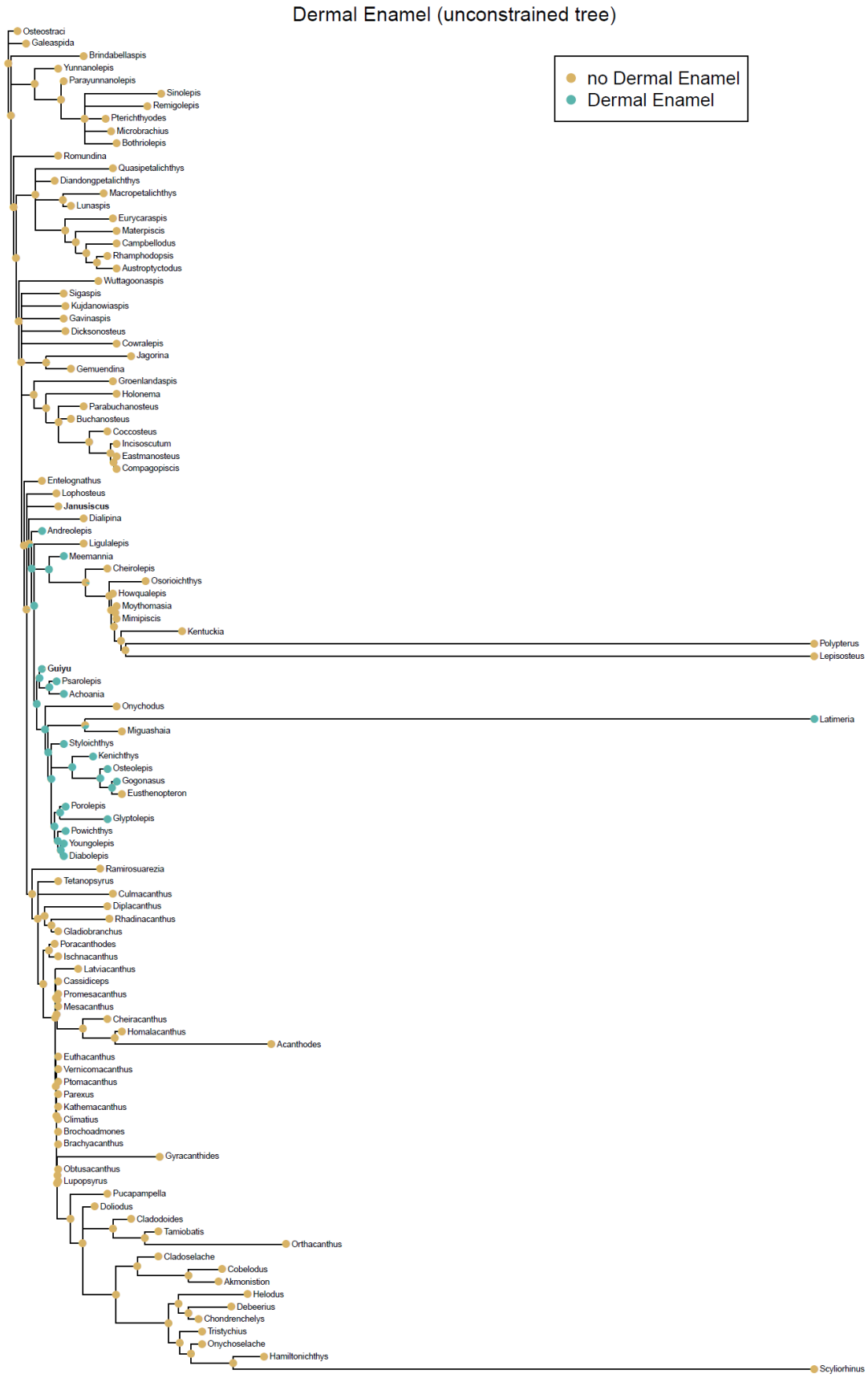
Dermal Enamel (unconstrained tree)
no Dermal Enamel
Dermal Enamel
Osteostraci
Galeaspida
Brindabellaspis
Yunnanolepis
Parayunnanolepis
Sinolepis
Remigolepis
Pterichthyodes
Microbrachius
Bothriolepis
Romundina
Quasipetalichthys
Diandongpetalichthys
Macropetalichthys
Lunaspis
Eurycaraspis
Materpiscis
Campbellodus
Rhamphodopsis
Austroptyctodus
Wuttagoonaspis
Sigaspis
Kujdanowiaspis
Gavinaspis
Dicksonosteus
Cowralepis
Jagorina
Gemuendina
Groenlandaspis
Holonema
Parabuchanosteus
Buchanosteus
Coccosteus
Incisoscutum
Eastmanosteus
Compagopiscis
Entelognathus
Lophosteus
Janusiscus
Dialipina
Andreolepis
Ligulalepis
Meemannia
Cheirolepis
Osorioichthys
Howqualepis
Moythomasia
Mimipiscis
Kentuckia
Polypterus
Lepisosteus
Guiyu
Psarolepis
Achoania
Onychodus
Latimeria
Miguashaia
Styloichthys
Kenichthys
Osteolepis
Gogonasus
Eusthenopteron
Porolepis
Glyptolepis
Powichthys
Youngolepis
Diabolepis
Ramirosuarezia
Tetanopsyrus
Culmacanthus
Diplacanthus
Rhadinacanthus
Gladiobranchus
Poracanthodes
Ischnacanthus
Latviacanthus
Cassidiceps
Promesacanthus
Mesacanthus
Cheiracanthus
Homalacanthus
Acanthodes
Euthacanthus
Vernicomacanthus
Ptomacanthus
Parexus
Kathemacanthus
Climatius
Brochoadmones
Brachyacanthus
Gyracanthides
Obtusacanthus
Lupopsyrus
Pucapampella
Doliodus
Cladodoides
Tamiobatis
Orthacanthus
Cladoselache
Cobelodus
Akmonistion
Helodus
Debeerius
Chondrenchelys
Tristychius
Onychoselache
Hamiltonichthys
Scyliorhinus

M

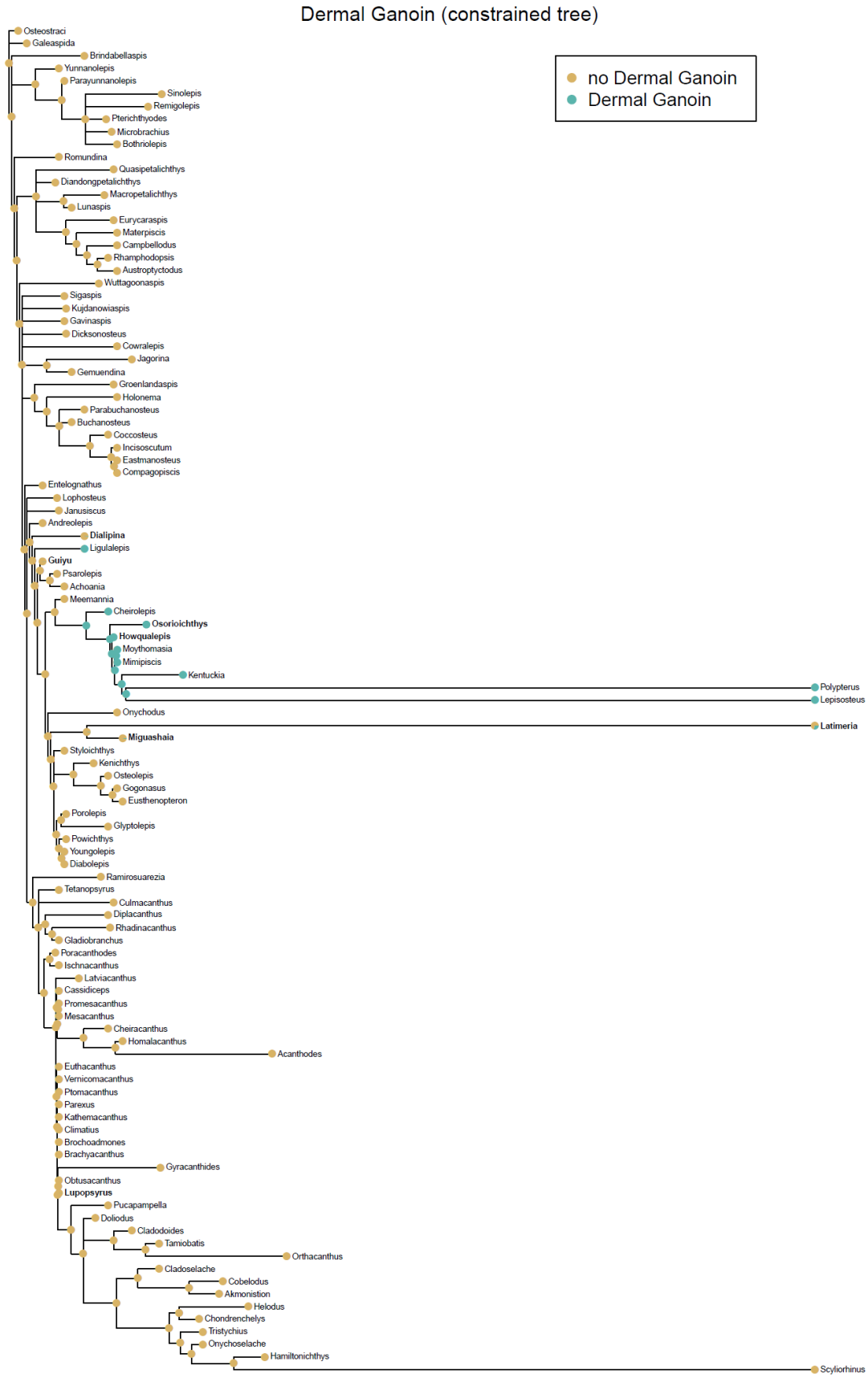
Dermal Ganoin (constrained tree)
no Dermal Ganoin
Dermal Ganoin
Osteostraci
Galeaspida
Brindabellaspis
Yunnanolepis
Parayunnanolepis
Sinolepis
Remigolepis
Pterichthyodes
Microbrachius
Bothriolepis
Romundina
Quasipetalichthys
Diandongpetalichthys
Macropetalichthys
Lunaspis
Eurycaraspis
Materpiscis
Campbellodus
Rhamphodopsis
Austroptyctodus
Wuttagoonaspis
Sigaspis
Kujdanowiaspis
Gavinaspis
Dicksonosteus
Cowralepis
Jagorina
Gemuendina
Groenlandaspis
Holonema
Parabuchanosteus
Buchanosteus
Coccosteus
Incisoscutum
Eastmanosteus
Compagopiscis
Entelognathus
Lophosteus
Janusiscus
Andreolepis
Dialipina
Ligulalepis
Guiyu
Psarolepis
Achoania
Meemannia
Cheirolepis
Osorioichthys
Howqualepis
Moythomasia
Mimipiscis
Kentuckia
Polypterus
Lepisosteus
Onychodus
Latimeria
Miguashaia
Styloichthys
Kenichthys
Osteolepis
Gogonasus
Eusthenopteron
Porolepis
Glyptolepis
Powichthys
Youngolepis
Diabolepis
Ramirosuarezia
Tetanopsyrus
Culmacanthus
Diplacanthus
Rhadinacanthus
Gladiobranchus
Poracanthodes
Ischnacanthus
Latviacanthus
Cassidiceps
Promesacanthus
Mesacanthus
Cheiracanthus
Homalacanthus
Acanthodes
Euthacanthus
Vernicomacanthus
Ptomacanthus
Parexus
Kathemacanthus
Climatius
Brochoadmones
Brachyacanthus
Gyracanthides
Obtusacanthus
Lupopsyrus
Pucapampella
Doliodus
Cladodoides
Tamiobatis
Orthacanthus
Cladoselache
Cobelodus
Akmonistion
Helodus
Chondrenchelys
Tristychius
Onychoselache
Hamiltonichthys
Scyliorhinus

N

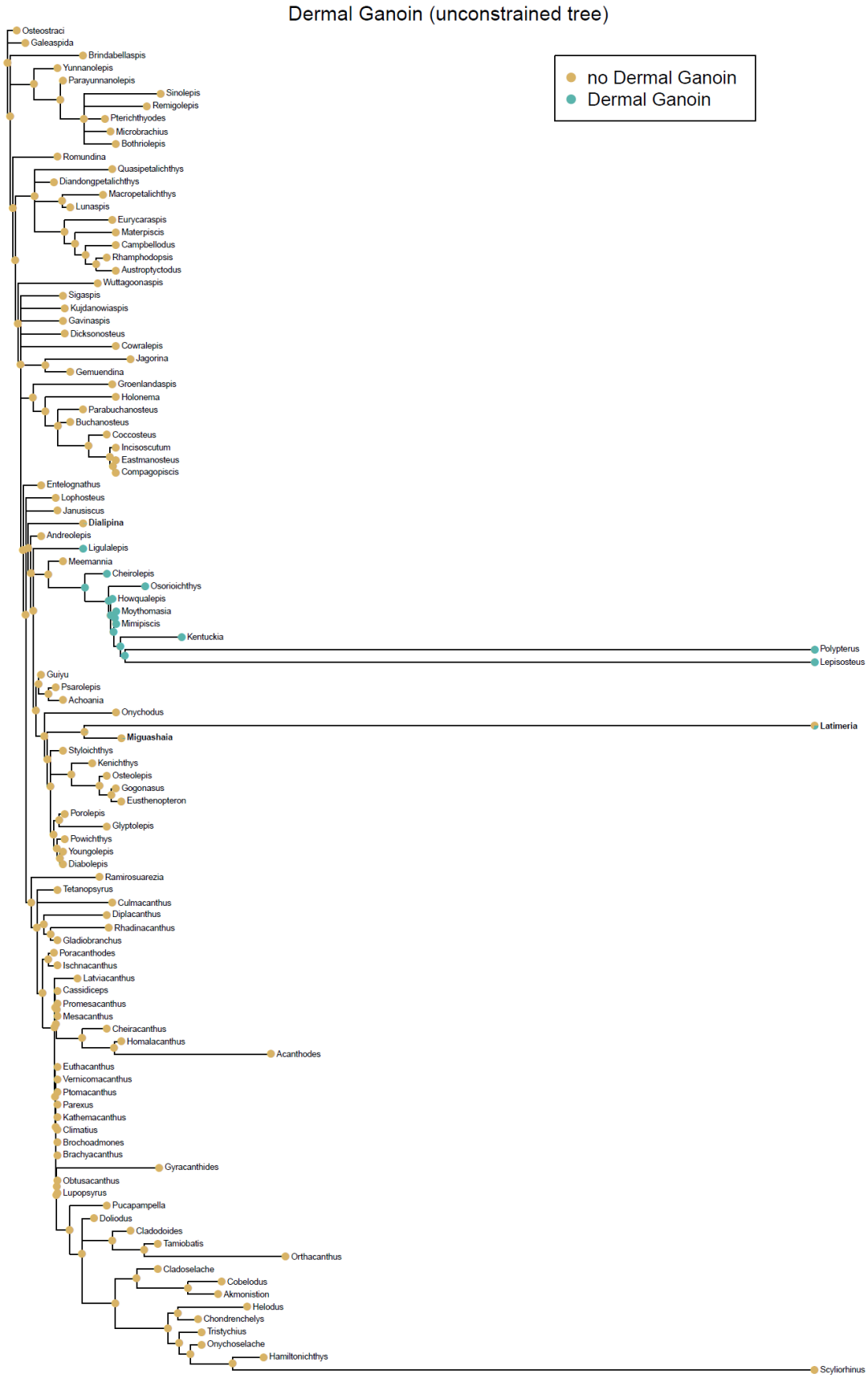
Dermal Ganoin (unconstrained tree)
no Dermal Ganoin
Dermal Ganoin
Osteostraci
Galeaspida
Brindabellaspis
Yunnanolepis
Parayunnanolepis
Sinolepis
Remigolepis
Pterichthyodes
Microbrachius
Bothriolepis
Romundina
Quasipetalichthys
Diandongpetalichthys
Macropetalichthys
Lunaspis
Eurycaraspis
Materpiscis
Campbellodus
Rhamphodopsis
Austroptyctodus
Wuttagoonaspis
Sigaspis
Kujdanowiaspis
Gavinaspis
Dicksonosteus
Cowralepis
Jagorina
Gemuendina
Groenlandaspis
Holonema
Parabuchanosteus
Buchanosteus
Coccosteus
Incisoscutum
Eastmanosteus
Compagopiscis
Entelognathus
Lophosteus
Janusiscus
Dialipina
Andreolepis
Ligulalepis
Meemannia
Cheirolepis
Osorioichthys
Howqualepis
Moythomasia
Mimipiscis
Kentuckia
Polypterus
Lepisosteus
Guiyu
Psarolepis
Achoania
Onychodus
Latimeria
Miguashaia
Styloichthys
Kenichthys
Osteolepis
Gogonasus
Eusthenopteron
Porolepis
Glyptolepis
Powichthys
Youngolepis
Diabolepis
Ramirosuarezia
Tetanopsyrus
Culmacanthus
Diplacanthus
Rhadinacanthus
Gladiobranchus
Poracanthodes
Ischnacanthus
Latviacanthus
Cassidiceps
Promesacanthus
Mesacanthus
Cheiracanthus
Homalacanthus
Acanthodes
Euthacanthus
Vernicomacanthus
Ptomacanthus
Parexus
Kathemacanthus
Climatius
Brochoadmones
Brachyacanthus
Gyracanthides
Obtusacanthus
Lupopsyrus
Pucapampella
Doliodus
Cladodoides
Tamiobatis
Orthacanthus
Cladoselache
Cobelodus
Akmonistion
Helodus
Chondrenchelys
Tristychius
Onychoselache
Hamiltonichthys
Scyliorhinus

O

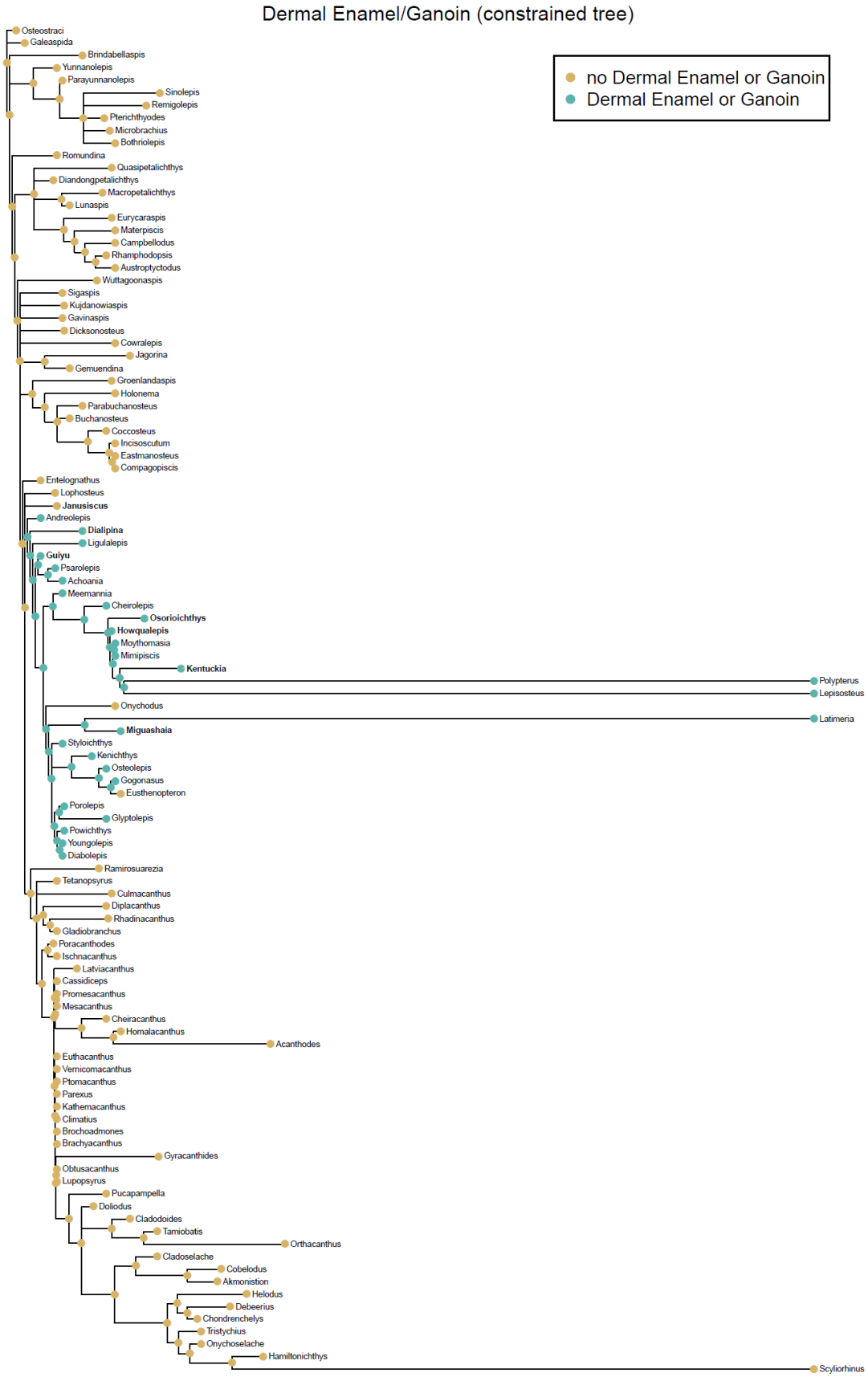
Dermal Enamel/Ganoin (constrained tree)
no Dermal Enamel or Ganoin
Dermal Enamel or Ganoin
Osteostraci
Galeaspida
Brindabellaspis
Yunnanolepis
Parayunnanolepis
Sinolepis
Remigolepis
Pterichthyodes
Microbrachius
Bothriolepis
Romundina
Quasipetalichthys
Diandongpetalichthys
Macropetalichthys
Lunaspis
Eurycaraspis
Materpiscis
Campbellodus
Rhamphodopsis
Austroptyctodus
Wuttagoonaspis
Sigaspis
Kujdanowiaspis
Gavinaspis
Dicksonosteus
Cowralepis
Jagorina
Gemuendina
Groenlandaspis
Holonema
Parabuchanosteus
Buchanosteus
Coccosteus
Incisoscutum
Eastmanosteus
Compagopiscis
Entelognathus
Lophosteus
Janusiscus
Andreolepis
Dialipina
Ligulalepis
Guiyu
Psarolepis
Achoania
Meemannia
Cheirolepis
Osorioichthys
Howqualepis
Moythomasia
Mimipiscis
Kentuckia
Polypterus
Lepisosteus
Onychodus
Latimeria
Miguashaia
Styloichthys
Kenichthys
Osteolepis
Gogonasus
Eusthenopteron
Porolepis
Glyptolepis
Powichthys
Youngolepis
Diabolepis
Ramirosuarezia
Tetanopsyrus
Culmacanthus
Diplacanthus
Rhadinacanthus
Gladiobranchus
Poracanthodes
Ischnacanthus
Latviacanthus
Cassidiceps
Promesacanthus
Mesacanthus
Cheiracanthus
Homalacanthus
Acanthodes
Euthacanthus
Vernicomacanthus
Ptomacanthus
Parexus
Kathemacanthus
Climatius
Brochoadmones
Brachyacanthus
Gyracanthides
Obtusacanthus
Lupopsyrus
Pucapampella
Doliodus
Cladodoides
Tamiobatis
Orthacanthus
Cladoselache
Cobelodus
Akmonistion
Helodus
Debeerius
Chondrenchelys
Tristychius
Onychoselache
Hamiltonichthys
Scyliorhinus

P

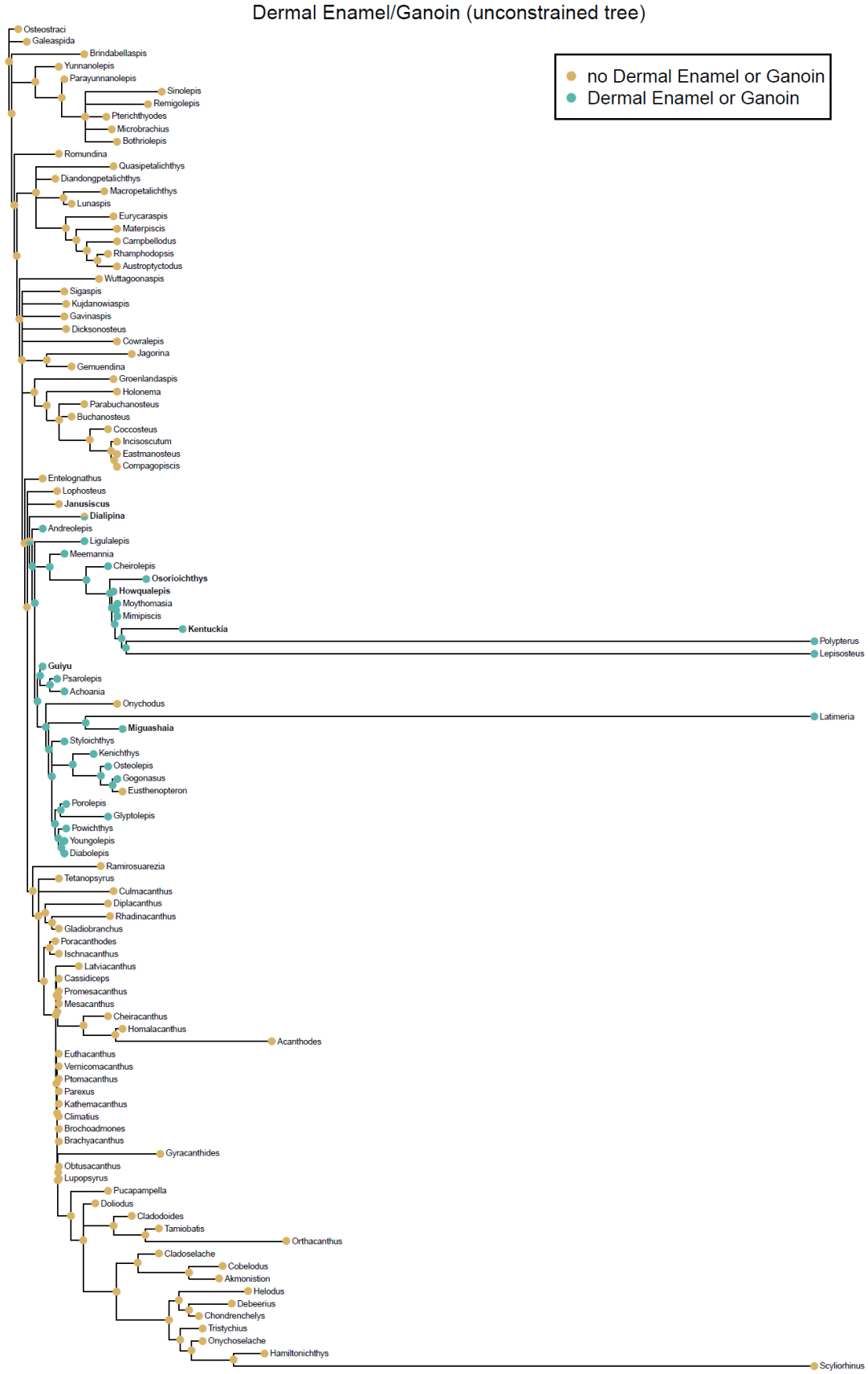
Dermal Enamel/Ganoin (unconstrained tree)
no Dermal Enamel or Ganoin
Dermal Enamel or Ganoin
Osteostraci
Galeaspida
Brindabellaspis
Yunnanolepis
Parayunnanolepis
Sinolepis
Remigolepis
Pterichthyodes
Microbrachius
Bothriolepis
Romundina
Quasipetalichthys
Diandongpetalichthys
Macropetalichthys
Lunaspis
Eurycaraspis
Materpiscis
Campbellodus
Rhamphodopsis
Austroptyctodus
Wuttagoonaspis
Sigaspis
Kujdanowiaspis
Gavinaspis
Dicksonosteus
Cowralepis
Jagorina
Gemuendina
Groenlandaspis
Holonema
Parabuchanosteus
Buchanosteus
Coccosteus
Incisoscutum
Eastmanosteus
Compagopiscis
Entelognathus
Lophosteus
Janusiscus
Dialipina
Andreolepis
Ligulalepis
Meemannia
Cheirolepis
Osorioichthys
Howqualepis
Moythomasia
Mimipiscis
Kentuckia
Polypterus
Lepisosteus
Guiyu
Psarolepis
Achoania
Onychodus
Latimeria
Miguashaia
Styloichthys
Kenichthys
Osteolepis
Gogonasus
Eusthenopteron
Porolepis
Glyptolepis
Powichthys
Youngolepis
Diabolepis
Ramirosuarezia
Tetanopsyrus
Culmacanthus
Diplacanthus
Rhadinacanthus
Gladiobranchus
Poracanthodes
Ischnacanthus
Latviacanthus
Cassidiceps
Promesacanthus
Mesacanthus
Cheiracanthus
Homalacanthus
Acanthodes
Euthacanthus
Vernicomacanthus
Ptomacanthus
Parexus
Kathemacanthus
Climatius
Brochoadmones
Brachyacanthus
Gyracanthides
Obtusacanthus
Lupopsyrus
Pucapampella
Doliodus
Cladodoides
Tamiobatis
Orthacanthus
Cladoselache
Cobelodus
Akmonistion
Helodus
Debeerius
Chondrenchelys
Tristychius
Onychoselache
Hamiltonichthys
Scyliorhinus

Q

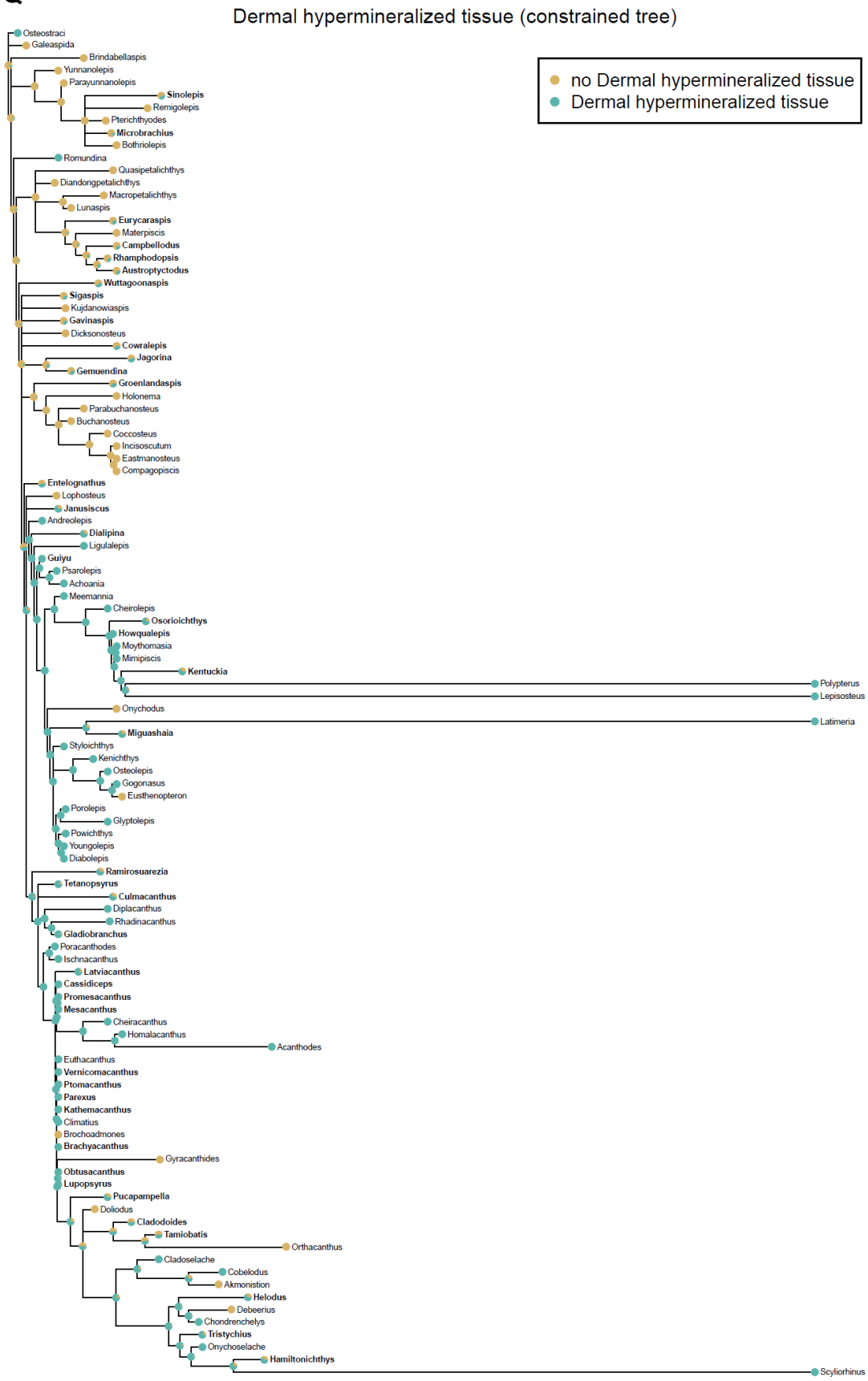
Dermal hypermineralized tissue (constrained tree)
no Dermal hypermineralized tissue
Dermal hypermineralized tissue
Osteostraci
Galeaspida
Brindabellaspis
Yunnanolepis
Parayunnanolepis
Sinolepis
Remigolepis
Pterichthyodes
Microbrachius
Bothriolepis
Romundina
Quasipetalichthys
Diandongpetalichthys
Macropetalichthys
Lunaspis
Eurycaraspis
Materpiscis
Campbellodus
Rhamphodopsis
Austroptyctodus
Wuttagoonaspis
Sigaspis
Kujdanowiaspis
Gavinaspis
Dicksonosteus
Cowralepis
Jagorina
Gemuendina
Groenlandaspis
Holonema
Parabuchanosteus
Buchanosteus
Coccosteus
Incisoscutum
Eastmanosteus
Compagopiscis
Entelognathus
Lophosteus
Janusiscus
Andreolepis
Dialipina
Ligulalepis
Guiyu
Psarolepis
Achoania
Meemannia
Cheirolepis
Osorioichthys
Howqualepis
Moythomasia
Mimipiscis
Kentuckia
Polypterus
Lepisosteus
Onychodus
Latimeria
Miguashaia
Styloichthys
Kenichthys
Osteolepis
Gogonasus
Eusthenopteron
Porolepis
Glyptolepis
Powichthys
Youngolepis
Diabolepis
Ramirosuarezia
Tetanopsyrus
Culmacanthus
Diplacanthus
Rhadinacanthus
Gladiobranchus
Poracanthodes
Ischnacanthus
Latviacanthus
Cassidiceps
Promesacanthus
Mesacanthus
Cheiracanthus
Homalacanthus
Acanthodes
Euthacanthus
Vernicomacanthus
Ptomacanthus
Parexus
Kathemacanthus
Climatius
Brochoadmones
Brachyacanthus
Gyracanthides
Obtusacanthus
Lupopsyrus
Pucapampella
Doliodus
Cladodoides
Tamiobatis
Orthacanthus
Cladoselache
Cobelodus
Akmonistion
Helodus
Debeerius
Chondrenchelys
Tristychius
Onychoselache
Hamiltonichthys
Scyliorhinus

R

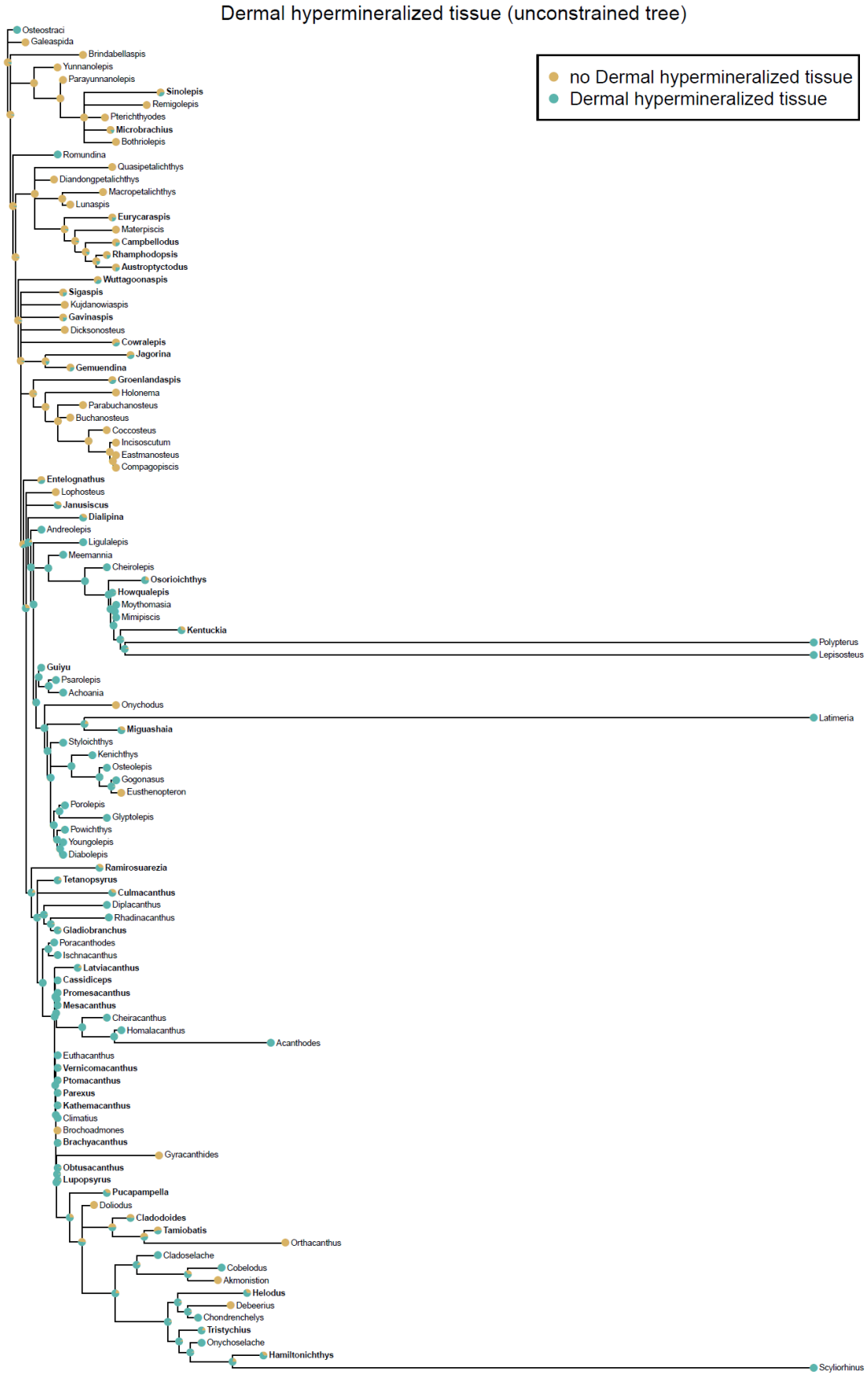
Dermal hypermineralized tissue (unconstrained tree)
no Dermal hypermineralized tissue
Dermal hypermineralized tissue
Osteostraci
Galeaspida
Brindabellaspis
Yunnanolepis
Parayunnanolepis
Sinolepis
Remigolepis
Pterichthyodes
Microbrachius
Bothriolepis
Romundina
Quasipetalichthys
Diandongpetalichthys
Macropetalichthys
Lunaspis
Eurycaraspis
Materpiscis
Campbellodus
Rhamphodopsis
Austroptyctodus
Wuttagoonaspis
Sigaspis
Kujdanowiaspis
Gavinaspis
Dicksonosteus
Cowralepis
Jagorina
Gemuendina
Groenlandaspis
Holonema
Parabuchanosteus
Buchanosteus
Coccosteus
Incisoscutum
Eastmanosteus
Compagopiscis
Entelognathus
Lophosteus
Janusiscus
Dialipina
Andreolepis
Ligulalepis
Meemannia
Cheirolepis
Osorioichthys
Howqualepis
Moythomasia
Mimipiscis
Kentuckia
Polypterus
Lepisosteus
Guiyu
Psarolepis
Achoania
Onychodus
Latimeria
Miguashaia
Styloichthys
Kenichthys
Osteolepis
Gogonasus
Eusthenopteron
Porolepis
Glyptolepis
Powichthys
Youngolepis
Diabolepis
Ramirosuarezia
Tetanopsyrus
Culmacanthus
Diplacanthus
Rhadinacanthus
Gladiobranchus
Poracanthodes
Ischnacanthus
Latviacanthus
Cassidiceps
Promesacanthus
Mesacanthus
Cheiracanthus
Homalacanthus
Acanthodes
Euthacanthus
Vernicomacanthus
Ptomacanthus
Parexus
Kathemacanthus
Climatius
Brochoadmones
Brachyacanthus
Gyracanthides
Obtusacanthus
Lupopsyrus
Pucapampella
Doliodus
Cladodoides
Tamiobatis
Orthacanthus
Cladoselache
Cobelodus
Akmonistion
Helodus
Debeerius
Chondrenchelys
Tristychius
Onychoselache
Hamiltonichthys
Scyliorhinus

S

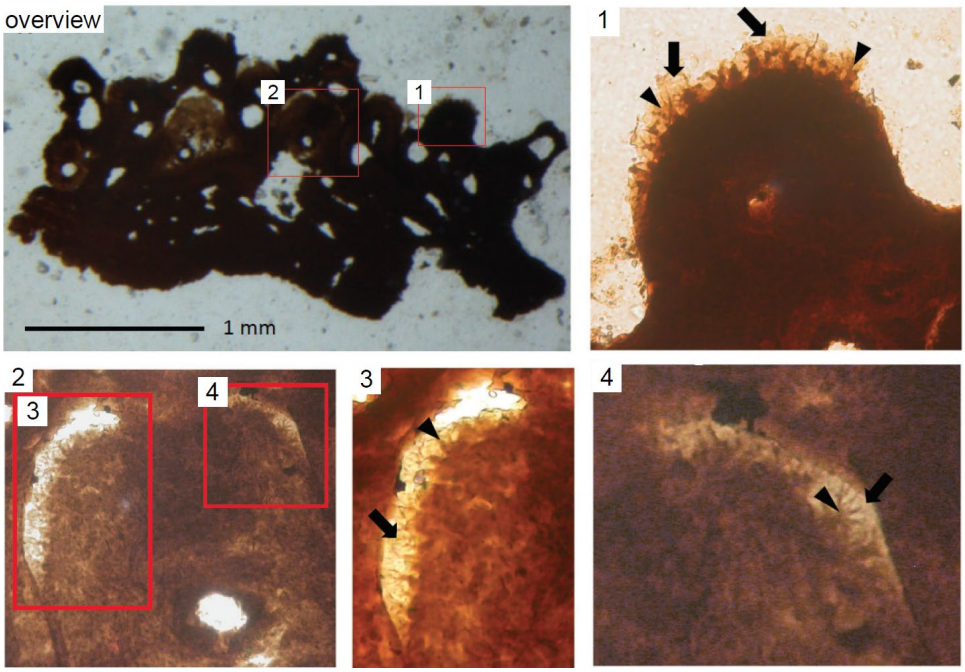

Figure S3. Reconstructing ancestral states of hypermineralized tissues, Related to Figure 5.

(A) Constrained tree used in ancestral state estimation. The GAP clade is constrained to a stem-osteichthyan affinity. Reliabilities of branches are shown at nodes as posterior probabilities.

(B) Unconstrained tree used in ancestral state estimation. The affinity of the GAP clade was unconstrained in the analysis and is resolved to a stem-sarcopterygian affinity. Reliabilities of branches are shown at nodes as posterior probabilities.

(C) Prediction of ancestral states of dental acrodin - GAP clade stem-osteichthyans, shown as pie charts.

(D) Prediction of ancestral states of dental acrodin - GAP clade unconstrained, shown as pie charts.

(E) Prediction of ancestral states of dental enameloid - GAP clade stem-osteichthyans, shown as pie charts.

(F) Prediction of ancestral states of dental enameloid - GAP clade unconstrained, shown as pie charts.

(G) Prediction of ancestral states of dermal enameloid - GAP clade stem-osteichthyans, shown as pie charts.

(H) Prediction of ancestral states of dermal enameloid - GAP clade unconstrained, shown as pie charts.

(I) Prediction of ancestral states of dental enamel - GAP clade stem-osteichthyans, shown as pie charts.

(J) Prediction of ancestral states of dental enamel - GAP clade unconstrained, shown as pie charts.

(K) Prediction of ancestral states of dermal enamel - GAP clade stem-osteichthyans, shown as pie charts.

(L) Prediction of ancestral states of dermal enamel - GAP clade unconstrained, shown as pie charts.

(M) Prediction of ancestral states of dermal ganoin - GAP clade stem-osteichthyans, shown as pie charts.

(N) Prediction of ancestral states of dermal ganoin - GAP clade unconstrained, shown as pie charts.

(O) Prediction of ancestral states of dermal enamel+ganoin - GAP clade stem-osteichthyans, shown as pie charts.

(P) Prediction of ancestral states of dermal enamel or ganoin - GAP clade unconstrained, shown as pie charts.
(Q) Prediction of ancestral states of dermal enamel, ganoin, or enameloid - GAP clade stem-osteichthyans, shown as pie charts.
(R) Prediction of ancestral states of dermal enamel, ganoin, or enameloid - GAP clade unconstrained, shown as pie charts.
(S) Cladoselache skin denticles [specimen P.9294 (NHMUK)]. Detail of boxed areas (1-4) in overview is enlarged. The dentin tubules (arrowheads), protruding through the enameloid layer (arrow), are clearly visible.

	lpq20	lpq8	lpq7	enam	scpp5	scpp7	lpq6	ambn	lpq5	lpq4	scpp3dl	scpp3cl	scpp3bl	scpp3al	odam	lpq3	scpp9	lpq2	lpq1
Coverage[1]	173	16	5	1761	6385	1768	3689	825	12	4	0	0	189	237	209	1119	69	336	2755
FPKM	54	6	2	548	2204	547	1118	262	4	2	0	0	101	106	66	338	21	102	1181
Conf[2]	4	3	1	8	35	31	45	7	1	1	0	0	45	22	5	12	4	9	62

(continued)

	dmp1	scpp1	dsppl1	ibsp	mepe1	mepe2	Spp1	lpq17	lpq16b	lpq16a	lpq15	lpq14	lpq13	lpq12	lpq19	lpq11	lpq18	lpq1	lpq9
Coverage[1]	33	237	33	632	513	991	1089	66	305	264	1010	79	126	951	386	1043	1201	3180	108
FPKM	12	72	11	211	193	313	326	20	125	101	341	23	38	317	117	331	383	1037	35
Conf[2]	1	5	1	7	22	35	11	2	21	16	8	9	5	6	4	9	7	13	7

Table S1. Expression levels gar SCPP genes in the skin, Related to Figure 2. Relative expression levels of SCPP genes in the skin were estimated as fragments per kilobase of transcript per million mapped reads (FPKM values) (Trapnell et al., 2010). [1]Coverage shows the estimate for the absolute depth of read coverage across the whole transcript. [2]Conf represents the 95% confidence interval.

	Dermal characters					Dental characters		
Taxa	Enameloid	Ganoin	Enamel	Enamel+Ganoin	Enamel+Ganoin+Enameloid	Acrodin	Enameloid	Enamel
Galeaspida	0	0	0	0	0	–	–	–
Osteostraci	1	0	0	0	1	–	–	–
Acanthodes	1	0	0	0	1	0	0/1	0/1
Achoania	0	0	1	1	1	0/1	0/1	0/1
Akmonistion	0	0	0	0	0	0	1	0
Austroptyctodus	0/1	0	0	0	0/1	0/1	0/1	0/1
Bothriolepis	0	0	0	0	0	–	–	–
Brachyacanthus	0/1	0	0	0	0/1	–	–	–
Brindabellaspis	0	0	0	0	0	0/1	0/1	0/1
Brochoadmones	0	0	0	0	0	0/1	0/1	0/1
Buchanosteus	0	0	0	0	0	0/1	0/1	0/1
Campbellodus	0/1	0	0	0	0/1	0/1	0/1	0/1
Cassidiceps	0/1	0	0	0	0/1	0/1	0/1	0/1
Cheiracanthus	1	0	0	0	1	0/1	0/1	0/1
Cheirolepis	0	1	0	1	1	1	0	0
Chondrenchelys	1	0	0	0	1	0/1	0/1	0/1
Cladodoides	0/1	0	0	0	0/1	0/1	0/1	0/1
Cladoselache	1	0	0	0	1	0	1	0
Climatius	1	0	0	0	1	0/1	0/1	0/1
Cobelodus	1	0	0	0	1	0/1	0/1	0/1
Coccosteus	0	0	0	0	0	0/1	0/1	0/1
Compagopiscis	0	0	0	0	0	0	0	0
Cowralepis	0/1	0	0	0	0/1	0/1	0/1	0/1
Culmacanthus	0/1	0	0	0	0/1	0/1	0/1	0/1
Debeerius	–	–	0	0	0	–	–	–
Diabolepis	0	0	1	1	1	0	0	1
Dialipina	0	0/1	0	0/1	0/1	0/1	0/1	0/1
Diandongpetalichthys	0	0	0	0	0	0/1	0/1	0/1
Dicksonosteus	0	0	0	0	0	0/1	0/1	0/1
Diplacanthus	1	0	0	0	1	–	–	–
Doliodus	0	0	0	0	0	0/1	0/1	0/1
Eastmanosteus	0	0	0	0	0	0/1	0/1	0/1
Entelognathus	0/1	0	0	0	0/1	–	–	–
Eurycaraspis	0/1	0	0	0	0/1	0/1	0/1	0/1
Eusthenopteron	0	0	0	0	0	0	0	1
Euthacanthus	1	0	0	0	1	–	–	–
Gavinaspis	0/1	0	0	0	0/1	0/1	0/1	0/1
Gemuendina	0/1	0	0	0	0/1	0/1	0/1	0/1
Gladiobranchus,	0/1	0	0	0	0/1	–	–	–
Glyptolepis	0	0	1	1	1	0	0	1
Gogonasus	0	0	1	1	1	0	0	1
Groenlandaspis	0/1	0	0	0	0/1	0/1	0/1	0/1
Guiyu	0	0/1	0/1	0/1	0/1	0/1	0/1	0/1
Gyracanthides	0	0	0	0	0	–	–	–
Scyliorhinus	1	0	0	0	1	0	1	0
Hamiltonichthys	0/1	0	0	0	0/1	0	1	0
Helodus	0/1	0	0	0	0/1	0	1	0
Holonema	0	0	0	0	0	0	0	0
Homalacanthus	1	0	0	0	1	–	–	–
Howqualepis	0	0/1	0	0/1	0/1	0/1	0/1	0/1
Incisoscutum	0	0	0	0	0	0/1	0/1	0/1
Ischnacanthus	1	0	0	0	1	0	1	0
Jagorina	0/1	0	0	0	0/1	0/1	0/1	0/1
Janusiscus	0/1	0	0/1	0/1	0/1	0/1	0/1	0/1

Kathemacanthus	0/1	0	0	0	0/1	-	-	-
Kenichthys	0	0	1	1	1	0/1	0/1	0/1
Kentuckia	0	0/1	0	0/1	0/1	0/1	0/1	0/1
Kujdanowiaspis	0	0	0	0	0	0/1	0/1	0/1
Latviacanthus	0/1	0	0	0	0/1	0	0	0
Ligulalepis	0	1	0	1	1	1	0	0
Lophosteus	0	0	0	0	0	0	0	0
Lunaspis	0	0	0	0	0	0/1	0/1	0/1
Lupopsyrus	0/1	0/1	0	0/1	0/1	-	-	-
Macropetalichthys	0	0	0	0	0	0/1	0/1	0/1
Materpiscis	0	0	0	0	0	0/1	0/1	0/1
Meemannia	0	0	1	1	1	0/1	0/1	0/1
Mesacanthus	0/1	0	0	0	0/1	-	-	-
Microbrachius	0/1	0	0	0	0/1	0/1	0/1	0/1
Miguashaia	0/1	0/1	0	0/1	0/1	0	0	1
Lepisosteus	0	1	0	1	1	1	0	1
Polypterus	0	1	0	1	1	1	0	1
Mimipiscis	0	1	0	1	1	1	0	0
Moythomasia	0	1	0	1	1	1	0	0
Obtusacanthus	0/1	0	0	0	0/1	-	-	-
Onychodus	0	0	0	0	0	0	0	1
Onychoselache	1	0	0	0	1	0	1	0
Orthacanthus	0	0	0	0	0	0	1	0
Osorioichthys	0	0/1	0	0/1	0/1	1	0	0
Osteolepis	0	0	1	1	1	0/1	0/1	0/1
Parabuchanosteus	0	0	0	0	0	0/1	0/1	0/1
Parayunnanolepis	0	0	0	0	0	0/1	0/1	0/1
Parexus	0/1	0	0	0	0/1	0	0	0
Poracanthodes	1	0	0	0	1	0/1	0/1	0/1
Porolepis	0	0	1	1	1	0	0	1
Powichthys	0	0	1	1	1	0	0	1
Promesacanthus	0/1	0	0	0	0/1	-	-	-
Psarolepis	0	0	1	1	1	0	0	0
Pterichthyodes	0	0	0	0	0	0/1	0/1	0/1
Ptomacanthus	0/1	0	0	0	0/1	0/1	0/1	0/1
Pucapampella	0/1	0	0	0	0/1	0/1	0/1	0/1
Quasipetalichthys	0	0	0	0	0	0/1	0/1	0/1
Ramirosuarezia	0/1	0	0	0	0/1	0/1	0/1	0/1
Remigolepis	0	0	0	0	0	0/1	0/1	0/1
Rhadinacanthus	1	0	0	0	1	-	-	-
Rhamphodopsis	0/1	0	0	0	0/1	0	0	0
Romundina	1	0	0	0	1	0/1	0/1	0/1
Sigaspis	0/1	0	0	0	0/1	0/1	0/1	0/1
Sinolepis	0/1	0	0	0	0/1	0/1	0/1	0/1
Styloichthys	0	0	1	1	1	0/1	0/1	0/1
Latimeria	0	0/1	1	1	1	0	0	1
Tamiobatis	0/1	0	0	0	0/1	0/1	0/1	0/1
Tetanopsyrus	0/1	0	0	0	0/1	-	-	-
Tristychius	0/1	0	0	0	0/1	0/1	0/1	0/1
Vernicomacanthus	0/1	0	0	0	0/1	0	0	0
Wuttagoonaspis	0/1	0	0	0	0/1	0/1	0/1	0/1
Youngolepis	0	0	1	1	1	0	0	1
Yunnanolepis	0	0	0	0	0	0/1	0/1	0/1
Andreolepis	0	0	1	1	1	0	0	0

Table S2. Presence or absence of enameloid, ganoin, enamel, enamel or ganoin, enamel, ganoin, or enameloid in the dermal skeleton, and acrodin, enameloid, and enamel on teeth, Related to Figure 5. 0, 1, and 0/1 represent the absence, presence, and unknown status of the tissue, respectively. "-" in dental characters represents the absence of teeth.

Taxa	Minimum age (Mya)	Reference
Galeaspida	432.6	
Osteostraci	437.4	
Acanthodes	298	King et al. 2016
Achoania	412	King et al. 2016
Akmonistion	327	King et al. 2016
Austroptyctodus	383	King et al. 2016
Bothriolepis	383	King et al. 2016
Brachyacanthus	415	King et al. 2016
Brindabellaspis	401	King et al. 2016
Brochoadmones	415	King et al. 2016
Buchanosteus	408	King et al. 2016
Campbellodus	383	King et al. 2016
Cassidiceps	415	King et al. 2016
Cheiracanthus	388	King et al. 2016
Cheirolepis	388	King et al. 2016
Chondrenchelys	338	King et al. 2016
Cladodoides	375	King et al. 2016
Cladoselache	360	King et al. 2016
Climatius	415	King et al. 2016
Cobelodus	325	King et al. 2016
Coccosteus	388	King et al. 2016
Compagopiscis	383	King et al. 2016
Cowralepis	383	King et al. 2016
Culmacanthus	385	King et al. 2016
Debeerius	320	King et al. 2016
Diabolepis	412	King et al. 2016
Dialipina	401	King et al. 2016
Diandongpetalichthys	417	King et al. 2016
Dicksonosteus	411	King et al. 2016
Diplacanthus	388	King et al. 2016
Doliodus	395	King et al. 2016
Eastmanosteus	383	King et al. 2016
Entelognathus	424	King et al. 2016
Eurycaraspis	385	King et al. 2016
Eusthenopteron	380	King et al. 2016
Euthacanthus	415	King et al. 2016
Gavinaspis	412	King et al. 2016
Gemuendina	408	King et al. 2016
Gladiobranchus	415	King et al. 2016
Glyptolepis	388	King et al. 2016
Gogonasus	383	King et al. 2016
Groenlandaspis	385	King et al. 2016
Guiyu	424	King et al. 2016
Gyracanthides	359.3	Warren et al. 2000
Scyliorhinus	0	
Hamiltonichthys	302	King et al. 2016
Helodus	311	King et al. 2016
Holonema	383	King et al. 2016
Homalacanthus	380	King et al. 2016
Howqualepis	385	King et al. 2016
Incisoscutum	383	King et al. 2016
Ischnacanthus	415	King et al. 2016
Jagorina	375	King et al. 2016
Janusiscus	415	King et al. 2016
Kathemacanthus	415	King et al. 2016
Kenichthys	396	King et al. 2016
Kentuckia	347	King et al. 2016
Kujdanowiaspis	411	King et al. 2016
Latviacanthus	404	King et al. 2016
Ligulalepis	401	King et al. 2016
Lophosteus	416	Cunningham et al. 2012
Lunaspis	408	King et al. 2016
Lupopsyrus	415	King et al. 2016
Macropetalichthys	390	King et al. 2016
Materpiscis	383	King et al. 2016
Meemannia	412	King et al. 2016
Mesacanthus	415	King et al. 2016
Microbrachius	386	King et al. 2016
Miguashaia	380	King et al. 2016
Lepisosteus	0	
Polypterus	0	
Mimipiscis	383	King et al. 2016
Moythomasia	383	King et al. 2016

Obtusacanthus	415	King et al. 2016
Onychodus	383	King et al. 2016
Onychoselache	336	King et al. 2016
Orthacanthus	290	King et al. 2016
Osorioichthys	367	King et al. 2016
Osteolepis	388	King et al. 2016
Parabuchanosteus	401	King et al. 2016
Parayunnanolepis	412	King et al. 2016
Parexus	415	King et al. 2016
Poracanthodes	417	King et al. 2016
Porolepis	411	King et al. 2016
Powichthys	411	King et al. 2016
Promesacanthus	415	King et al. 2016
Psarolepis	416	King et al. 2016
Andreolepis	424	Chen et al. 2016
Pterichthyodes	389	King et al. 2016
Ptomacanthus	415	King et al. 2016
Pucapampella	388	King et al. 2016
Quasipetalichthys	385	King et al. 2016
Ramirosuarezia	392	King et al. 2016
Remigolepis	366	King et al. 2016
Rhadinacanthus	386.9	Lukševičs et al. 2010
Rhamphodopsis	388	King et al. 2016
Romundina	415	King et al. 2016
Sigaspis	412	King et al. 2016
Sinolepis	358.5	Zhu et al. 2000
Styloichthys	412	King et al. 2016
Latimeria	0	
Tamiobatis	360	King et al. 2016
Tetanopsyrus	415	King et al. 2016
Tristychius	336	King et al. 2016
Vernicomacanthus	415	King et al. 2016
Wuttagoonaspis	393	King et al. 2016
Youngolepis	412	King et al. 2016
Yunnanolepis	415	King et al. 2016

Table S3. Tip ages used for the ancestral state estimation, Related to Figure 5.

Transparent Methods

Bioinformatic analyses

We searched for SCPP genes in RNA-seq datasets (GenBank accession numbers: SRX796494 and SRX1016233-SRX1016241 for lungfish, SRX796491 and SRX1386644- SRX1386647 for bichir, and SRX424533 and SRX424534 for sturgeon) by tblstn (http://www.ncbi.nlm.nih.gov/) (Altschul et al., 1990) using amino acid sequences of gar orthologs as queries (Kawasaki et al., 2017).

Relative expression levels of gar SCPP genes were estimated as FPKM values (Trapnell et al., 2010), calculated for a dataset of gar skin (GenBank accession number, SRP042013) (Braasch et al., 2016) using Galaxy (https://usegalaxy.org/) (Afgan et al., 2016). The dataset was retrieved from the EBI SRA database, trimmed using Trimmatic (Bolger et al., 2014), aligned with the gar genome sequence (LepOcu1) using TopHat (Kim et al., 2013). FPKM values and confidence intervals were calculated using Cufflinks (Trapnell et al., 2010) based on BAM files obtained by the TopHat analysis. All default conditions were used in Galaxy analysis, except additional options in Trimmomatic (ILLUMINACLIP and MINLEN=50) and Cufflinks (multi-read correction). Genomic coordinates of SCPP genes were determined using Splign (http://www.ncbi.nlm.gov./) (Kapustin et al., 2008), and used for the Cufflinks analysis.

Molecular analysis

All animals used in our study (gar, 16-55 cm in total length; zebrafish, 3.0 cm in total length; bichir, 20 cm in total length; and lungfish, 20 cm in total length; sex not determined for these animals) were sacrificed according to the guidelines issued by the Ministry of Justice in Japan. SCPP genes identified in bichir and lungfish RNA-seq datasets were confirmed by PCR using cDNA libraries made from a tooth plate (lungfish) and tooth germs (bichirs), as described (Braasch et al., 2016). These libraries were made using SMART cDNA library construction kit (Takara Bio), and PCR products were size fractionated by agarose gel electrophoresis, purified from the agarose gel using the FastGene Gel/PCR Extraction Kit (Nippon Genetics), and ligated into T-vector pMD20 (Takara Bio). The ligation mix was then used to transform *E.*

coli HST08 Premium Competent Cells (Takara Bio). Exon-intron borders were also determined by PCR using genomic DNA as the substrate. For expression analysis of bichir *scpp5*, total RNA molecules were isolated using RNAiso Plus (Takara Bio) and cDNA was synthesized using the PrimerScript II 1st strand cDNA synthesis kit (Takara bio). Primer sequences used for RT-PCR are as follows: 5'-GAGACTTGCGATCTTCTCTTCTG-3' and 5'-GTGAATTGACCTGAGGCAGGA-3' for *scpp5*; and 5'-CACAGTTTGCCAGATGGTCC-3' and 5'-CACCACCAATTGCCTTGCTC-3' for *gapdh*.

ISH analysis

For ISH analysis, jaws and skin of gar and zebrafish were fixed with neutralized 4% paraformaldehyde, decalcified with Morse's solution (10% w/v sodium citrate and 22.5% v/v formic acid), dehydrated through a graded ethanol series and xylene, embedded in paraffin, sectioned in the coronal plane at 4 μm in thickness, and mounted on glass slides. These glass slides were deparaffined, treated with Proteinase K (20 mg/ml) for 10 min, and used for hybridization (50% formamide, 10 mM Tris pH7.6, 1xDenhart's solution, 5% dextran sulfate, 600 mM NaCl, 0.25% SDS, 1 mM EDTA, and 100μg/ml *Escherichia coli* tRNA) at 70C (Nakatomi et al., 2006). A specific portion of *scpp5*, *ambn*, and *enam* were amplified from the cDNA libraries (primer sequences: 5'-GTTGGTGCTACAGCAGGAAGT-3' and 5'-GTTGTTGCTTCCCTGAACTG-3' for gar *ambn*; 5'-AAGGCCTCAGCTTCGTCCAG-3' and 5'-ACTCCTTCTCGTTGACTTCGT-3' for gar *enam*; 5'-TATTCTGAGGAGTCACCAA-3' and 5'-ATTCTGACTTGGCTGGACG-3' for gar *scpp5*; 5'-ACTTCATCAACAGGTGCCCAATC-3' and 5'-TGAAAGCTCCGTGACCTGAATCT-3' for zebrafish *ambn*; and 5'-CTGCCCCTGACAGTGGCAGTAATG-3' and 5'-CATCAGGCCCAACAACAGTGGTGT-3' for zebrafish *enam*), cloned using the pGEM-T Easy Vector (Promega), and labeled with digoxigenin using the DIG RNA Labeling Kit (Roche), and used for hybridization. After hybridization, glass slides were washed with 2xSSC. Hybridization signals were detected using Anti-Digoxigenin-AP, Fab fragments (Roche) and NBT/BCIP Solution (Roche), as specified.

IHC analysis

For IHC analysis, jaws and scales were fixed (4% paraformaldehyde-0.2% glutaraldehyde, 0.05M HEPES buffer pH7.4), dehydrated, and embedded in LR-White resin (LR-W, London Resin), and processed for the Protein A-gold (PAG) method (Sasagawa et al., 2012). For light microscopic analysis, semi-thin sections were made from LR-W resin block, mounted on glass slides, masked with 5% goat serum in phosphate buffered saline (PBS), and reacted with the antibody diluted 1:100 or 1:200 in PBS containing 0.5% bovine serum albumin (PBS-BSA) at 4C. These sections were washed with PBS, incubated with the PAG conjugate (gold nanoparticles 5nm, BBI) diluted 1:100 with PBS-BSA, washed with PBS, treated with the silver enhancer solution (50 mM citrate buffer, 0.85% hydroquinone, 0.1% maleic acid, 0.11% silver lactate, and 1% acacia powder) (Uchida et al., 1991) for 10 min in a dark box, and rinsed with water. These sections were then immersed in photographic fixatives, and stained with fast red or toluidine blue (Sasagawa et al., 2012).

For TEM analysis, ultrathin sections obtained from LR-W resin block were mounted on nickel grids, floated on a drop of 1% goat serum and then the antibody diluted 1:200-1:400 in PBS-BSA. These sections were subsequently washed with PBS-BSA, treated with 1% goat serum and then with the PAG conjugate diluted 1:10 in PBS-BSA. These sections were stained with platinum blue and lead citrate (additionally stained with phosphotungstic acid for some samples), and examined using TEM (JEM-1010, JEOL) (Sasagawa et al., 2016). In some sections, immunoreactions were enhanced using the silver enhancer solution (Uchida et al., 1991) or the Silver Enhancer Kit (Kirkegaard & Perry Laboratories). Polyclonal antibodies to gar Scpp5 were raised against YRQQPQQQN (SIGMA-ALDRICH).

Phylogenetic analysis

We augmented an existing phylogenetic dataset (Qiao et al., 2016) with codings for *Scyliorhinus*, *Lepisosteus*, *Polypterus*, and *Latimeria,* representing the three major living clades of jawed vertebrates. We also coded *Andreolepis,* a putative stem-osteichthyan (Qu et al., 2015), and coded *Ligulalepis* as

present for dental acrodin (Schultze, 2016; Schultze, 2018). Morphological data were analyzed using the Mkv+G model in MrBayes 3.2.7 (Ronquist et al., 2012). We constrained the positions of the extant taxa to mitigate long branch effects: *Scyliorhinus* with *Helodus, Chondrenchelys, Debeerius, Tristychius, Hamiltonichthys, Onychoselache* (Qiao et al., 2016); *Latimeria* with *Miguashaia* (Arratia and Schultze, 2015); and *Polypterus, Lepisosteus, Kentuckia* with *Moythomasia, Mimipiscis* (Giles et al., 2017). We conducted two phylogenetic analyses of this dataset, one in which the GAP clade were constrained to be stem-osteichthyans (King et al., 2017; Lu et al., 2017), and the other in which these taxa were topologically unconstrained, yielding a stem-sarcopterygian affinity (Lu et al., 2016; Qiao et al., 2016; Choo et al., 2017). Each analysis used four independent runs of four chains over 10,000,000 generations, sampling every 10,000 generations, with 25% of burnin. Convergence was assessed using Tracer 1.7 (Rambaut et al., 2018). Results were summarized using majority rule consensus trees (Figures S3A and S3B).

Ancestral state estimation

We compiled data on the distribution of five dermal (enameloid, ganoin, enamel, ganoin/enamel, hypermineralized tissue) and three dental (acrodin, enameloid, enamel) skeletal characters (Table S2); we confirmed the presence of dental enameloid in *Cladoselache* (Figure S3S).

Branch lengths were estimated using the function *timePaleoPhy* in the R package (https://www.R-project.org/) *paleotree* (Bapst, 2012) using the 'equal' method (Brusatte et al., 2008), with the root age increased by 5 million years. Tip ages are from King *et al.* (King et al., 2017) (Table S3) but the root (Tinn and Märss, 2018), and the crown clades of chondrichthyans, sarcopterygians, actinopterygians, osteichthyans, and gnathostomes (Benton et al., 2015) were calibrated to be minimally as old as oldest fossil representative. Using these time-scaled topologies, we estimated ancestral states using Stochastic Character Mapping (Huelsenbeck et al., 2003) in the R package *phytools* (Revell, 2012). Each character was coded as a binary presence or absence state for all taxa; uncertain tip states were assigned an equal prior probability of 0.5. Taxa were excluded from an analysis when the character was

inapplicable. By running all separate analyses for each character, there is zero modelled co-variance between each character. Stochastic character mapping was run using the *make.simmap* function (Bollback, 2006) in *phytools* but with a single *Q* matrix for all simulations under the 'all rates different' and a naïve equal prior probability for absence or presence at the root. Each character model ran for 1000 simulations and each iteration used the same 'empirical' *Q* matrix with the highest likelihood transition probabilities. Results were summarized using the *describe.simmap* function and the posterior probabilities of node and tip states were plotting on each tree.

Supplemental References

Afgan, E., Baker, D., van den Beek, M., Blankenberg, D., Bouvier, D., Cech, M., Chilton, J., Clements, D., Coraor, N., Eberhard, C., et al. (2016). The Galaxy platform for accessible, reproducible and collaborative biomedical analyses: 2016 update. Nucleic Acids Res. *44*, W3-W10.

Altschul, S.F., Gish, W., Miller, W., Myers, E.W., and Lipman, D.J. (1990). Basic local alignment search tool. J. Mol. Biol. *215*, 403-410.

Arratia, G., and Schultze, H.-P. (2015). A new fossil actinistian from the Early Jurassic of Chile and its bearing on the phylogeny of Actinistia. J. Vertebr. Paleontol. *35*, e983524.

Bapst, D.W. (2012). paleotree: an R package for paleontological and phylogenetic analyses of evolution. Methods Ecol. Evol. *3*, 803-807.

Benton, M.J., Donoghue, P.C.J., Asher, R.J., Friedman, M., Near, T.J., and Vinther, J. (2015). Constraints on the timescale of animal evolutionary history. Palaeontol. Electronica *18*,

Bolger, A.M., Lohse, M., and Usadel, B. (2014). Trimmomatic: a flexible trimmer for Illumina sequence data. Bioinformatics *30*, 2114-2120.

Bollback, J.P. (2006). SIMMAP: stochastic character mapping of discrete traits on phylogenies. BMC Bioinformatics *7*, 88.

Braasch, I., Gehrke, A.R., Smith, J.J., Kawasaki, K., Manousaki, T., Pasquier, J., Amores, A., Desvignes, T., Batzel, P., Catchen, J., et al. (2016). The spotted gar genome illuminates vertebrate evolution and facilitates human-teleost comparisons. Nat. Genet. *48*, 427-437.

Brusatte, S.L., Benton, M.J., Ruta, M., and Lloyd, G.T. (2008). Superiority, competition, and opportunism in the evolutionary radiation of dinosaurs. Science *321*, 1485-1488.

Chen, D., Blom, H., Sanchez, S., Tafforeau, P., and Ahlberg, P.E. (2016). The stem osteichthyan *Andreolepis* and the origin of tooth replacement. Nature 539, 237-241.

Choo, B., Zhu, M., Qu, Q., Yu, X., Jia, L., and Zhao, W. (2017). A new osteichthyan from the late Silurian of Yunnan, China. PLoS One *12*, e0170929.

Cunningham, J.A., Rucklin, M., Blom, H., Botella, H., and Donoghue, P.C. (2012). Testing models of dental development in the earliest bony vertebrates, *Andreolepis* and *Lophosteus*. Biol. Lett. *8*, 833-837.

Giles, S., Xu, G.H., Near, T.J., and Friedman, M. (2017). Early members of 'living fossil' lineage imply later origin of modern ray-finned fishes. Nature *549*, 265-268.

Goldsmith, M.I., Fisher, S., Waterman, R., and Johnson, S.L. (2003). Saltatory control of isometric growth in the zebrafish caudal fin is disrupted in long fin and rapunzel mutants. Dev. Biol. *259*, 303-317.

Huelsenbeck, J.P., Nielsen, R., and Bollback, J.P. (2003). Stochastic mapping of morphological characters. Syst. Biol. *52*, 131-158.

Kapustin, Y., Souvorov, A., Tatusova, T., and Lipman, D. (2008). Splign: algorithms for computing spliced alignments with identification of paralogs. Biol. Direct. *3*, 20.

Kawasaki, K. (2009). The SCPP gene repertoire in bony vertebrates and graded differences in mineralized tissues. Dev. Genes Evol. *219*, 147-157.

Kawasaki, K., and Amemiya, C.T. (2014). SCPP genes in the coelacanth: tissue mineralization genes shared by sarcopterygians. J. Exp. Zool. B Mol. Dev. Evol. *322*, 390-402.

Kawasaki, K., Mikami, M., Nakatomi, M., Braasch, I., Batzel, P., J, H.P., Sato, A., Sasagawa, I., and Ishiyama, M. (2017). SCPP genes and their relatives in gar: rapid expansion of mineralization genes in osteichthyans. J. Exp. Zool. B Mol. Dev. Evol. *328*, 645-665.

Kim, D., Pertea, G., Trapnell, C., Pimentel, H., Kelley, R., and Salzberg, S.L. (2013). TopHat2: accurate alignment of transcriptomes in the presence of insertions, deletions and gene fusions. Genome Biol. *14*, R36.

King, B., Qiao, T., Lee, M.S.Y., Zhu, M., and Long, J.A. (2017). Bayesian morphological clock methods resurrect placoderm monophyly and reveal rapid early evolution in jawed vertebrates. Syst. Biol. 66, 499-516.

Lu, J., Giles, S., Friedman, M., den Blaauwen, J.L., and Zhu, M. (2016). The oldest actinopterygian highlights the cryptic early history of the hyperdiverse ray-finned fishes. Curr. Biol. 26, 1602-1608.

Lu, J., Giles, S., Friedman, M., and Zhu, M. (2017). A new stem sarcopterygian illuminates patterns of character evolution in early bony fishes. Nat. Commun. *8*, 1932.

Lukševičs, E., Lebedev, O.A., and Zakharenko, G.V. (2010). Palaeozoogeographical connections of the Devonian vertebrate communities of the Baltica Province. Part I. Eifelian–Givetian. Palaeoworld *19*, 94-107.

Nakatomi, M., Morita, I., Eto, K., and Ota, M.S. (2006). Sonic hedgehog signaling is important in tooth root development. J. Dent. Res. *85*, 427-431.

Qiao, T., King, B., Long, J.A., Ahlberg, P.E., and Zhu, M. (2016). Early Gnathostome Phylogeny Revisited: Multiple Method Consensus. PLoS One *11*, e0163157.

Qu, Q., Haitina, T., Zhu, M., and Ahlberg, P.E. (2015). New genomic and fossil data illuminate the origin of enamel. Nature *526*, 108-111.

Rambaut, A., Drummond, A.J., Xie, D., Baele, G., and Suchard, M.A. (2018). Posterior Summarization in Bayesian Phylogenetics Using Tracer 1.7. Syst. Biol. *67*, 901-904.

Revell, L.J. (2012). phytools: an R package for phylogenetic comparative biology (and other things). Methods Ecol. Evol. *3*, 217-223.

Ronquist, F., Teslenko, M., van der Mark, P., Ayres, D.L., Darling, A., Hohna, S., Larget, B., Liu, L., Suchard, M.A., and Huelsenbeck, J.P. (2012). MrBayes 3.2: efficient Bayesian phylogenetic inference and model choice across a large model space. Syst. Biol. *61*, 539-542.

Sasagawa, I., Oka, S., Mikami, M., Yokosuka, H., Ishiyama, M., Imai, A., Shimokawa, H., and Uchida, T. (2016). Immunohistochemical and Western Blotting Analyses of Ganoine in the Ganoid Scales of Lepisosteus oculatus: an Actinopterygian Fish. J. Exp. Zool. B Mol. Dev. Evol. *326*, 193-209.

Sasagawa, I., Yokosuka, H., Ishiyama, M., Mikami, M., Shimokawa, H., and Uchida, T. (2012). Fine structural and immunohistochemical detection of collar enamel in the teeth of Polypterus senegalus, an actinopterygian fish. Cell Tissue Res. *347*, 369-381.

Schultze, H.-P. (2018). Hard tissues in fish evolution: history and current issues. Cybium *42*, 29-39.

Schultze, H.-P. (2016). Scales, enamel, cosmine, ganoine, and early osteichthyans. C. R. Palevol. *15*, 83-102.

Tanabe, T., Aoba, T., Moreno, E.C., Fukae, M., and Shimuzu, M. (1990). Properties of phosphorylated 32 kd nonamelogenin proteins isolated from porcine secretory enamel. Calcif. Tissue Int. *46*, 205-215.

Tinn, O., and Märss, T. (2018). The earliest osteostracan *Kalanaspis delectabilis* gen. et sp nov. from the mid-Aeronian (mid-Llandovery, lower Silurian) of Estonia. J. Vertebr. Paleontol. *38*, e1425212.

Trapnell, C., Williams, B.A., Pertea, G., Mortazavi, A., Kwan, G., van Baren, M.J., Salzberg, S.L., Wold, B.J., and Pachter, L. (2010). Transcript assembly and quantification by RNA-Seq reveals unannotated transcripts and isoform switching during cell differentiation. Nat. Biotechnol. *28*, 511-515.

Uchida, T., Tanabe, T., Fukae, M., Shimizu, M., Yamada, M., Miake, K., and Kobayashi, S. (1991). Immunochemical and immunohistochemical studies, using antisera against porcine 25 kDa amelogenin, 89 kDa enamelin and the 13-17 kDa nonamelogenins, on immature enamel of the pig and rat. Histochemistry *96*, 129-138.

Warren, A., Currie, B.P., Burrow, C., and Turner, S. (2000). A redescription and reinterpretation of *Gyracanthides murrayi* Woodward 1906 (Acanthodii, Gyracanthidae) from the Lower Carboniferous of the Mansfield Basin, Victoria, Australia. J. Vertebr. Paleontol. *20*, 225-242.

Yamakoshi, Y., Pinheiro, F.H., Tanabe, T., Fukae, M., and Shimizu, M. (1998). Sites of asparagine-linked oligosaccharides in porcine 32 kDa enamelin. Connect. Tissue Res. *39*, 39-46; discussion 63-37.

Zhu, M., Wang, N.-Z., and Wang, J.-Q. (2000). Devonian macro-and microvertebrate assemblages of China. Cour. For. Sekenbg. *223*, 361-372.